# Characterization of two novel proteins containing the rhodanese homology domain: YgaP and YbbB of *Escherichia coli*

by

Farzana Ahmed

Dissertation submitted to the Faculty of the Virginia Polytechnic Institute and State University in partial fulfillment of the requirements for the degree of

Doctor of Philosophy
in
Biochemistry

_____
Timothy J. Larson, Chair

_____
David R. Bevan

_____
Dennis R. Dean

_____
Jiann-Shin Chen

_____
David L. Popham

August 7, 2003
Blacksburg, Virginia

Keywords: YgaP, YbbB, rhodanese, seleno-tRNA, 2-selenouridine

# Characterization of two novel proteins containing the rhodanese homology domain: YgaP and YbbB of *Escherichia coli*

Farzana Ahmed

Timothy J. Larson, Chair

Department of Biochemistry

## ABSTRACT

Rhodanese homology domains are ubiquitous structural modules found in eubacteria, eukaryotes and archaea. The rhodanese homology domain may comprise the entire structure of a protein. Alternatively it is found as tandemly repeated modules in which the C-terminal domain displays the properly structured active site. Finally it is found as a member of many multidomain proteins. Although some members of this family of proteins show sulfurtransferase activity *in vitro*, their specific physiological functions remain largely undefined. Fusion of a rhodanese domain to different protein domains of known or unknown functions provides important clues to the diverse roles for these proteins.

Nine proteins containing the rhodanese homology domain are predicted in *Escherichia coli*. In this work, two of these proteins: YgaP and YbbB were characterized using bioinformatics, biochemical and genetic approaches. YgaP is a single domain rhodanese that is predicted to contain an amino-terminal rhodanese domain (118 amino acids) and a hydrophobic carboxy-terminal domain (56 amino acids). The *ygaP* gene was cloned into a vector that directed overexpression of a membrane-associated rhodanese activity. The cellular location of YgaP was determined by using sucrose density layer ultracentrifugation. YgaP and rhodanese activity co-sedimented with the cytoplasmic membrane marker D-lactate dehydrogenase, and was not present in the outer membrane fractions, indicating YgaP is a cytoplasmic membrane protein. A polyhistidine-tagged

variant of YgaP was subsequently solubilized from the membrane by detergent extraction and purified by metal chelate chromatography. Similar to the other characterized rhodaneses, purified YgaP-$His_6$ as well as the membrane-associated native form of the protein displayed a double displacement (ping-pong) mechanism. YgaP is unique in that it is the first membrane-associated rhodanese to be described. To understand the physiological role of YgaP, a strain with *ygaP* gene disruption was constructed. No obvious phenotype resulted from deletion of *ygaP*.

The *ybbB* gene of *E. coli* has an interesting genome organization in several Gram-negative bacteria including *Pseudomonas aeruginosa* and *Azotobacter vinelandii* where it is predicted to be in the same operon with *selD*, encoding selenophosphate synthetase. Thus the role of YbbB in selenium metabolism was investigated. A strain with *ybbB* gene deletion was constructed and tested for its ability to incorporate $^{75}Se$ into tRNA and protein. It was shown that the disruption of *ybbB* prevented specific incorporation of selenium into tRNA but not into proteins *in vivo*. The modified nucleoside missing in tRNAs of the Δ*ybbB* strain was identified as 5-methylaminomethyl-2-selenouridine ($mnm^5se^2U$), which has previously been shown to be present in the wobble position of the anticodon of *E. coli* $tRNAs^{Lys,\ Glu\ and\ Gln}$. Data from HPLC analysis showed that the deletion of *ybbB* did not affect the production of 5-methylaminomethyl-2-thiouridine ($mnm^5s^2U$), the precursor to $mnm^5se^2U$, suggesting that YbbB is not required for sulfur transfer but is rather involved in selenation of tRNAs. YbbB was subsequently expressed with a C-terminal histidine tag and purified for initial characterization. Purified YbbB-$His_6$ migrated as a 43 kDa monomer under denaturing conditions and displayed spectral properties that suggested its interaction with tRNA. Finally, it was shown that Cys97, which aligns with the active site cysteine of rhodanese and is conserved in all known YbbB homologs, is required for YbbB activity. However, Cys96, which is not conserved, is not required for activity.

*This work is dedicated to the memory of my dad, Sufi M. Ahmed: A great scientist, a great man, without whom I would not have taken this less traveled path.*

# Acknowledgements

I would like to express my deep appreciation and respect for my advisor, Dr. Timothy J. Larson, for his ceaseless support, encouragement, continued guidance and patience during my research years in his lab. His strong scientific knowledge, remarkable memory together with his unique blend of humility, compassion and respect for others has been a source of inspiration for me and will continue to be so in the future.

My sincere thanks to my committee, Dr. David R. Bevan, Dr. Jiann-Shin Chen, Dr. Dennis R. Dean and Dr. David L. Popham for their suggestions and guidance which has led me towards the completion of this degree. I also want to thank Dr. Bevan for his molecular modeling class, Dr. Dean and Dr. Popham for introducing me to prokaryotic gene expression in a very interesting way and to Dr. Chen for allowing me to rotate in his lab in the first year of graduate study.

I would like to express my gratitude to Dr. Hess, for chairing my preliminary exam and for his support and encouragement during the preparation for the exam. I am truly thankful to other faculty members of the department: Dr. Kennelly, Dr. White, Dr. Potts, Dr. Gregory, Dr. Newton, Dr. Sitz, Dr. Luckhart, Dr. Gillaspy and Dr. Tu for teaching me biochemistry and molecular biology. Thanks to Dr. Keenan under whom I enjoyed working as a teaching assistant. I am thankful to Kim Harich for helping me with MALDI Mass spectrometry.

I want to thank Dr. Theressa C. Stadtman of NIH along with her lab members Matt Wolfe and Gerard Lacourciere for generous collaboration in the YbbB project.

Thanks to Janet Donahue, for her kindness, assistance and continuous effort for creating a happy and warm atmosphere in the lab.

My warmest appreciation to the past and present members of the Larson lab: Hui Cheng, Bekir Col, Promjit Jutabha and Keith Ray with whom I not only exchanged scientific ideas but also shared many happy and memorable moments in my life. Additionally, I would like to thank Jeremy Hunt, Randy Mauldin, Senay Sengul, Debbie Johnson and other past undergraduate researchers in the lab who have made the last several years an enjoyable experience.

I would also like to acknowledge the people in different labs that shared their equipments and reagents with me including Ben Potters, Debbie Wright, Sue Anderson, Valerie Cash and Randy Saunders. Many thanks to Julianna Toth for her technical assistance during my rotation in Dr. Chen's lab. I am thankful to Murat Kasap, Brian Lower, Hong Li, Archana Mukhopadhyay, Renhui Li and Karsten Klage for their friendship and for teaching me many valuable things.

I am deeply indebted to my mother and my sister for their love, support and continued encouragement throughout my life. Most especially I would like to thank my husband, Raqibul Mostafa for making this journey worthwhile. I'm grateful to Allah for providing me with the opportunity to pursue this degree.

# Table of Contents

# List of Figures

# List of Tables

# Chapter One

# Introduction

## 1.1 Rhodanese homology domain

Rhodanese homology domains are ubiquitous structural modules found in eukaryotes, eubacteria and archaea (1). They are composed of an active site loop and two structural motifs, designated CH2A and CH2B, which are essential features of rhodanese homology domains (2). CH2A is a strand-helix-strand region and CH2B consists of a strand followed by a helix. The rhodanese homology domain may comprise the entire structure of a protein. Alternatively it is found as tandemly repeated modules in which the C-terminal domain displays the properly structured active site. Finally it is found as a member of many multidomain proteins (FIG. 1.1). The crystal structures of bovine (Rhobov) and *Azotobacter vinelandii* (RhdA) rhodaneses (3;4) show that these proteins are composed of two identically folded domains of limited sequence similarity but very similar three dimensional structures, called hereafter rhodanese domains or modules. Each domain was about 120 amino acids in length and displayed an $\alpha/\beta$ topology, with a central parallel five stranded beta-sheet surrounded by alpha-helices on both sides (3;4). The structural similarity between the two domains of Rhobov and RhdA suggests that rhodaneses arose by divergent evolution from a common ancestor protein. The two domains are considered to have arisen by gene duplication which, under selective pressure, maintained conformational similarity but lost sequence conservation (3). Although the two domains of Rhobov and RhdA have similar conformations, only the C-

terminal domain possesses the catalytic cysteine in its active site, which is replaced by Asp in the active site loop of the N-terminal domain. The C-terminal domain will be called the catalytic domain and the N-terminal domain, the pseudorhodanese domain. The cysteine residue present in the active site of the catalytic domain is the first residue of a six-amino acid active-site loop that folds in a cradle like structure defining the enzyme's catalytic pocket (4).

Until recently the rhodanese folds were not observed in any other protein structures. However, the recent crystal structure determination of two human cell cycle control phosphatases, Cdc25A and Cdc25B, revealed that these two proteins display three dimensional folds identical to the rhodanese domain with the active site cysteine residue present in its conserved position (2;5). However the active site loop of Cdc25 has seven amino acid residues instead of six for sulfurtransferases, which is suggested to be required for binding phosphate.

Besides Cdc25, catalytic rhodanese domain was also identified in proteins composed of single rhodanese domains with the six-amino acid active site loop bearing the catalytic cysteine. The recent chracterization of the GlpE protein, a thiosulfate sulfurtransferase (TST) from *E. coli*, showed that it is a single domain rhodanese, composed of only the catalytic rhodanese domain, which suggested that the N-terminal pseudorhodanese domain present in Rhobov and RhdA is not essential for catalysis (6;7). Besides GlpE, the periplasmic sulfide dehydrogenase from *Wolinella succinogenes*, also described as a sulfurtransferase (polysulfide:cyanide sulfurtransferase), has a single rhodanese domain (8). The single rhodanese domain has been found associated with proteins involved in specific stress responses including the phage shock protein PspE

from *E. coli*, heat shock protein 67B2 from *Drosophila melanogester* and the *Vibrio cholera* shock protein Q9KN65. The arsenic resistance protein (9) Acr2 from yeast also has a catalytic rhodanese domain, which has an active site loop similar to Cdc25 phosphatases (1).

The pseudorhodanese domain lacking the active site cysteine has been found in the N-terminal non-catalytic domain of mercaptopyruvate sulfurtransferases from rat and *E. coli* (10-12), in two distinct families of MAP-kinase phosphatases (13), in about one third of the several dual specific phosphatases and in several ubiquitin hydrolases from yeast and human (2;14). The function of the pseudorhodanese domain has not been elucidated. However in bovine rhodanese this domain is suggested to be involved in substrate recognition which could come in the vicinity of the active site through the folding of a loop over the C-terminal domain (15). The pseudorhodanese domain has also been suggested to have regulatory functions in dual-specific phosphatases and ubiquitin hydrolases, possibly in signal transduction.

The catalytic rhodanese domain has been found in association with other domains of known or unknown functions. This domain is present at the C-terminus of ThiI, an *E. coli* protein involved in thiamin and 4-thiouridine biosynthesis (16-18), at the C-terminal domain of MoeB from bacteria, fungi, plants and animals, which has been shown to be involved in the transfer of sulfur for molybdopterin biosynthesis in *Aspergillus nidulans* (19) and also at the C-terminal domain of uncharacterized NADH disulfide oxidoreductases from *Lactococcus lactis*, *Vibrio cholera* (COG0446), *Archaeoglobis fulgidus* and *Bacillus anthracis*, thought to be involved in NADH dependent reduction of disulfide bonds. Several other proteins contain the catalytic rhodanese domain at the C-

terminus including a peptidyl prolyl *cis-trans* isomerase from *Arabidopsis thaliana*, two ArsR-like metalloregulators from *Mycobacterium tuberculosis* and HesB from *Xylella fastidiosa* that has a IscA-like domain fused to a rhodanese domain. IscA and its homologs serve as alternate scaffolds for Fe-S cluster assembly in prokaryotes and eukaryotes (20). The presence of rhodanese homology domain in different proteins and in combination with other domains suggest diverse biological roles for this family of proteins.

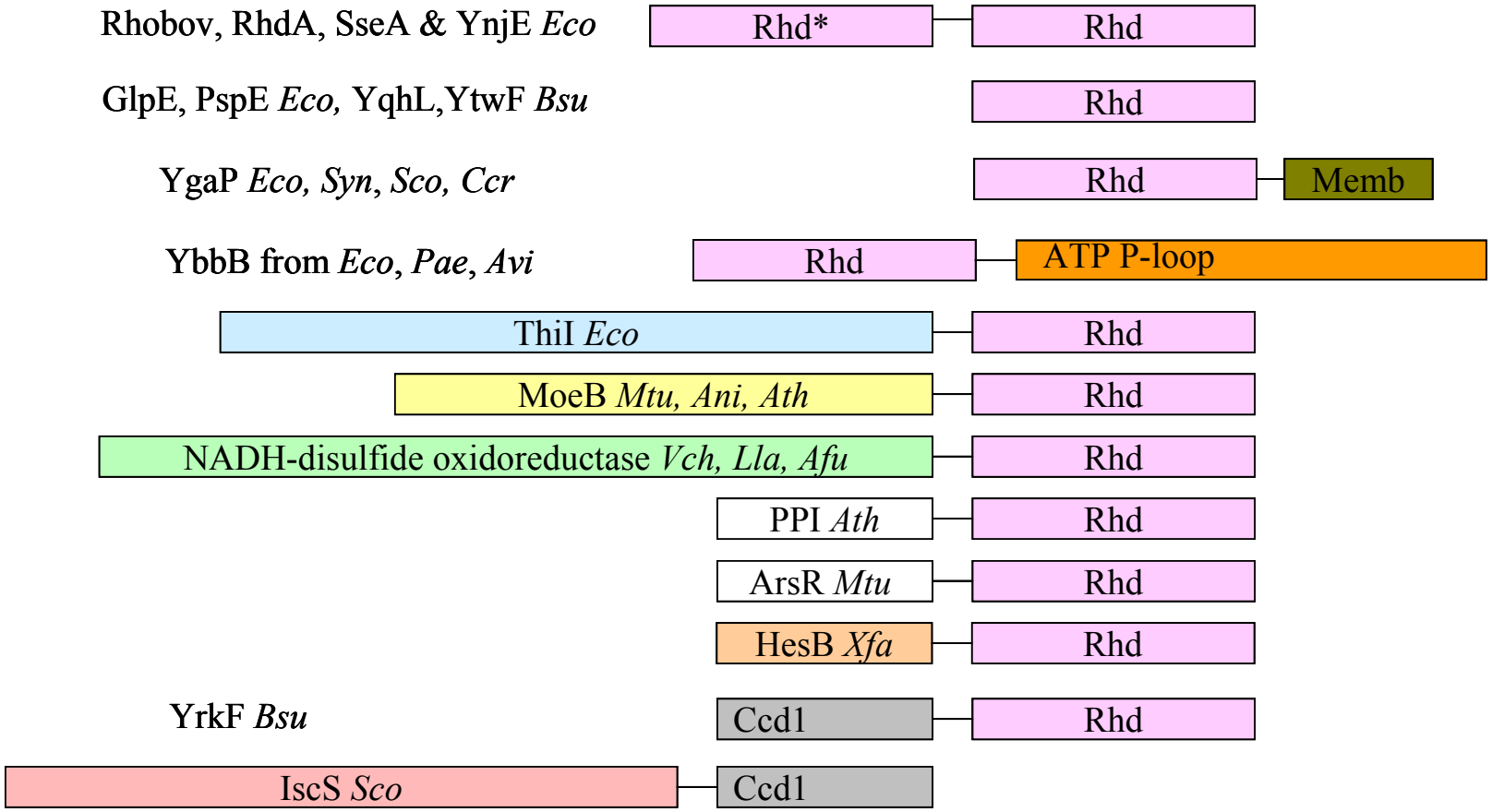


**FIG. 1.1. Domain architecture of proteins containing single, tandem and fusion of rhodanese homology domain**

Rhd, catalytic rhodanese domain; Rhd*, pseudorhodanese domain; Memb, predicted membrane domain, Ccd1, conserved cysteine domain 1; PPI, peptidyl prolyl *cis-trans* isomerase. *Eco*, *E. coli*; *Bsu*, *Bacillus subtilis*, *Syn, Synechocystis*; *Sco, Streptomyces coelicolor*; *Ccr, Caulobacter crecentus; Pae, Pseudomonas aeruginosa*; *Avi, Azotobacter vinelandii*; *Mtu*, *Mycobacterium tuberculosis*; *Ani*, *Aspergillus nidulans*; *Ath*, *Arabidopsis thaliana*; *Vch*, *Vibrio cholera*; *Lla*, *Lactococcus lactis*; *Afu*, *Archaeoglobis fulgidus*; *Xfa*, *Xylella fastidiosa*

## 1.2. Sulfurtransferases

Sulfurtransferases are widely distributed enzymes that catalyze the transfer of a sulfane sulfur atom from a donor molecule to an acceptor substrate (21). Rhodanese and mercaptopyruvate sulfurtransferase (MST) are proteins belonging to the sulfurtransferase family of enzymes containing the rhodanese homology domain. The distinct characteristics of these two enzymes and their prevalence in different organisms are described below.

### 1.2.1. Thiosulfate:cyanide sulfurtransferase (Rhodanese, E.C 2.8.1.1)

Rhodaneses are enzymes that catalyze the *in vitro* transfer of sulfane sulfur atom from thiosulfate to cyanide forming thiocyanate and sulfite as shown below:

$$SSO_3^{2-} + CN^- \rightarrow SCN^- + SO_3^{2-}$$

Besides thiosulfate and cyanide serving as sulfur donor and acceptor molecules, the enzyme also uses thiosulfonates ($RSO_2S^-$), polysulfide ($RSS^-$) and thiocysteine as sulfur donors and sulfite, sulfinate and thiol compounds as sulfur acceptor substrates (22;23). Rhodaneses were first discovered in mammalian tissues. S. Lang reported that certain animal tissues contain enzymes that catalyze the reaction between thiosulfate and cyanide to form thiocyanate and sulfite (24). S. Lang called the enzyme rhodanese, derived from the German word rhodanid meaning thiocyanate. Rhodanese is a mitochondrial enzyme that is especially abundant in mammalian liver and kidney. Current knowledge of rhodanese structure and function is derived from an enzyme from

bovine liver mitochondria (3). Rhodanese from bovine liver has been isolated and characterized in great detail in terms of both its structure (3;24) and mechanism of action (25;26). The enzyme is a single polypeptide of 293 amino acid residues with a molecular weight of 32,900. Kinetic measurements of bovine rhodanese showed that enzyme catalysis occurs by a double displacement (ping-pong) mechanism where the enzyme cycles between a sulfur-free form (E-Cys-$S^-$) and a persulfide containing intermediate (E-Cys-$SS^-$) (25;27). During the course of the reaction the sulfur donor covalently binds the sulfur free form of the enzyme and the first product is released. The persulfide form of the enzyme then binds to the sulfur acceptor and transfers its sulfane sulfur to form the second product and the enzyme is released again in the sulfur-free form. Crystal structure analysis and anion inhibition studies of bovine rhodanese indicate the presence of a cationic site in the enzyme that binds the anionic substrate (3;27). The positive charges, Arg-186 and Lys-249, close to the active site Cys-247 might participate in binding of the substrate thiosulfate (3). It is hypothesized that the cationic site also serves as an electrophilic group polarizing the sulfur-sulfur bond of the substrate so that it is readily cleaved by an enzyme nucleophile; the active site sulfhydryl group. Chemical inactivation of the enzyme was shown to be associated with modification of Arg-186, which indicated the importance of this residue in the sulfur transfer function of rhodanese (26).

Besides the bovine enzyme, rhodaneses have been detected in other mammalian tissues, in birds, plants and in a wide variety of bacteria. Rhodanese isozymes were found in a wide range of human tissues, with kidney and liver showing the highest levels of activity (28). In addition the enzyme was purified from rat liver and characterized to

some extent (29). A comprehensive search of the *A. thaliana* genome identified about 18 proteins containing the rhodanese homology domain. Two of these proteins were identified as single domain rhodaneses having thiosulfate sulfurtransferase activities (rhodanese) (30;31).

Rhodanese enzymes have also been identified and /or isolated from various bacterial sources including nitrogen-fixing *Azotobacter vinelandii* (4;32) soil *bacteria Acinetobacter calcoaceticus lwoffi* (33), *Bacillus subtilis* (34), and from *E. coli* (35). In *A. vinelandii* the *rhdA* gene was shown to encode a rhodanese (RhdA) (32). RhdA displayed some sequence similarity to bovine rhodanese (22% identical residues) including the conservation of the active site cysteine. However, the other residues in the active site of RhdA displayed extensive substitutions with respect to the vertebrate enzymes.

In *E. coli* at least two distinct rhodaneses were described by Volini et al (35). One called the accessible rhodanese, due to its release by freeze-thaw treatment, was purified and characterized extensively. Although the catalytic properties of this *E. coli* enzyme were similar to bovine rhodanese, its molecular size of 14 kDa, indicated that it is a single domain rhodanese. However, the *E. coli* gene encoding the rhodanese and the amino acid sequence was not determined at that time. Recently, it was shown that the *glpE* gene of the *glp* regulon of *E. coli* encodes a 12 kDa rhodanese (6). Although the overall sequence identity between GlpE and mammalian rhodaneses was low (17%), the active site cysteine and the secondary motifs were conserved in GlpE. Kinetic analysis of purified GlpE showed that the enzyme follows a double displacement mechanism similar to other characterized rhodaneses. The crystal structure of GlpE was determined, which revealed

that GlpE displayed three-dimensional folds identical to the Rhobov and RhdA enzymes (7;36). The physiological function of GlpE is not known. Thioredoxin-1 was found to serve as a sulfur acceptor substrate for GlpE which indicated that thioredoxin 1 and related dithiol proteins could serve as physiological substrates for GlpE (6).

### 1.2.2. Mercaptopyruvate sulfurtransferase (MST, E.C 2.8.1.2)

Mercaptopyruvate sulfurtransferase belonging to the sulfurtransferase family of enzymes uses 3-mercaptopyruvate as the sulfur donor instead of thiosulfate and catalyzes the transfer of sulfur to a variety of thiophiles including cyanide, thiols, sulfite and sulfinate (37;38).

$$HSCH_2COCOO^- + CN^- \longleftrightarrow SCN^- + CH_3COCOO^-$$

or

$$HSCH_2COCOO^- + RSH \longleftrightarrow RSSH + CH_3COCOO^-$$

MST was first discovered in rat liver about 50 years ago (39;40), but compared to rhodanese the enzyme was not characterized extensively due to its instability. The enzyme is widely distributed in prokaryotes and eukaryotes and located mainly in the cytosol, although the enzyme was also detected in the mitochondria (41). The rat liver MST was purified to near homogeneity (42) and a recombinant form of the enzyme was expressed in *E. coli* and later characterized (10). Amino acid sequence of MST revealed 60% identity to rat liver rhodanese, with a striking similarity around the active site (10). An active site cysteine ($Cys^{246}$ in MST) and an arginine residue ($Arg^{185}$ in MST) in rhodaneses are conserved in MST. However, two other active site residues in rhodaneses

(Arg$^{247}$ and Lys$^{248}$) are replaced by Gly and Ser in MST. Substitution of the active site Arg and Lys residues of rhodaneses by Gly and Ser respectively, caused a decrease in rhodanese activity with simultaneous increase in MST activity (42). In another study, MST was shown to be partly converted to a rhodanese by replacement of Gly$^{248}$ and Ser$^{249}$ in the active site by the rhodanese residues (Arg and Lys) (10). These results showed that MST and rhodaneses are interconvertable and the difference in the ratio of their activities is caused by specific residues in the active site (42).

MSTs were also identified in plants. Two cDNA clones from *A. thaliana* were islolated and characterized (43;44). Both proteins preferred 3-mercaptopyruvate to thiosulfate as substrate and one was located in the mitochondria while the other was in the cytosol.

Although MST was isolated and characterized from *E. coli* a long time ago, the gene coding for this enzyme was unknown (45). Recently, the *E. coli sseA* gene was identified and the corresponding protein was shown to have MST activity (11;12). SseA is the first prokaryotic MST to be identified and characterized in detail. The active site motif in SseA (CSGVTA) is identical to those found in eukaryotic MSTs suggesting this active site loop confers specificity for 3-mercaptopyruvate over thiosulfate as substrate (11). In fact the interaction of SseA with thiosulfate was shown to be unfavorable.

## 1.3. Proposed physiological roles of sulfurtransferases

Although sulfurtransferases from different organisms have been characterized in detail their physiological functions remain unknown. Some of the proposed functions include cyanide detoxification, biosynthesis of sulfur-containing cofactors, mobilization

of sulfur for biosynthesis or repair of Fe-S clusters, biosynthesis of thionucleosides, selenium metabolism, and different aspects of sulfur metabolism.

### 1.3.1. Biosynthesis of sulfur containing cofactors

Sulfur containing cofactors, namely thiamin, biotin, molybdopterin and lipoic acid, are essential components in living organisms that play key roles in various enzyme catalyzed reactions. The basic pathways for the biosynthesis of these cofactors have been described to some extent; however the steps or the specific mechanism for incorporation of sulfur into some of these cofactors is not completely understood. The presence of a rhodanese domain at the C-terminus of *E. coli* ThiI, an enzyme required for thiamin and thionucleoside synthesis, and MoeB, a molybdopterin synthase sulfurase from bacteria, fungi, plant and animal indicates that rhodaneses might be involved in biosynthesis of these cofactors.

Thiamin or vitamin B1 (FIG. 1.3.1) is a water-soluble B-complex vitamin, which is an essential component of human diet. Thiamin deficiency causes beriberi, a disease that affects cardiovascular, nervous, muscular and gastrointestinal systems. Thiamin is the precursor of the coenzyme thiamin pyrophosphate that serves as a cofactor of important enzymes of carbohydrate metabolism including α-keto acid decarboxylase, α-keto acid dehydrogenase, transketolase and acetolactate synthase (46;47) . Thiamin biosynthesis involves the separate synthesis of the thiazole and the pyrimidine ring, which are coupled together to form thiamin (48). The sulfur-containing thiazole ring is derived from tyrosine, cysteine, and deoxy-D-xylulose-phosphate (47;48). In *E. coli* at least six gene products (ThiFSGH, ThiI and IscS) are involved in biosynthesis of the thiazole moiety of thiamin. First, ThiF catalyzes adenylation of the C-terminal glycine of

ThiS to form ThiS-COAMP. The acyl adenylate intermediate is subsequently converted into ThiS thiocarboxylate (ThiS-COSH) by the action of IscS and ThiI with sulfur being derived from cysteine. The ThiS-COSH serves as the immediate sulfur donor in thiazole assembly (47-49). ThiI from *E. coli* and some other organisms have a rhodanese domain comprised of ~100 residues at the C-terminus of the protein. ThiI was shown to act as a sulfurtransferase for transferring sulfur from IscS to ThiS and to uridine of tRNAs (17;50;51). IscS is a cysteine desulfurase that initiates the mobilization of sulfur from cysteine. In the database Clusters of Orthologous Groups (52) of proteins there are 11 ThiI orthologs. Many of the ThiI orthologs do not have a rhodanese domain fused to the C-terminus of the protein. These ThiI proteins may employ a stand-alone rhodanese in the biosynthesis of thiamin and 4-thiouridine in those organisms.

The mechanism of sulfur incorporation into molybdopterin (FIG. 1.3.1) is similar to that of the thiazole ring of thiamin. Molybdopterin is a tricyclic pyranopterin that has a unique dithiolene group for binding molybdenum to form the molybdenum cofacor (MoCo) (53). The molybdenum cofactor is found in the catalytic active center of all molybdoenzymes except nitrogenase. The MoCo biosynthetic pathway involves three major steps: the conversion of guanine nucleotide to precursor Z, the incorporation of the dithiolene moiety in precursor Z to form molybdopterin and the ligation of the molybdenum to the dithiolene to form MoCo (53-55). MPT synthase, a heterotetrameric enzyme composed of two small (MoaD) and two large subunits (MoaE) catalyzes the transfer of sulfur to precursor Z for formation of MPT (53;56). MoeB, an MPT synthase sulfurase catalyzes the formation of a thiocarboxylate at the C-terminal Gly of activated MoaD and this thiocarboxylate serves as the immediate sulfur donor for MPT synthesis

(53;57). MoeB shares sequence similarity to ThiF while MoaD and ThiS share 29% sequence identity (56). It is known that cysteine is the ultimate source of sulfur, and IscS and its homologs, CSD and CsdB are capable of mobilizing sulfur from L-cysteine to precursor Z for synthesis of MPT *in vitro* with CSD having the highest catalytic activity (55). The MoeB homologs of mycobacterium, plant, fungi and human have a rhodanese domain fused at the C-terminal of the protein. In *Aspergillus nidulan*, a cysteine residue in the C-terminal rhodanese domain of CnxF, the MoeB homolog in this organism, was suggested to be involved in thioester formation between the MPT synthase and the MPT synthase sulfurase (19). The C-terminal rhodanese domain of MOCS3, a human MoeB homolog was also suggested to be involved in sulfur transfer for MPT biosynthesis (58). Since *E. coli* MoeB does not possess a C-terminal rhodanese motif, it is possible that one or more of the rhodaneses in *E. coli* participate in sulfur transfer to MPT synthase for MPT synthesis.

The mechanistic enzymology of sulfur incorporation into biotin and lipoic acid (FIG. 1.3.1) has intrigued researchers for many years. The incorporation of sulfur into biotin and lipoic acid occurs at the final step of their respective pathways, which are catalyzed by the *bioB* and the *lipA* gene products respectively (59). *bioB* encodes biotin synthase (BioB) that inserts the sulfur atom between the unactivated methyl and C-6 methylene carbon atoms of dethiobiotin to form biotin (60). Recent reports indicate that BioB is a Fe-S cluster-containing dimeric enzyme which serves as the immediate sulfur donor for conversion of dethiobiotin into biotin (61;62). The conversion requires biotin synthase, S-adenosylmethionine, cysteine, NADPH, dithiothreitol, $Fe^{2+}$, flavodoxin and flavodoxin reductases (59;63). The type and number of Fe-S cluster in BioB has been a

matter of controversy. Work by Ugulava et al. suggested the presence of two different clusters in biotin synthase, a [4Fe-4S] center that converts dethiobiotin to biotin radical and a [2Fe-2S] cluster that provides the sulfur atom for incorporation into this radical (64). However the process of restoring the depleted Fe-S cluster is not clear, but may involve NifS/IscS proteins. In fact NifS from *A. vinelandii* and bovine rhodanese has been shown to transfer sulfur from cysteine or thiosulfate for restoring the [2Fe-2S] cluster of apoprotein of biotin synthase from *E. coli* (65). BioB has been reported to display cysteine desulfurase activity that can transfer sulfur from free cysteine. The reaction is proposed to proceed via the formation of a cysteine persulfide on BioB that serves as the sulfur donor to dethiobiotin (66). In view of these findings it is suggested that BioB functions through a complex system involving Fe-S cluster, persulfide and free radicals (66).

Like BioB, LipA (lipoate synthase) catalyzes incorporation of sulfur to form the carbon-sulfur bond. In this case two sulfur atoms are inserted into octanoic acid to form lipoic acid (67;68). LipA also displays amino acid sequence similarity to BioB and contains Fe-S clusters (59;69). These findings suggest that LipA follows a similar mechanism to BioB. However, the exact mechanism of sulfur transfer into lipoic acid remains to be elucidated.

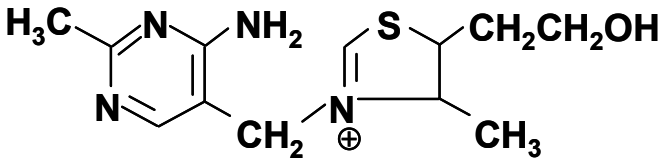


Thiamin

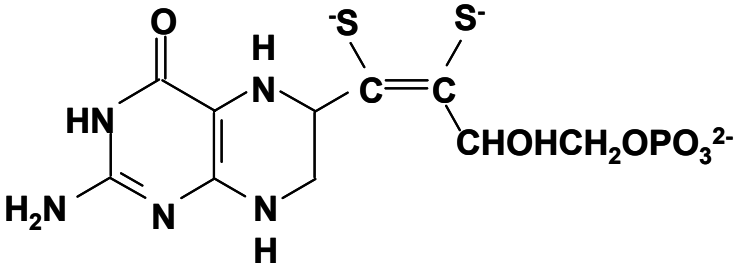


Molybdopterin

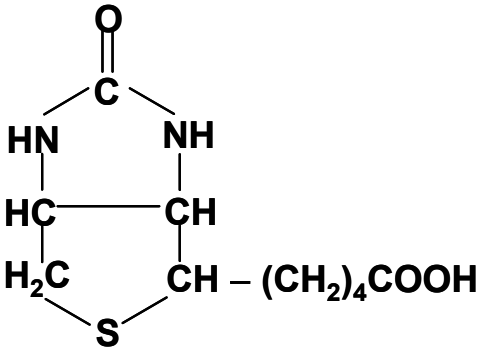


Biotin

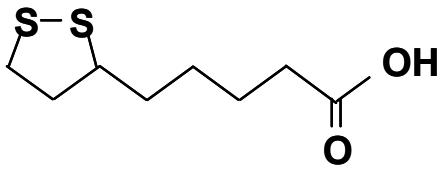


Lipoic Acid

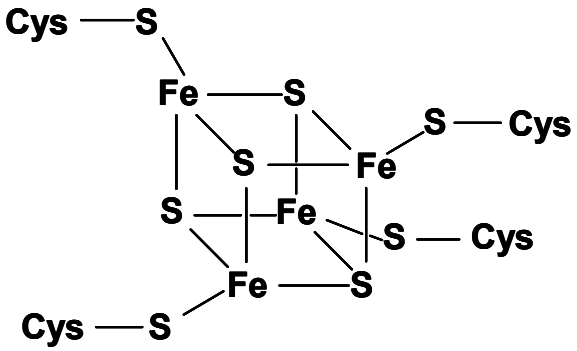


$Fe_4S_4$ cluster

**FIG. 1.3.1. Structure of sulfur-containing cofactors and $Fe_4S_4$ cluster**

## 1.3.2. Thionucleosides in tRNAs

Modified nucleosides are present in tRNAs from all organisms which are derivatives of the four normal nucleosides adenosine (A), guanosine (G), uridine (U) and cytidine (C). At present more than 80 different modified nucleosides have been characterized (70) with the largest diversity of this modification present at the anticodon wobble position 34 of tRNA or immediately 3' adjacent to the anticodon triplet at position 37.

At least 10 different thiolated nucleosides have been identified and characterized in tRNAs from different organisms among which four occur naturally in *E. coli*. These are 4-thiouridine ($s^4U$) (FIG. 1.4.2), 2-thiocytidine ($s^2C$), 5-methylaminomethyl-2-thiouridine ($mnm^5s^2U$) and 6-N-dimethyl-2-methylthioadenosine ($ms^2i^6A$). The biosynthetic pathway for 4-thiouridine in tRNA has been elucidated. It was shown that the modification of uridine at position 8 of tRNA to 4-thiouridine requires the enzymatic activity of IscS (50;71), a cysteine desulfurase and ThiI, a rhodanese involved in thiamin biosynthesis (17). The mechanism of sulfur transfer initially involves the mobilization of sulfur from cysteine to IscS forming IscS-SSH persulfide at the active site cysteine of IscS, which is then transferred to the cysteine residue (Cys-456) at the rhodanese domain of ThiI, forming a ThiI-SSH persulfide. At the final step the modified ThiI protein, in the presence of $Mg^{2+}$ and ATP transfers the sulfur to the tRNA forming a subset of tRNAs with 4-thiouridine ($s^4U$) at position 8 of the tRNAs (16;17;72). Cys-456 at the rhodanese domain of ThiI that aligns with the active site cysteine of rhodaneses was shown to be essential for catalysis since a ThiI variant carrying a Cys to Ala mutation was unable to synthesize 4-thiouridine tRNAs (17;18).

The functional roles of tRNA modification represent the fine-tuning of the many functions of tRNA in protein translation (71). The 4-thiouridine in tRNA has been suggested to serve as a photo-sensor for near-UV radiation (16). In exposure to UV light an intramolecular cross-link occurs between the $s^4U$ at position 8 and the cytidine at position 13 of the tRNA molecule of bacteria, which renders the tRNA ineffective as a substrate for aminoacylation. This results in accumulation of uncharged tRNA in the organism leading to growth arrest (16).

tRNA modification, particularly of the thiolated type, have been found to influence tRNA aminoacylation (73), codon anticodon specificity (74), reading frame maintenance (75) and binding of the tRNA to the ribosome (76). The 2-thiouridine ($s^2U$) present at the anticodon wobble position of $tRNA^{Glu}$ is required for recognition by amino acyl tRNA synthetase (73). The presence of $mnm^5s^2U$ at the same position of $tRNA^{Lys}$ is essential for its interaction with AAA or AAG programmed ribosomes (76). $s^2U$ has been also associated with maintenance of the reading frame, since mutants lacking this modified base show a significant increase in frame shifting, a trait found in many mutants deficient in tRNA modification (75). Recently lack of $s^2U$ in the wobble position of tRNA has been linked to different aspects of human diseases. The MERFF disease (myoclonus epilepsy associated with ragged-red fibers) occurs due to a point mutation in the $tRNA^{Lys}$ gene (A8344G) and this point mutation causes a lack of $s^2U$ in the wobble position of $tRNA^{Lys}$ (77). This anticodon base modification defect present in $tRNA^{Lys}$ disturbs codon antiocodon pairing that results in severely reduced translational efficiency, which could lead to the onset of MERRF.

### 1.3.3. Iron-sulfur clusters

Iron-sulfur (Fe-S) clusters are found in numerous proteins that perform a wide range of functions including electron transfer, catalysis in redox and non-redox reactions and sensing of regulatory processes (78). Various types of Fe-S clusters are present in different proteins; however, the [2Fe-2S] and [4Fe-4S] clusters (FIG. 1.3.1) are most common. The pioneering work of Dean and associates demonstrated the role of two *nif* gene products (NifS and NifU) in the assembly of Fe-S cluster in the nitrogenase protein in *A. vinelandii* (79). NifS is a pyridoxal phosphate dependent cysteine desulfurase that initiates Fe-S cluster formation by producing elemental sulfur from cysteine (80). NifS catalyzes the transfer of the sulfur from cysteine to a conserved cysteine residue in its active site, forming a NifS-bound persulfide intermediate, which serves as the immediate sulfur donor for Fe-S cluster synthesis (81;82). Under reducing conditions, the persulfide sulfur released from NifS combines with an iron source and generates the Fe-S cluster of nitrogenase. The NifU protein is known to serve as a scaffold for the assembly of the newly made Fe-S cluster before incorporating into other apoFe-S proteins (83).

In addition to the Nif machinery other distinct systems, termed Isc (iron-sulfur cluster) and Suf are present in bacteria for assembly of Fe-S clusters. Unlike the Nif proteins that only participate in maturation of nitrogenase, the Isc proteins have a general role in the biosynthesis of Fe-S proteins (84). The Isc gene cluster in several bacteria including *Azotobacter vinelandii*, *E. coli*, *Haemophilus influenza* and *Pseudomonas aeruginosa* is composed of *iscR, iscS, iscU, iscA, hscB, hsc A* and *fdx* (85). Genes homologous to these are found in all bacterial genomes, which indicate that *isc* gene products have crucial roles in all organisms. IscS, the homolog of NifS displays cysteine

desulfurase activity and follows a similar mechanism for transferring sulfur from cysteine to its target sites. The IscU protein has similarity to the N-terminal domain of NifU and it also serves as a scaffold for intermediates during Fe-S cluster assembly. The IscA protein and its Nif counterpart are proposed to be alternate scaffolds for Fe-S cluster biosynthesis (86). In addition to Fe-S cluster biosynthesis the IscS protein has a more global role. It has been shown to provide sulfur for the biosynthesis of sulfur-containing cofactors thiamin, molybdopterin and thionucleosides (50;71;87).

Two other IscS homologs, CSD (CsdA) and CsdB are also present in *E. coli* that have cysteine desulfurase activity. However CSD prefers L-cysteine sulfinic acid as substrate (88) and CsdB has greater specificity for selenocysteine over cysteine (89). CsdB, also known as SufS, is part of the Suf system in *E. coli*, which is the third bacterial system for assembly of Fe-S clusters (90). The components of this system are encoded by an unassigned operon (*sufABCDSE*) and are suggested to participate in an Isc independent minor pathway for the assembly of Fe-S clusters (90).

### 1.3.4. Rhodaneses in selenium metabolism

Rhodaneses have also been implicated to play a role in selenium metabolism. These enzymes are known to occur as a sulfur-free form and a persulfide-containing form, where the sulfur is carried on the active site cysteine that functions to deliver sulfur to the acceptor substrates. Recently, Stadtman and her group demonstrated that persulfide free bovine rhodanese could react with selenite ($SeO_3^{2-}$) in the presence of reduced glutathione to form a selenium-substituted rhodanese (E-Se) (91). This selenium-bound rhodanese was able to serve as a selenium donor to selenophosphate

synthetase (SelD) for *in vitro* synthesis of selenophosphate, which is the selenium precursor for selenocysteine of proteins and seleno-tRNAs.

## 1.4. Selenium in protein and tRNA

Selenium is an essential trace mineral that has fundamental importance to human health. Selenium is present in selenoproteins and seleno-tRNAs of bacteria (92;93), archaea (94;95), plants (96) and mammals (97;98). In selenium-dependent enzymes selenium generally occurs as a selenocysteine residue at the active site, that functions as a redox center. Although the presence of several redox type selenoproteins in prokaryotes has been known for several years, until recently glutathione peroxidase was the only known selenoprotein from eukaryotes (99). This enzyme catalyzes the reduction of peroxides to harmless products and thus protects the cells from oxidative damage caused by reactive oxygen species. The subsequent discovery of other eukaryotic selenocysteine-containing enzymes like tetraiodothyronine 5'-deiodinase that converts thyroxin to thyroid hormone (92) and thioredoxin reductase that participates in reduction of ribonucleotides to deoxyribonucleotides needed for DNA synthesis (100), provides examples of an even more ubiquitous role of selenium in growth and developmental processes of different animals. Recently several other mammalian seleno-proteins have been discovered that are assumed to serve fundamental physiological functions.

Selenium deficiency has been identified in parts of the world where the selenium content of soil is low. Two human selenium deficiency diseases, Keshan disease, an endemic cardiomyopathy and Kashin-Beck disease, a deforming arthritis were first identified in areas of China where the soil is extremely low in selenium (101). However,

both these conditions are believed to have other causative factors. Current research indicates the importance of selenium to other health conditions particularly in relation to immune response and cancer prevention, which are also not exclusively linked to the enzymic function of selenium-containing compounds in the cell.

### 1.4.1. Incorporation of selenocysteine into protein

The basic pathway for incorporation of selenium as selenocysteine into protein has been characterized in detail. In 1986 the parallel discoveries of August Bock and his collaborators in Munchen and by P. R. Harrison and his collaborators in Glasgow showed that the genes encoding the selenoproteins bacterial formate dehydrogenase and bovine glutathione peroxidase contain an in-frame TGA codon within their coding sequence that directs the incorporation of selenocysteine into the proteins (102;103). The biosynthesis of selenocysteine and its incorporation into proteins require the function of at least four gene products (SelA, B, C and D) (104;105) (FIG. 1.4.1). *selC* encodes for the tRNA specific for selenocysteine that carries the anticodon UCA complementary to UGA. $tRNA^{Sec}$ is charged with L-serine by the action of seryl-tRNA synthetase (SerS) and this serves as the adapter at which the seryl moiety is converted into the selenocysteine derivative. This conversion is catalyzed by selenocysteine synthase (SelA) with the aid of monoselenophosphate serving as the selenium substrate. Monoselenophosphate is synthesized from selenide and ATP by the action of selenophosphate synthetase, the product of *selD*. At the final step, a specialized translation factor, SelB similar to the elongation factor EF-TU, interacts with guanine nucleotide, Sec-$tRNA^{Sec}$ and the SECIS element in mRNA and directs the insertion of selenocysteine at UGA (105). SECIS

element is a secondary stem loop structure in selenoprotein mRNAs positioned immediately downstream of the UGA codon of selenocysteine that binds SelB, GTP Sec-tRNA$^{Sec}$ ternary complex and determines the position of selenocysteine incorporation in the nascent polypeptide chain.

In *E. coli*, there are three genes coding for selenium-containing formate dehydrogenases, which are expressed constitutively or under anaerobic conditions (102;106;107). Other bacterial selenocysteine-containing proteins include glycine reductase from several species of *Clostridium* and formate dehydrogeanse from *Salmonella* and *Clostridium* (99). Selenium-dependent formate dehydrogenase and hydrogenase are also present in the archaeon, *Methanococcus* (94).

Nicotinic acid hydroxylase (108), xanthine dehydrogenase and purine hydroxylase (109) are examples of selenoproteins detected in certain anaerobic bacteria that do not contain selenocysteine. In these enzymes selenium is present in a labile cofactor. Selenium is also present as selenomethionine in numerous proteins from prokaryotic and eukarotic sources where it occurs as a random substitute for methionine (110).

## 1.4.2. Selenophosphate synthesis

Selenophosphate is the highly reactive, reduced selenium compound that serves as the selenium donor for selenocysteine-containing enzymes (111) and seleno-tRNAs (95). Selenophosphate synthetases (SelD) from *E. coli* (112) and *Haemophilus influenzae* (113) have been characterized that catalyze the synthesis of monoselenophosphate from selenide and ATP *in vitro*, in the presence of ATP and high levels of free selenide (1-5

mM) (112). However the $K_m$ value for selenide (20 μM) was far above the optimal concentration (0.1-1 μM) needed for growth of bacterial species and mammalian cultured cells, suggesting that there may be a separate mechanism for providing adequate amounts of selenide to selenophosphate synthetase. In fact, levels of 10 μM are toxic for growth of bacterial species.

NifS from *A. vinelandii* is a pyridoxal phosphate containing enzyme that catalyzes the removal of sulfur from L-cysteine to produce alanine (80). NifS is also able to catalyze the removal of selenium from L-selenocysteine (82). Recently it was shown that replacement of selenide by NifS and L-selenocysteine in an *in vitro* selenophosphate synthetase assay resulted in an increased rate of selenophosphate production (114). This result indicated that NifS and L-selenocysteine serve as better substrates for selenophosphate synthetase than free selenide. It was also demonstrated *in vitro* that the three NifS homologs in *E. coli*, IscS, CSD and CsdB can effectively mobilize selenium from free selenocysteine to selenophosphate synthetase (115). Since CsdB showed greater specificity for selenocysteine than the other NifS homologs it was suggested that CsdB may be the *E. coli* counter part of mammalian selenocysteine lyase that could function as a selenide delivery protein to selenophosphate synthetase for formation of selenophosphate (89).

### 1.4.3. Selenium incorporation into tRNA

Selenium is also present in tRNA species from bacteria (93), archaea (95), plant (96), and mammals (98;116). Several bacterial tRNAs contain selenium as a 2-selenouridine residue in the wobble position 34 of the anticodons of these tRNAs. Isoaccepting species of lysine, glutamate and glutamine tRNAs are the most abundant

seleno-tRNAs (117;118) that contain 2-selenouridine residue in the form of 5-methylaminomethyl-2-selenouridine (FIG. 1.4.2) (119-121). In *E. coli*, lysine, glutamate and glutamine isoacceptor tRNAs account for about 13% of total tRNA population (122), a fraction of which modify into seleno-tRNAs. The pathway for incorporation of selenium into tRNA has been partly characterized (FIG. 1.4.1). The uridine at the wobble position of the anticodon is thiolated to form 2-thiouridine, catalyzed by MnmA and IscS (87;123). However the exact mechanism of this reaction is not clear. The 2-thiouridine at this position is further modified to 5-methylaminomethyl-2-thiouridine ($mnm^5s^2U$) by the product of *mnmE* (124). Although it is known that 2-thiouridine tRNA is the precursor to 2-selenouridine tRNA and that selenophosphate is the selenium donor substrate, the exact mechanism of selenium incorporation has not been defined. The requirement of selenophosphate as a substrate for seleno-tRNA synthesis was demonstrated by the study of *selD* mutants in *E. coli* and *Salmonella typhimurium* that were unable to produce seleno-tRNAs *in vivo* (125;126). A partially purified enzyme from a *selD* mutant of *S. typhimurium* catalyzed the conversion 2-thiouridine in the added tRNA substrate into 2-selenouridine in the presence of SelD, selenide and ATP (127). The results of the study showed that selenophosphate synthetase (SelD), selenide and ATP were required for selenophosphate synthesis, which served as the selenium donor for the enzyme that converts 5-methylaminomethyl-2-thiouridine to 5-methylaminomethyl-2-selenouridine. The enzyme was termed 2-selenouridine synthase as it did not require additional ATP for the reaction. Bulk thio-tRNA preparations from *E. coli* and wild type *S. typhimurium* served equally well as the tRNA substrate for the selenium incorporation reaction catalyzed by the partially purified *Salmonella* enzyme.

However bulk tRNA isolated from the *E. coli mnmA* mutant strain that lacks 2-thiouridine, did not serve as a substrate. The gene coding for the 2-selenouridine synthase and the properties of the enzyme were not determined.

The significance of selenium-modified tRNAs is not clear. In *Clostridium sticklandii* selenium-modified $tRNA^{Glu}$ was proposed to be essential for aminoacylation with glutamate (117). Later it was shown (128) that when $mnm^5s^2U$ was present in the anticodon of $tRNA^{Glu}$ the recognition of GAA was four fold greater than GAG. However substitution of the sulfur with selenium in $mnm^5s^2U$ forming $mnm^5se^2U$ eliminated the preference for GAA. These results indicated that selenium-modified tRNAs are probably involved in fine tuning processes and not necessarily critical requirements for proper cell functions.

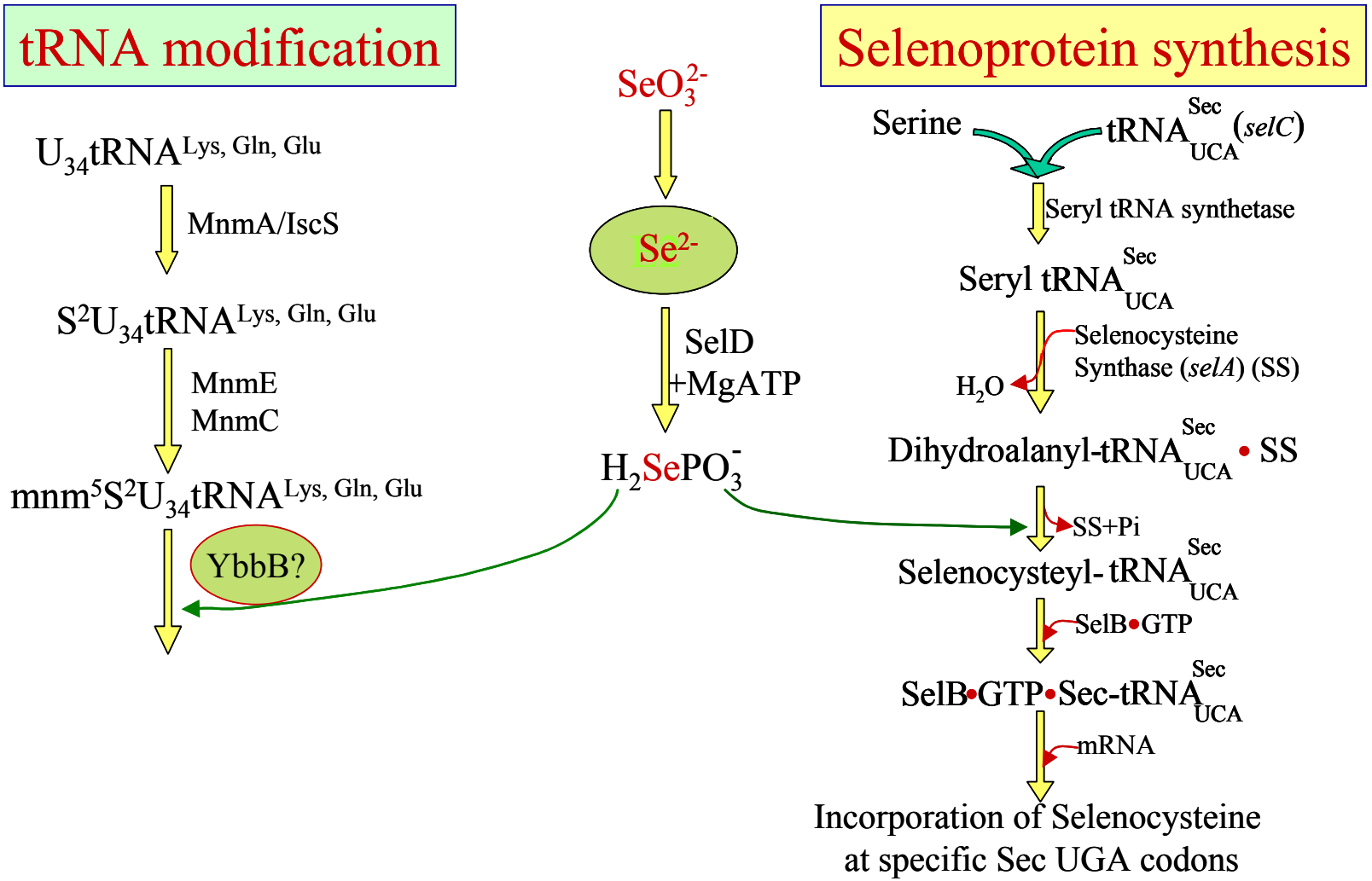


**FIG. 1.4.1. Pathway for selenium incorporation into protein and tRNA**

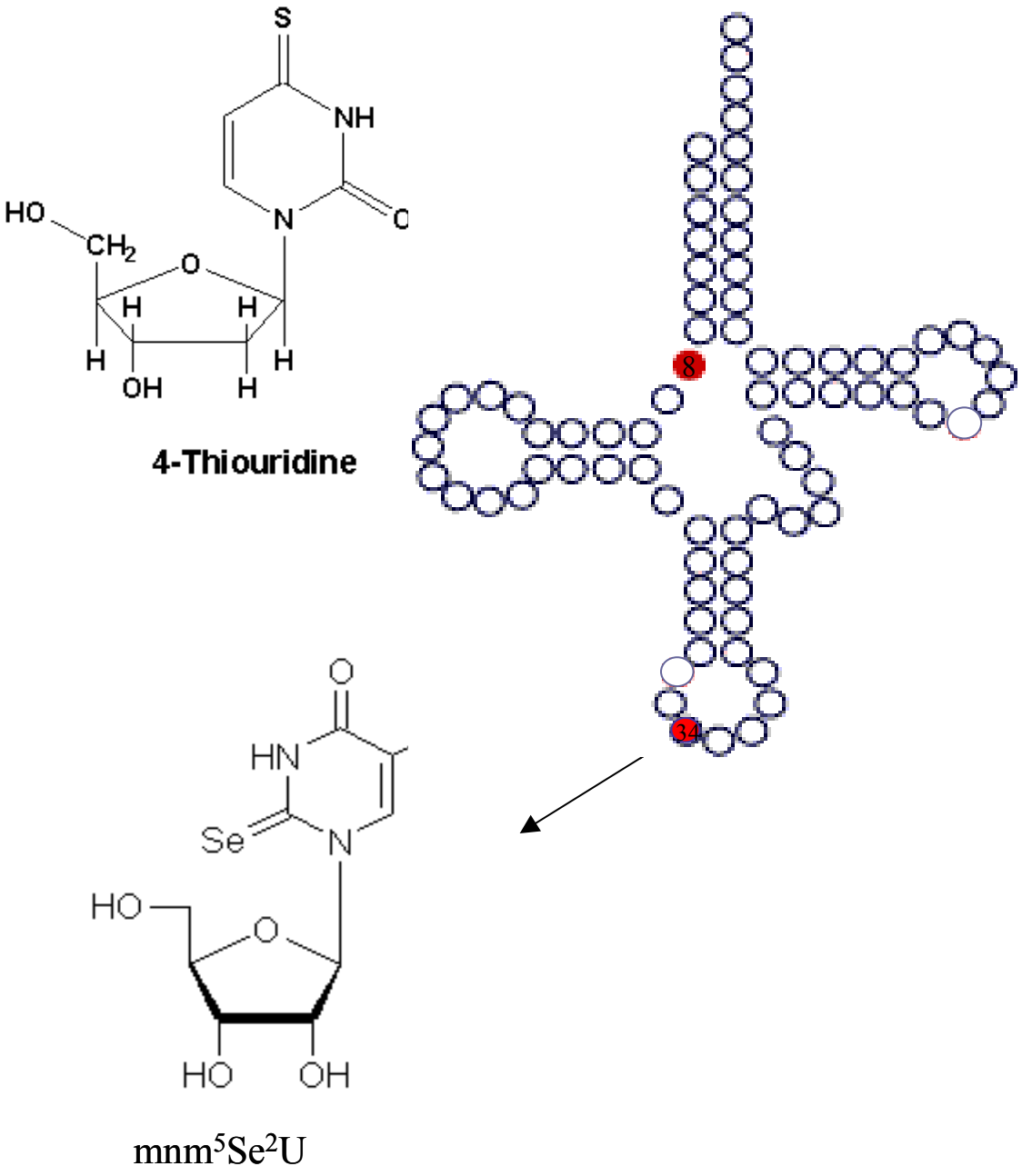


**FIG. 1.4.2. Two common locations for tRNA modification**
2-thiouridine and 5-methylaminomethyl-2-thiouridine are also located at the wobble position 34 of tRNA.

## 1.5. Present Work

In *E. coli*, nine proteins containing the rhodanese homology domain were identified by BLAST search (FIG. 1.5.1). Among them GlpE (6), PspE (129;130) and ThiI (17) were found to have rhodanese activity and one of them called SseA had mercaptopyruvate sulfurtransferase activity (11;12).

GlpE and PspE have been purified and characterized in detail. GlpE is encoded by the *glpE* gene, which is a member of the *glp* regulon of *E. coli*. PspE, the smallest known rhodanese is encoded by the *pspE* gene that is present in the phage shock protein operon (131;132). Both GlpE and PspE are single-domain rhodaneses that are located in the cytoplasm and periplasm respectively (6;130). The purified enzymes exist as a mixture of sulfur-free and persulfide-containing forms. During catalysis, a cysteine persulfide is formed at the active site cysteine of GlpE and PspE that serves as the sulfur donor substrate to the acceptor molecule. Like bovine Rhodanese, both GlpE and PspE were shown to display a double displacement mechanism. Anion inhibition studies showed that PspE, like the bovine rhodanese was inhibited by most anions while GlpE showed little inhibition by anions.

The other rhodanese, ThiI is a multidomain protein that has an N-terminal THUMP domain, a central P-loop ATPase domain and a C-terminal rhodanese domain. The THUMP domain has sequence similarity to proteins involved in RNA modification and is suggested to be involved in RNA binding (133). The ATPase domain and the rhodanese domain catalyze the biosynthesis of 4-thiouridine. ThiI has also been shown to be involved in the biosynthesis of the thiazole ring of thiamin.

The present work involves the identification and characterization of two other proteins containing the rhodanese homology domain in *E. coli*: YgaP and YbbB. YgaP is a single domain rhodanese with a C-terminal extension containing hydrophobic residues. Computer algorithms indicated the presence of two transmembrane regions at the C-terminus of YgaP, which suggested that the protein might be associated with the membrane. YgaP homologs with an amino-terminal rhodanese domain and a carboxy-terminal transmembrane domain are present in a wide variety of bacteria including *Caulobacter crescentus*, *Synechocystis sp PCC 6803*, *Pseudomonas aeruginosa*, *Pasteurella multicoda* and also in *Shigella flexneri* and *Salmonella typhimurium*. A his-tag variant of YgaP was purified by metal affinity chromatography and the catalytic properties of the enzyme were determined. A strain with *ygaP* gene deletion was constructed and used as a tool to study relevance of YgaP in the organism.

YbbB, the other rhodanese-like protein has a rhodanese domain at the N-terminus and a P-loop motif in the C-terminal domain of the protein. The genome context of *ybbB* in several Gram-negative bacteria including *P. aeruginosa* and *A. vinelandii* (FIG. 1.5.2) has indicated that *ybbB* is located in a putative operon downstream of *selD* that encodes selenophosphate synthetase. This discovery suggested that YbbB might be involved in some aspects of selenium metabolism. In the present study, a strain with a chromosomal *ybbB* gene deletion was constructed to investigate the role of YbbB in selenium metabolism.

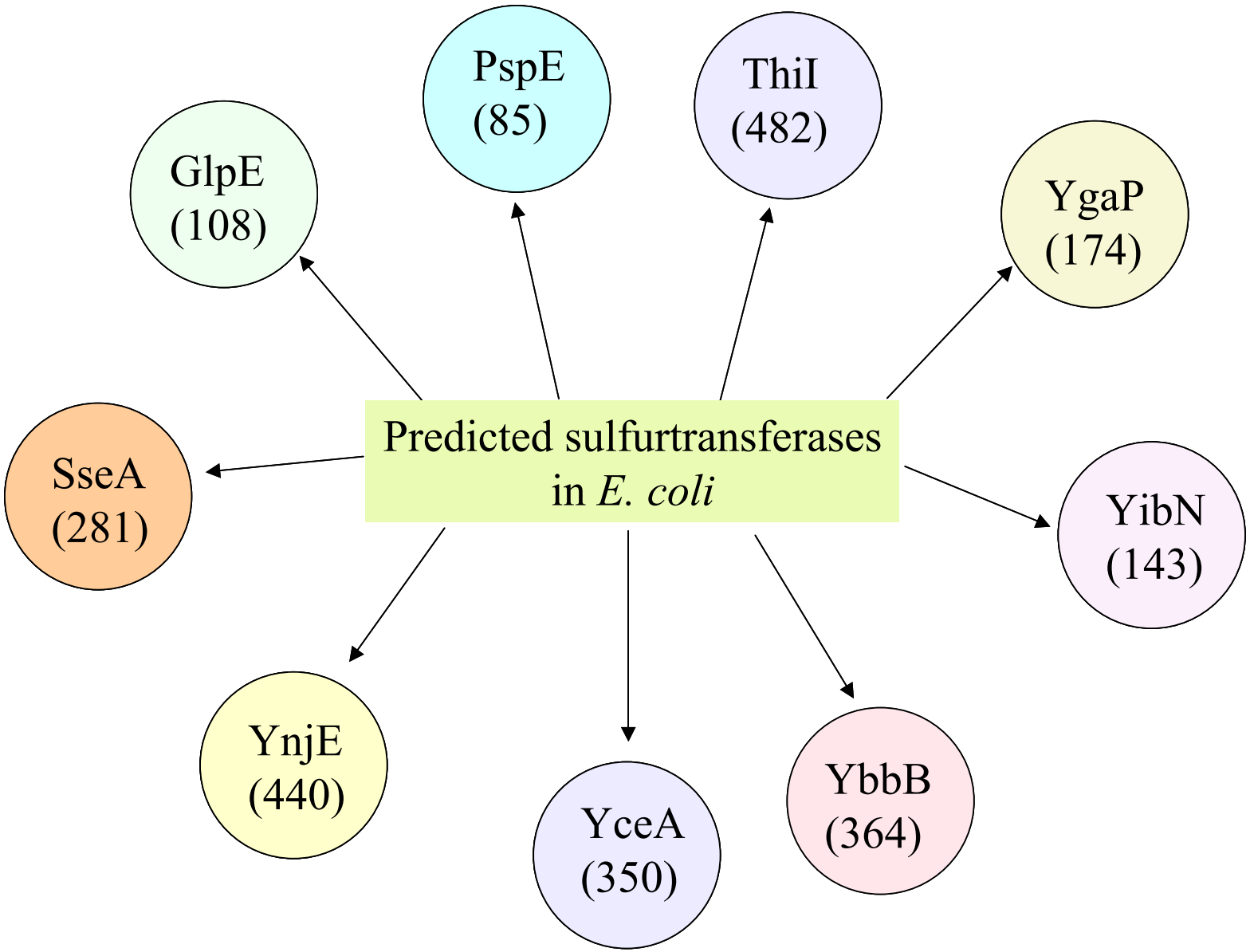


**FIG. 1.5.1. Proteins containing rhodanese homology domain in *E. coli***

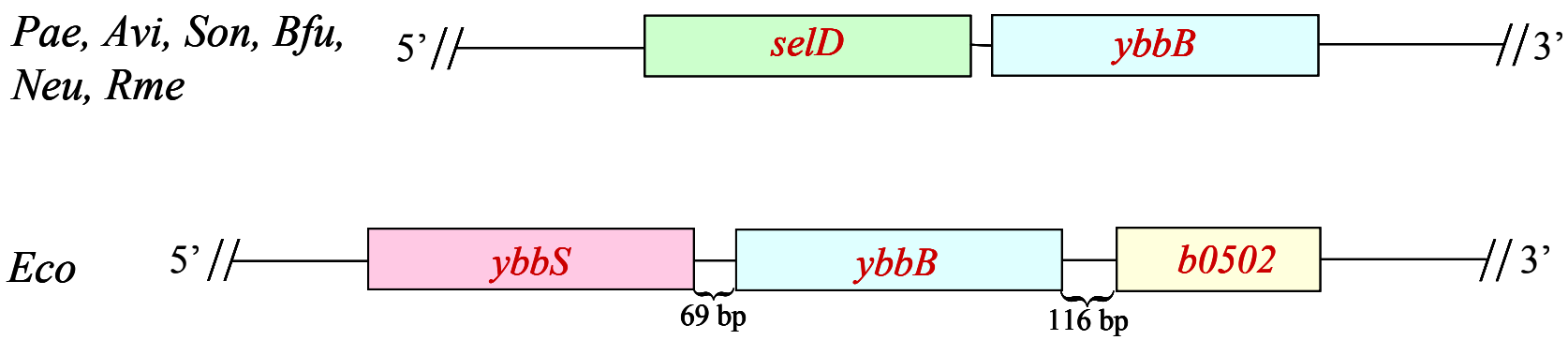


**FIG. 1.5.2. Genome context of *ybbB***

Genome context of *ybbB* in *E. coli* (*Eco*) and other gram-negative bacteria. *Pae, Pseudomonas aeruginosa*; *Avi Azotobacter vinelandii*; *Son*, *Shewanella oneidensis*; *Bfu*, *Burkholderia fungorium*; *Neu*, *Nitrosomonas europaea*; *Rme*, *Ralstonia mettalidurans*. In *Magnetococcus* the *selD-ybbB* gene order is reversed. In *E. coli* the *ybbS* gene is upstream of *ybbB* and predicted to encode a putative transcriptional regulator of the LysR family. *b0502* is downstream of *ybbB* and encodes a protein of unknown function.

# Chapter Two

## YgaP, a novel membrane associated rhodanese from *Escherichia coli*

## 2.1. Introduction

Sulfurtransferases are widely distributed enzymes that carry out sulfur trafficking in biological systems. Rhodaneses (thiosulfate:cyanide sulfurtransferase, EC 2.8.1.1) are one of the earliest and well characterized sulfurtransferases that catalyze the transfer of sulfane sulfur from thiosulfate to cyanide forming thiocyanate and sulfite.

$$SSO_3^{2-} + CN^- \rightarrow SCN^- + SO_3^{2-}$$

In *E. coli* at least two distinct rhodaneses were described by Volini et al. (35;134). One of them, known as the accessible rhodanese, was released from the cell by freeze-thaw treatment. The other was called the cytoplasmic rhodanese as the enzyme activity was found only after disruption of the cells by sonication. However, the genes for these two rhodaneses were not mapped nor were the sequences for the proteins determined. Recently, the GlpE rhodanese of *E. coli* was identified and characterized in detail (6). GlpE was found to be a cytoplasmic enzyme encoded by the *glpE* gene belonging to the *glp* regulon. A strain having a chromosomal *glpE* deletion did not show a significant

decrease in rhodanese activity indicating the presence of other rhodaneses. A PSI BLAST search (135) using GlpE as the query identified eight additional proteins in *E. coli* containing rhodanese homology domains. All of these proteins displayed sequence similarity to GlpE and to the well-characterized bovine liver rhodanese. Proteins having rhodanese homology domains are found in most organisms and consist of conserved secondary and active site motifs found in all rhodaneses identified so far.

Besides GlpE, three other proteins with the rhodanese homology domain were identified as sulfurtransferases in *E. coli*. They are: PspE, a small periplasmic rhodanese (129;130); ThiI, a cytoplasmic enzyme needed for thiazole and 4-thiouridine synthesis (17) and SseA (11;12), a mercaptopyruvate sulfurtransferase (MST) also found in the cytoplasm. Mercaptopyruvate sulfurtransferases (MST) catalyze the transfer of sulfur from 3-mercaptopyruvate to cyanide forming thiocyanate and pyruvate.

$$HSCH_2COCOO^- + CN^- \longleftrightarrow SCN^- + CH_3COCOO^-$$

This work describes YgaP, one of the proteins of *E. coli* with the rhodanese homology domain. YgaP has sequence similarity to other rhodaneses including GlpE and the second domain of bovine rhodanese. YgaP is unique in having an N-terminal rhodanese domain fused to a predicted transmembrane domain at the C-terminus. In this work we show that YgaP is a rhodanese that has a unique cellular location different from other known rhodaneses. Subcellular fractionation and sucrose density layer ultracentrifugation were used to determine the cellular location of YgaP. A polyhistidine-tagged variant of YgaP was subsequently overexpressed and purified.

Purified YgaP-$His_6$ was characterized and the catalytic properties were compared to other rhodaneses.

Although rhodaneses from *E. coli* and other organisms have been purified and characterized, their physiological functions are largely still undefined. Some proposed roles include cyanide detoxification (136), mobilization of sulfur for biosynthesis or repair of Fe-S clusters (137-139) and mobilization of sulfur for biosynthesis of sulfur containing cofactors like thiamin, biotin, lipoic acid or molybdopterin. ThiI is one of the *E. coli* rhodaneses having a defined physiological function. It is involved in the biosynthesis of the thiazole ring of thiamin and $S^4U$ in tRNA (17;18;140). The physiological functions of the other *E. coli* rhodaneses remain unknown (with the exception of YbbB; see chapter 3). As an approach to define the physiological role of YgaP, a strain having a *ygaP* gene deletion was constructed and studied under various growth conditions. Since *E. coli* has several rhodanese paralogs, strains with multiple sulfurtranseferase gene disruptions, including Δ*ygaP*, were also constructed. These strains were studied under various conditions in attempts to identify the physiological roles for rhodaneses.

# 2.2.Materials and Methods

## 2.2.1. Bacterial strains and plasmids.

The bacterial strains and plasmids used or constructed in this study are listed in Table 2.2.1 and 2.2.2, respectively. All strains are K-12 derivatives except for BL21(DE3) and BL21*(DE3) which are derived from *E. coli* B. DH5αZ1 (141) was

used as a host during plasmid construction. BL21(DE3)(plysS) harboring pFA22 and BL21*(DE3) harboring pFA24 were used for overexpression of YgaP and YgaP-$His_6$ respectively. To construct the YgaP expression plasmid the gene for *ygaP* was amplified by PCR with primers YgaP1 and YgaP-R2 (Table 2.2.3). After cleavage with *Nde*I and *Hin*dIII the PCR product was cloned into the same sites of pT7-7 (142) yielding pFA22. To construct the plasmid vector pFA24 for overexpression and purification of YgaP-$His_6$ the gene for *ygaP* was amplified with primers YgaP1 and YgaPhisR (Table 2.2.3). The *Nde*I - *Sal*I cleaved PCR fragment was cloned into pGZ117 (143) between the T7 promoter and the region encoding a $His_6$ affinity tag and thrombin cleavage site. Replacement of the stop codon of *ygaP* with *Sal*I and subsequent cloning resulted in expression of YgaP-$His_6$ with C-terminal amino acid sequence RA | VDLVPR*$GSH_6$ where the residues to the right of the vertical line are the additional residues at the C-terminal end of YgaP; the asterisk indicates the thrombin cleavage site.

## 2.2.2. Growth media and conditions

Cultures were grown in Luria-Bertani (LB) (144) broth supplemented with the appropriate antibiotic (200 μg/ml ampicillin, 25 μg/ml kanamycin or 10 μg/ml tetracycline). All cultures were grown at 37$^{o}$C unless indicated otherwise. Overexpression of YgaP or YgaP-$His_6$ was achieved by growing BL21(DE3)(pLysS) (pFA22) or BL21*(DE3)(pFA24) respectively in 500 ml LB to an $OD_{600}$ of 0.6 - 0.8 and inducing with 0.5 mM isopropylthio-β-D-galactopyranoside (IPTG). Cultures were grown for 2.5 – 3 hours after induction and then harvested by centrifugation at 1000 × g for 5 minutes.

Strain BW25113 was used for creating strains with *ygaP* or multiple rhodanese gene deletions. For making competent cells, BW25113 was grown in SOB medium supplemented with ampicillin and 1 mM L-arabinose. The cells were grown at 30$^{o}$C to an $OD_{600}$ of 0.6 and made chemically competent by treating with $MgCl_2$ and $CaCl_2$ (145). The $Km^r$ cassette was excised from the Δ*ygaP*::$Km^r$-disrupted strain by transforming the cells with plasmid pCP20. pCP20 is an $Ap^r$ and $Cm^r$ plasmid that has a temperature sensitive origin of replication and thermal induction of yeast FLP recombinase synthesis (146). The ampicillin resistant transformants were selected at 30$^{o}$C and then colonies were purified on nonselective medium at 43°C. Loss of the $Km^r$ cassette and pCP20 was verified by plating the cells on medium supplemented with kanamycin and ampicillin or chloramphenicol.

To find out whether the *ygaP* mutant or other single and multiple rhodanese mutants were impaired in growth, the mutant strains were grown in minimal medium containing M9 or AB salts supplemented with one or more of the following: 0.2% glucose or 0.4% glycerol, 2 μg/ml thiamin and 0.01 mM $MgSO_4$. For testing thiamin, biotin or lipoic acid auxotrophy the mutant strains were grown in minimal medium with or without the required cofactors.

As an approach to test the ability of the mutants to synthesize molybdopterin, the single and the multiple mutants were grown on LB plates containing 20 mM $NaClO_3$ at 37°C under anaerobic conditions (147). A GasPak Plus anaerobic generator was placed in a closed container to obtain anaerobic conditions.

P1 transduction was done according to the methods described by Silhavy et al. (148). However, after incubation of the cell and lysate mixture for 30 min at 30°C, 10

mM sodium citrate was added to the transduction tubes prior to phenotypic expression and plating.

Table 2.2.1. Bacterial Strains

| Strain | Genotype | Derivation or Reference |
|---|---|---|
| MG1655 | $F^-$ *rph-1 ilvG rfb-50* $\lambda^-$ | (149) |
| TL524 | MG1655 Δ(*lacZYA-argF*)*U169* | (150) |
| BL21(DE3) | $F^-$ *ompT hsdS*$_B$ ($r_B^- m_B^-$) *gal dcm* (*λcIts857 ind1 Sam7 nin5 lacUV5-T7 gene1*) | (151) |
| BL21*(DE3) | BL21(DE3) *rne131* | (152) |
| BW25113 | *lacI*$^q$ *rrnB*$_{T14}$ Δ*lacZ*$_{WJ16}$ *hsdR514* Δ*araBAD*$_{AH33}$ Δ*rhaBAD*$_{LD78}$ | (145) |
| CAG18642 | MG1655 *srlD3131*::Tn*10* $\lambda^-$ *rph-1* | (153) |
| CAG18500 | MG1655 $\lambda^-$, *rph-1*, *thiC39*::Tn*10* | (153) |
| JRG33 | *lipA9*, *lacY1*, Δ*(gpt-proA)62*, *purB15*, *hisG4*(Oc), *gal K2*(Oc), $\lambda^-$, *Rac-O*, *rfbD1*, *mgl-51*, *rpsL35*(strR), *kdgK51*, *xylA5*, *mtl-1*, *thi-1* | (154) |
| R875 | *bioB17*, *lac-3350*, *IN(rrnD-rrnE)1*, $\lambda^-$ | (155) |
| VJS2890 | Δ*thiI*::$Km^r$ | (48) |
| S1247 | *bioA24*, *moaA29, zbh-283*::Tn*10* | (156) |
| FA001 | BW25113 Δ*ygaP*::$Km^r$ | This work |
| FA003 | BW25113 Δ*ygaP*::$Km^r$ *srlD3131*::Tn*10* | P1 (CAG18642) → FA001 Selection for $Tc^r$ |

| Strain | Genotype | Derivation or Reference |
|---|---|---|
| FA005 | TL524 Δ*ygaP*::Km$^r$ *srlD3131*::Tn*10* | P1 (FA003) → TL524 Selection for Km$^r$ |
| FA007 | BW25113 Δ*ygaP*::FRT | FLP-mediated removal of Km$^r$ from FA001[a] |
| FA009 | TL524 Δ*ygaP*::FRT *srlD3131*::Tn*10* | FLP-mediated removal of Km$^r$ from FA005[a] |
| FA012 | TL524 Δ*ygaP*::Km$^r$ | P1 (FA001) → TL524 Selection for Km$^r$ |
| FA013 | TL524 Δ *sseA*::Sp$^r$ Δ*ygaP*::Km$^r$ | P1 (FA001) → PJ1 |
| FA014 | TL524 Δ *sseA*::Sp$^r$ Δ*ynjE* Δ*ygaP*::Km$^r$ | P1 (FA001) → PJ6 |
| PJ1 | TL524 *sseA*::Sp$^r$ | Promjit Jutabha |
| PJ6 | TL524 Δ*ynjE*, *sseA*::Sp$^r$ | Promjit Jutabha |
| FA015 | TL524 Δ *sseA*::Sp$^r$ Δ*ygaP* | FLP-mediated removal of Km$^r$ of FA013[a] |
| FA016 | TL524 Δ *sseA*::Sp$^r$ Δ*ynjE* Δ*ygaP* | FLP-mediated removal of Km$^r$ of FA014[a] |
| FA018 | TL524 Δ *sseA*::Sp$^r$ Δ*ygaP* Δ*glpE*::Km$^r$ | P1(AL1) → FA015 |
| FA021 | TL524 Δ *sseA*::Sp$^r$ Δ*ynjE* Δ*ygaP* Δ*glpE*::Km$^r$ | P1(AL12) → FA016 |
| AL1 | BW25113 Δ*glpE*::Km$^r$ | Jen Brichetti |
| AL12 | BW25113 Δ*glpE*::Km$^r$ *malT*::Tn*10* | Jen Brichetti |

| Strain | Genotype | Derivation or Reference |
|---|---|---|
| FA024 | TL524 Δ *sseA*::Sp$^r$ Δ*ygaP* Δ*glpE* | FLP-mediated removal of Km$^r$ from FA018[a] |
| FA025 | TL524 Δ *sseA*::Sp$^r$ Δ*ynjE* Δ*ygaP* Δ*glpE* | FLP-mediated removal of Km$^r$ from FA021[a] |
| JLD17201 | TL524 Δ*glpE*::Km$^r$ | P1(AL1) → TL524 |
| JLD17204 | TL524 Δ*glpE*::*FRT* | FLP-mediated removal of Km$^r$ from JLD17201[a] |
| JLD17301 | TL524 Δ *sseA*::Sp$^r$ Δ*ygaP* Δ*glpE* Δ*pspE*::Km$^r$ | P1(HC1.1) → FA024 |
| JLD17302 | TL524 Δ *sseA*::Sp$^r$ Δ*ynjE* Δ*ygaP* Δ*glpE* Δ*pspE*::Km$^r$ | P1(HC1.1) → FA025 |
| HC1.1 | BW25113 Δ*pspE*::Km$^r$ | Hui Cheng |
| HC3.1 | BW25113 Δ*pspE*::Km$^r$ | Hui Cheng |
| JLD19901 | TL524 Δ *sseA*::Sp$^r$ Δ*ynjE* Δ*ygaP* Δ*glpE* Δ*pspE* | FLP-mediated removal of Km$^r$ from JLD17302[a] |
| JLD18801 | BW25113 Δ*yceA*::Km$^r$ | Janet Donahue |
| JLD19401 | TL524 Δ*yceA*::Km$^r$ | P1(JLD18801) → TL524 |
| JLD19902 | TL524 Δ *sseA*::Sp$^r$ Δ*ynjE* Δ*ygaP* Δ*glpE* Δ*pspE* Δ*yceA*::Km$^r$ | P1 (JLD19401)→ JLD19901 |
| JLD20502 | TL524 Δ *sseA*::Sp$^r$ Δ*ynjE* Δ*ygaP* Δ*glpE* Δ*pspE* Δ*yceA* | FLP-mediated removal of Km$^r$ of JLD19902[a] |

| Strain | Genotype | Derivation or Reference |
|---|---|---|
| FA026 | BW25113 Δ*ybbB*::Km$^r$ | This work |
| FA029 | BW25113 Δ*ybbB*::Km$^r$ *purK79*::Tn*10* | P1(CAG12171) → FA026 |
| FA036 | TL524 Δ *sseA*::Sp$^r$ Δ*ynjE* Δ*ygaP* Δ*glpE* Δ*pspE* Δ*yceA* Δ*ybbB*::Km$^r$ | P1 (FA029) → JLD20502 |
| FA037 | TL524 Δ*thiC39*::*Tn*10 | P1 (CAG18500) → TL524 |
| JLD26501 | TL524 Δ*thiI*::Km$^r$ | P1 (VJS2890) → TL524 |
| JLD26503 | TL524 *sseA*::Sp$^r$ Δ*ygaP* Δ*ynjE* Δ*glpE*, Δ*pspE* Δ*yceA* Δ*thiI*::Km$^r$ | P1 (VJS2890) → JLD20502 |
| JLD27003 | TL524 *sseA*::Sp$^r$ Δ*ygaP* Δ*ynjE* Δ*glpE*, Δ*pspE* Δ*yceA* Δ*thiI*::Km$^r$ Δ*recA*::Cm$^r$ | P1(BB1600) → JLD26503 |

[a] In each case where FLP-mediated removal of Km$^r$ cassette was employed, an FRT "scar" remains at the site of the deletion (eg, Δ*ygaP*::FRT).

Table 2.2.2. Plasmids

| Plasmid | Description | Derivation or reference |
|---|---|---|
| pBS-KS$^+$ | ColE1 origin Ap$^r$ | Stratagene |
| pCP15 | FRT flanked Km$^r$ cassette in a pUC19 derivative | (146) |
| pCP20 | FLP$^+$ Ap$^r$ Cm$^r$ rep$^{ts}$ | (146) |
| pKD46 | OriR101 Ap$^r$ repA$^{ts}$ *araC*-$P_{araB}$ λRed (γ β exo) | (145) |
| pT7-7 | ColEI origin, Ap$^r$, T7 promoter | (157) |
| pGZ117 | $(His)_6$ linker between *Sal*I and *Hin*dIII of pT7-7 | (143) |
| pFRT-K | Gene disruption plasmid, FRT-flanked Km$^r$ cassette in *Eco*RI/*Hin*dIII of pBS KS$^+$ | This work |
| pFA22 | *ygaP* cloned into *Nde*I and *Hin*dIII of pT7-7 | This work |
| pFA24 | *ygaP* cloned into *Nde*I and *Sal*I of pGZ117 | This work |
| pFA111 | 5' flanking region of *ygaP* cloned into *Not*I/*Bam*HI of pFRTK | This work |
| pFA121 | 3' flanking region of *ygaP* cloned into *Hin*dIII/SalI of pFA111 | This work |

Table 2.2.3. Oligonucleotides

| Name | Oligonucleotide sequence 5'-3'[a] | Restriction site |
|---|---|---|
| YgaP1 | GGAGTCcaTATGGCTTTGACAACC | *Nde*I |
| YgaP-R2 | TGGCAGAAGcTtAATCTCTCGACG | *Hin*dIII |
| YgaPhisR | TCGCgTCgacAGCTCGTTGGTTC | *Sal*I |
| YgaP2 | TCCaGATCTAATTACTGAGGCCGG | *BglII* |
| PNF1 | GCCtAGCGGCcGCAGAATGATGG | *Not*I |
| PNR1 | AAATGGaTccCAAAGCCATAGTGACTCCT | *Bam*HI |
| PCF1 | ATTAAGaaGCTTTGTTGGTGCCGG | *Hind*III |
| PCR1 | AATGgTCGAcAAATTCAGGGTTGTCA | *Sal*I |

[a] Lower case letters indicate base substitutions to create the underlined restriction sites.

### 2.2.3. Solubilization of YgaP

A soluble fraction containing YgaP was prepared from cells obtained from a 500 ml culture. After harvest, the cell pellet was resuspended in 20 ml of 25 mM Tris acetate (pH 8.6) and 1 mM ammonium thiosulfate buffer. The cells were lysed by two passages through a French pressure cell at 12,000 – 16,000 psi. The cell lysate was centrifuged at 6,000 × g for 15 minutes at 4$^{o}$C to remove cell debris and unbroken cells. The clarified supernatant was centrifuged at 100,000 × g for 90 minutes at 4$^{o}$C to separate the membrane fraction as pellet and the cytoplasmic fraction as supernatant. The membrane pellet was resuspended in 2 ml of 25 mM Tris acetate (pH 8.6) and 1 mM ammonium thiosulfate buffer and adjusted to 0.5% Triton X-100 and 2 mM $MgCl_2$. The mixture was kept on ice for one hour and occasionally mixed by gentle vortexing. The membrane fraction was then centrifuged at 100,000 × g for 60 minutes at 4$^{o}$C to obtain the integral membrane proteins in the detergent extract. SDS PAGE and rhodanese assay were performed for the cell free extract, cytoplasmic fraction, membrane fraction and the detergent extract.

### 2.2.4. Isolation of cytoplasmic membrane and outer membrane fractions

The location of YgaP in outer membrane versus inner membrane was determined by sucrose density layer ultracentrifugation essentially as described by Ito et al. (158). Cells obtained from a 500 ml culture of BL21(DE3)(plysS)(pFA22) were suspended in 5 ml of 20% sucrose containing 25 mM Tris acetate (pH 8.6) and 1 mM ammonium thiosulfate. The cell suspension was incubated on ice for 30 minutes with 1/5$^{th}$ volume of

freshly prepared lysozyme (3 mg/ml) in 0.1 M EDTA (pH 7.3). After disruption of the cells by sonication, the solution was diluted with an equal volume of 3 mM EDTA (pH 7.3) and centrifuged at 5000 × g for 30 min to remove cell debris and unbroken cells. The supernatant was collected and 2.5 ml was layered onto 5 ml of 15% sucrose-3 mM EDTA with a cushion of 7 ml of 53% sucrose-3 mM EDTA in the middle and 1 ml of 70% sucrose-3 mM EDTA at the bottom. After centrifugation at 28,000 rpm for 4 hours in a SW28 swinging bucket rotor, the inner and outer membrane fractions were recovered from the upper and lower interface regions respectively. The fractions were analyzed by SDS PAGE and assayed for rhodanese and lactate dehydrogenase activity. All steps were carried out at 0-4$^{o}$C.

### 2.2.5. Purification of YgaP-His$_6$

YgaP-His$_6$ was solubilized from the membrane fraction by detergent extraction as described above. The detergent extract containing approximately 1 mg of total protein was mixed in a 1.5 ml eppendorf tube with 0.2 ml of Talon-$Co^{2+}$ resin (BD Bioscience) previously equilibrated with ten bed volumes of extraction buffer containing 50 mM sodium phosphate and 300 mM NaCl (pH 8.0). The resin containing YgaP- His$_6$ was washed three times with ten bed volumes of the same buffer. The protein was eluted with two bed volumes of elution buffer containing 50 mM sodium phosphate, 300 mM NaCl and 150 mM imidazole (pH 7.0). The elution step was repeated two more times. The purification was carried out in batches. All fractions were assayed for rhodanese activity

and analyzed on SDS PAGE. The purest fractions (>95%) were pooled and stored at -20$^{o}$C.

SDS PAGE was performed on 15% polyacrylamide gels as described by Laemmli (159). Protein was visualized with Fast stain (Zoion Biotech, Inc.).

Protein concentrations were determined by the method of Bradford (160) using reagents purchased from Pierce Chemical Company. Bovine serum albumin was used as the standard and the manufacturer's microassay method was used.

## 2.2.6. MALDI TOF Mass spectrometry

MALDI TOF mass spectrometry was used to identify a second protein band seen on SDS polyacrylamide gel of purified YgaP-$His_6$. For MALDI MS analysis the samples were prepared in the following way.

The two Coomassie stained protein bands of interest were excised from the gel and placed in 1.5 ml eppendorf tubes. A gel slice from a protein-free region of gel was processed in parallel to serve as a control. The Coomassie dye was removed from the stained proteins by incubating the gel pieces with 100 µl of 25 mM ammonium bicarbonate containing 50% acetonitrile (v/v) for 10 min at room temperature with occasional agitation on a vortex mixer. This step was repeated two to three times until the gel pieces appeared shrunken and white/light blue in color. The gel pieces were dehydrated by adding 100 µl of acetonitrile and drying in a Speed Vac for 10 min. The protein was then reduced by addition of 100 µl of 10 mM dithiothreitol (DTT) in 25 mM ammonium bicarbonate. After incubating the gel pieces for about 30 min, the solution was removed and the protein was alkylated by addition of 100 µl of 50 mM

iodoacetamide in 25 mM ammonium bicarbonate (45 min). The solution was removed and the gel pieces were again dehydrated in acetonitrile as described above. The gel was then rehydrated in 200 μl of 25 mM ammonium bicarbonate buffer. This dehydration/rehydration step was repeated once more. Then the gel pieces were dried for approximately 30 min in a Speed vac. The dried gel pieces were then rehydrated with 20 μl of trypsin solution (20 ng/μl) and kept on ice for 10 min. This mixture was agitated for 5 min using a vortex mixer and 30 μl of 25 mM ammonium bicarbonate was added to cover the gel pieces. This mixture was then incubated for 16 hours at 37$^{o}$C. The trypsin digests were centrifuged and the digestion was stopped by addition of 5 μl of 5% trifluroacetic acid (TFA). The mixture was vortexed for 10 min and centrifuged to collect liquid at the bottom of the tube. The peptides were recovered from the gel pieces with Zip-Tips. The Zip-Tips were prepared by aspirating 10 μl of acetonitrile:0.1% TFA (1:1) solution (repeated three times). The tips were equlibrated with 10 μl 0.1% TFA. The peptides were bound to the Zip-Tips by aspirating and dispensing the digest solutions 10-20 times through the Zip-Tips. The Zip-Tips were washed with 10 μl of 0.1% TFA. The peptides were eluted from the Zip-Tip by aspirating and dispensing 3 μl of the matrix solution 3 times through the tips. For MALDI-MS analysis 3 μl of the peptide-matrix solution was dispensed dirtectly to the MALDI plate and allowed to dry. The matrix solution was a saturated solution of α-hydroxycinnamic acid in 0.1% TFA. Each sample was spotted in five places on the MALDI plate and mass spectra were obtained on a Kratos Kompact SEQ time of flight mass spectrometer. Theoretical peptide masses for YgaP-$His_6$ trypsin digest were obtained by entering the amino acid sequence of YgaP-

$His_6$ at http://us.expasy.org/tools/peptide-mass.html. YgaP-$His_6$ protein band served as a positive control.

## 2.2.7. Assay of thiosulfate sulfurtransferase activity (rhodanese assay)

Assay for measuring rhodanese activity was essentially as described previously for quantification of thiocyanate (23;35). The assay used thiosulfate as the sulfur donor and cyanide as the sulfur acceptor. The 0.5 ml assay mixture consisted of 100 mM Tris acetate (pH 8.6), 50 mM ammonium thiosulfate, 50 mM KCN and enzyme. The reactions were initiated by addition of KCN and terminated after 5 to 10 min by addition of 0.25 ml of 15% formaldehyde. Color was developed by addition of 0.75 ml of ferric nitrate solution [100 g of $Fe(NO_3)_3 . 9H_2O$ and 200 ml of 65% $HNO_3$ per 1,500 ml]. Reaction mixtures were centrifuged to pellet any insoluble material and the formation of thiocyanate was quantified by measuring absorbance at 460 nm (23). A reaction mixture containing all reagents except the enzyme was used as blank. One unit of enzyme is defined as the amount that catalyzes the production of 1 μmol of thiocyanate per min at 25°C and corresponds to an absorbance change of 2.8 at 460 nm.

## 2.2.8. Assay of D-Lactate dehydrogenase

D-Lactate dehydrogenase activity was determined by using a continuous spectrophotometric assay that monitors the reduction of MTT [3-(4,5 Dimethylthiazol)-2,5 diphenyl tetrazolium bromide] at 570 nm in the presence of the substrate D-lactate (161).

## 2.2.9. Construction of chromosomal *ygaP* deletion

The *ygaP* gene was disrupted using a modification of the method of Datsenko and Wanner (145) where λ Red recombinase facilitates replacement of the gene or region of interest with an antibiotic resistance cassette flanked by FRT sites. For construction of the *ygaP* deletion a 559 bp fragment from the N terminal flanking region of *ygaP* was amplified by PCR using primers PNFI and PNRI (Table 2.2.3). Similarly a 471 bp fragment consisting of the 3' flanking region of *ygaP* was amplified with primers PCFI and PCRI (Table 2.2.3) (FIG. 2.2.2). The deletion removes most of the gene leaving only 9 bp of the N-terminal coding region and 95 bp from the C-terminal region. The PCR product amplified from the N-terminal region was digested with *Not*I and *Bam*HI and ligated into the same sites of pFRT-K (Table 2.2.2), creating pFA111. For our experiments pFRT-K was constructed by introducing a 1.5 kb kanamycin-resistance cassette ($Km^r$) flanked by FRT sites (FLP recombinase site) from pCP15 (146) into the *Eco*RI-*Hin*dIII sites of pBluescript-$KS^+$ (Stratagene) (FIG. 2.2.1). Thus pFRT-K contains multiple cloning sites on each side of the $Km^r$ cassette for cloning chromosomal DNA sequence that target the gene disruption.

The PCR product amplified from the C-terminal region was subsequently digested with *Hind*III and *Sal*I and inserted into the same sites of pFA111 resulting in pFA121 (Table 2.2.2). PFA121 was linearized with *Not*I and *Sal*I and a 2.5 kb linear DNA fragment consisting of the $Km^r$-FRT cassette flanked by N and C terminal regions of *ygaP* deletion was generated. The construct resulted in deletion of 418 bp of *ygaP*. The linear DNA was introduced by transformation into strain BW25113(pKD46) by selection for kanamycin resistance, creating FA001 (Table 2.2.1). The $Km^r$ cassette was

excised from the genome of FA001 by introducing pCP20 (strain FA007) (146). pCP20 produces FLP recombinase that allows homologous recombination between the FRT sites flanking the $Km^r$ cassette. The *ygaP* gene deletion was verified by PCR using primers PNF1 and YgaP2 (Table 2.2.3). P1 mediated transductional mapping was performed using the nearby *srlD*::Tn*10* marker (from strain CAG18642). The *srlD*::Tn*10* marker was introduced into FA001 by P1 transduction creating FA003 (Table 2.2.1). As anticipated, the *ygaP*::$Km^r$ and *srlD*::Tn*10* were 20 % cotransducible. P1 lysates of FA001 and FA003 were made and Δ*ygaP*::$Km^r$ was moved to TL524 by P1 transduction creating FA012 and FA005 , respectively (Table 2.2.1). The resulting $Km^r$ transductants were purified and the $Km^r$ cassette was subsequently excised from FA005 by introducing pCP20, yielding strain FA009. PCR using primers PNF1 and YgaP2 was performed using DNA from strain FA005 as template to verify the expected gene replacement at the *ygaP* chromosomal locus.

## 2.2.10. Construction of strains with multiple sulfurtransferase gene disruptions

Bacteriophage P1-mediated transduction (148) was used for construction of strains with multiple sulfurtransferase gene disruptions. A P1 lysate was generally prepared from a donor strain carrying a single sulfurtransferase gene disruption and moved to the recipient strain by P1 transduction. The donor strain with the single gene disruption was created by replacing the gene of interest with an antibiotic resistance cassette, generally kanamycin, as described above. Wild-type strain TL524 was used as the recipient. Transductants carrying the newly disrupted gene were obtained by

selecting for kanamycin resistance. The $Km^r$ cassette was excised each time with pCP20-encoded FLP recombinase to allow introduction of additional sulfurtransferase gene disruption by P1 transduction. In this way strains having up to seven sulfurtransferase gene mutations were created (Table 2.2.1).

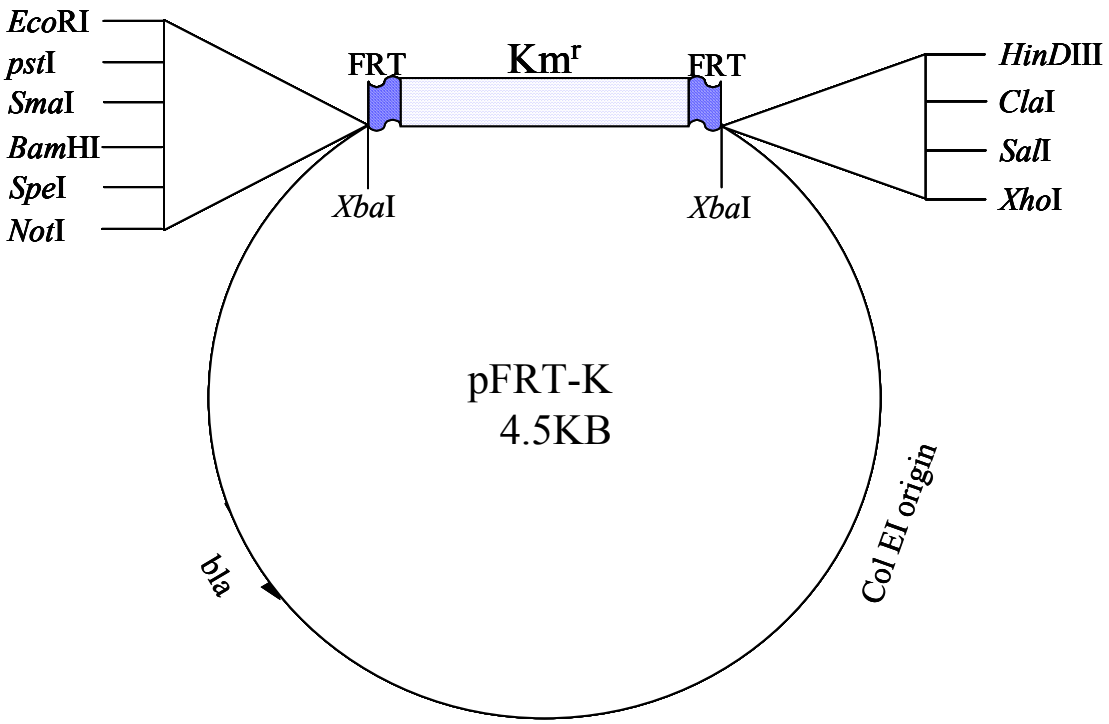


**FIG. 2.2.1. Plasmid pFRT-K used for constructing *ygaP* gene disruption.**
The multiple cloning sites are shown. FRT represents FLP recombinase target sites

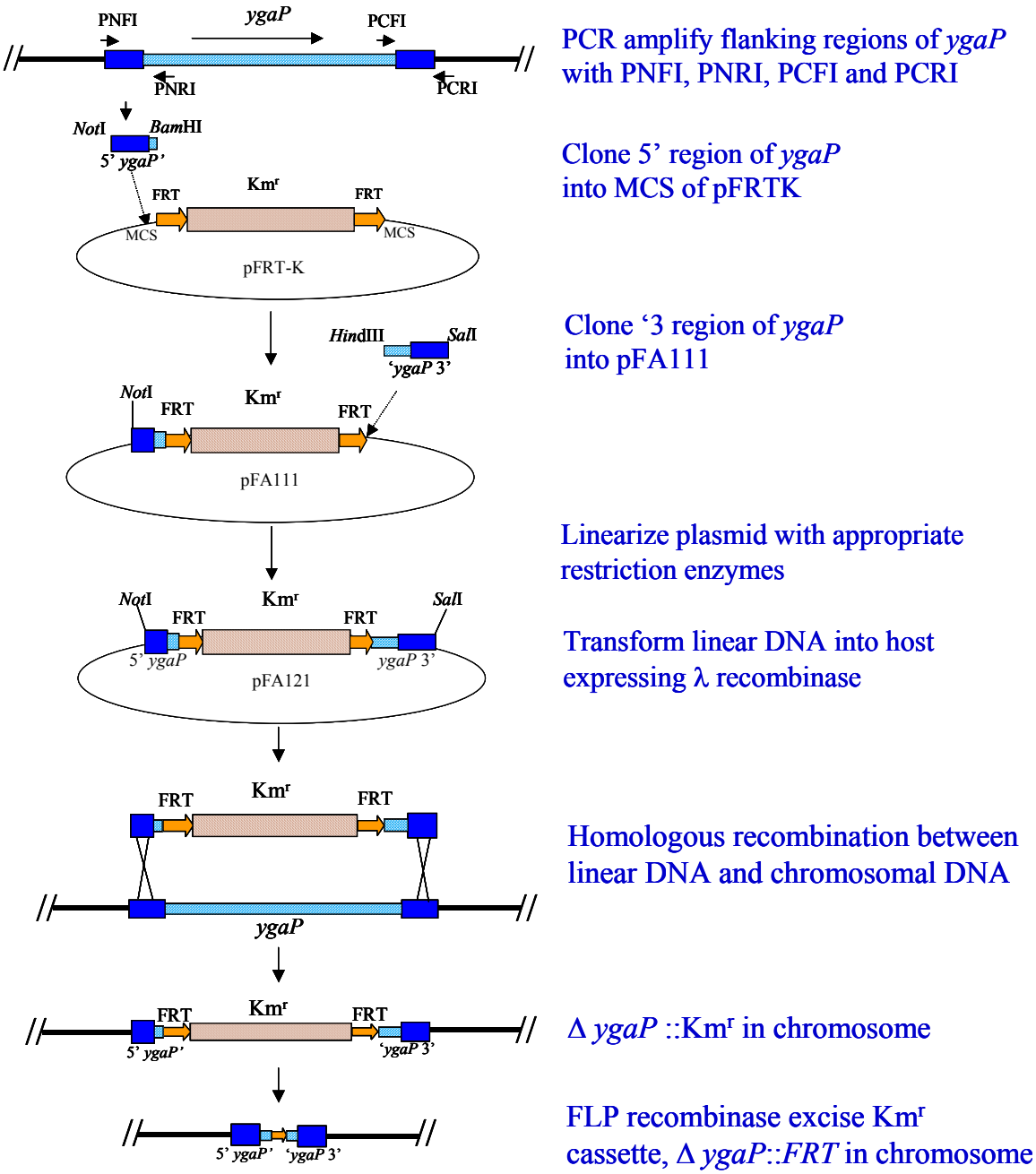


**FIG. 2.2.2. Construction of *ygaP* disruption in the genome**
The 5' and the 3' flanking regions of *ygaP* are represented in dark blue. y*gaP* is represented as blue dots.

## 2.3. Results

### 2.3.1. YgaP is a thiosulfate sulfurtransferase

In the database Cluster of Orthologous Groups (52), YgaP is identified as a rhodanese-related sulfurtransferase in COG0607 along with 93 other proteins. A PSI-BLAST search (135) using *E. coli* GlpE (6) as the query also revealed that YgaP along with seven other proteins from *E. coli* exhibit sequence similarity to known sulfurtransferases including bovine liver rhodanese. These proteins contain a conserved rhodanese homology domain (1;162) with an active site cysteine known to be essential for catalysis. FIG. 2.3.1 shows the sequence alignment of YgaP with other *E. coli* sulfurtransferases and with the second domain of bovine rhodanese and rat MST.

```
                                                                                                  partial
           |---- CH2A motif-----|                |----Active site----| |----CH2B motif-
Consensus:  UUD-R----U  GHU---U------U---------UU--C--G---------U----U---U--U-G----U
Rhod2       LVDSRAQGRY  GHIPGSVNMPFMNF      TKPLIATCRKGVTACHIALAAYLCGKPD-VAIYDGSWFEW
GlpE(108AA) LVDIRDPQSF  GHAVQAFHLTNDTL-(X)9-DTPVMVMCYHGNSSKGAAQYLLQQGYDV-VYSIDGGFEAW
YgaP(174AA) LIDIRDADEY  EHIPEADLAPLSVL      HEQIIFHCQAGKRTSNNADKLAAIAAPAEIFLLEDGIDGW
PspE(104AA) WIDVRVPEQY  EHVQGAINIPLKEV      NDTVKVYCNAGRQSGQAKEILSEMGYTH-VEN-AGGLKDI
YibN(143AA) VVDLRQRDDF  GHIAGSINLLPSEI      DKPVIVVDGSGMQCQEPANALTKAGFAQ-VFVLKEGVAGW

ThiI(482AA) ILDIRSID-L  EGID-VVSLPFYKL      NKTWLLWCERGVMSRLQALYLREQGFNN-VKVYRP-----

MST-Rat     VVDARAAGRF  GHIPGSVNIPFTEF      SKPLVATCGSGVTACHVVLGAFLCGKPD-VPVYDGSWVEW
SseA2(281AA)IIDARPAARF  GHIPGALNVPWTEL      DKPIIVSCGSGVTAAVVLLALATLDVPN-VKLYDGAWSEW
YbbB(364AA) IIDVRAPIEF  EHGAMPAAINLPLM      NPQGILCCARGGQRSHIVQSWLHAAGID-YPLVEGGYKAL
YceA(350AA) FIDMRNHYEY  GHFENALEIPADTF      DKKIVMYCTGGIRCEKASAWMKHNGFNK-VWHIEGGIIEY
YnjE(440AA) LVSIRSWPEF  GHA-GSDSTHMEDF      EQQVSFYCGTGWRASETFMYARAMGWKN-VSVYDGGWYEW
```

**FIG. 2.3.1. Sequence Alignment of YgaP**

Alignment of the conserved regions of YgaP with other putative *E. coli* sulfurtransferases and to the C-terminal domain of bovine rhodanese (Rhod2). U, uncharged; PspE, YgaP, YibN, ThiI, YbbB, YnjE, YceA are rhodanese-like proteins from *E. coli*; SseA2 is the second domain of the SseA protein from *E. coli*; MST-Rat is the rat mercaptopyruvate sulfurtransferase. The active site cysteine is represented in bold red and conserved residues are represented in other colors.

Analysis of the amino acid sequence of YgaP revealed a region near the C-terminus rich in hydrophobic residues. The presence of such hydrophobic residues suggested the possibility of YgaP being a membrane protein. Sulfurtransferase activities were determined in cell free extracts and membrane fractions of strain BL21(DE3)(plysS)(pFA22), which overexpresses YgaP. Thiosulfate:cyanide sulfurtransferase (rhodanese) activity was present in cell free extracts of this YgaP overexpressing strain. Very little increase in rhodanese activity was observed in cell free extracts compared to the vector control (Table 2.3.1). However most of the rhodanese activity in the crude extract of *E.coli* is contributed by two soluble proteins GlpE and PspE (6;129). After separation of soluble proteins by centrifugation, a 240-fold increase in rhodanese specific activity was found associated with the particulate fraction of the YgaP-overexpressing strain (Table 2.3.1). This suggested that the rhodanese activity in the membrane fraction was contributed by YgaP. The increase in rhodanese activity corresponded to an overexpression of YgaP in the cell free extract and the membrane fraction as illustrated by SDS PAGE (Fig. 2.3.2). The rhodanese activity in the membrane fraction of the vector control was only 10% of that in the crude extract indicating that YgaP is only a minor contributor of total rhodanese activity.

Table 2.3.1. Rhodanese specific activity in subcellular fractions of strains overexpressing YgaP

| Protein Fractions | Plasmid | | Fold |
|---|---|---|---|
| | pT7-7 | pFA22 | |
| Crude Extract | 0.3 | 1.4 | 5 |
| Membrane Fraction | 0.03 | 7.2 | 240 |

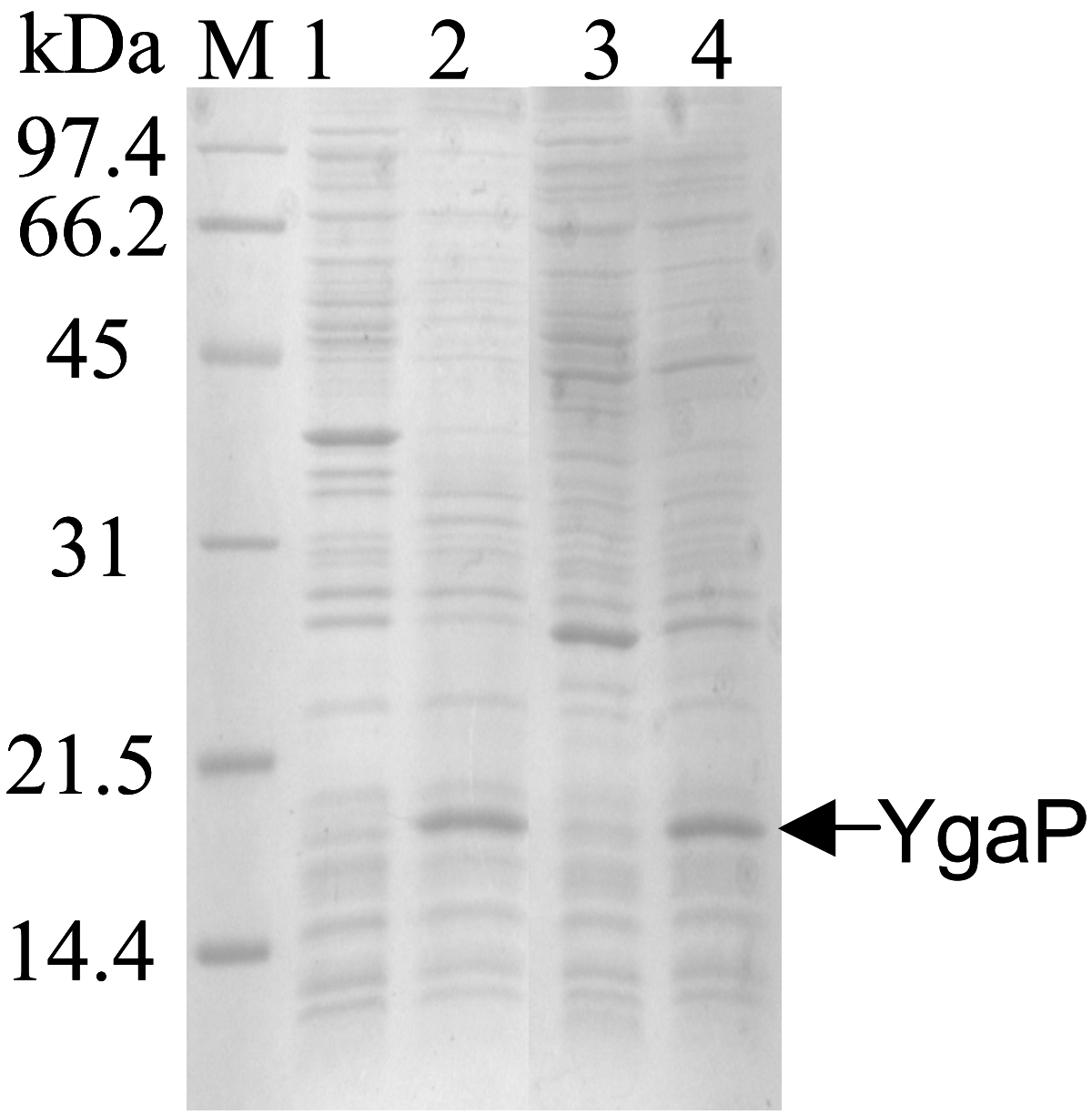


**FIG. 2.3.2. Overexpression of YgaP**
Crude extracts and membrane fractions from BL21(DE3)(plysS)(pFA22) were analyzed by SDS PAGE. Lane M, molecular mass markers. Lanes 1 and 3, crude extract and membrane fractions from BL21(DE3) (plysS) (pT7-7). Lanes 2 and 4, crude extract and membrane fractions from BL21(DE3) (plysS) (pFA22).

## 2.3.2. Cellular location of YgaP.

Since YgaP has a large block of hydrophobic residues near the C-terminus, two different computer algorithms were used for prediction of membrane topology (TMHMM, SOSUI). Both programs predicted that YgaP has two transmembrane helices near the C-terminus and that there is a 60% probability of the N-terminal rhodanese domain of YgaP to be present in the cytoplasm. Treatment of membrane fractions of a strain overexpressing YgaP with Triton X-100 and $MgCl_2$ resulted in solubilization of YgaP. These conditions are known to selectively solubilize integral proteins of the inner membrane, while leaving major outer membrane proteins in their native location (163).

To verify the location of YgaP within the cytoplasmic membrane, the inner and outer membrane fractions of a strain overexpressing YgaP were isolated by sucrose density layer ultracentrifugation (158). Fractions were collected and analyzed for rhodanese activity and for marker proteins of the inner and outer membranes. Lactate dehydrogenase (LDH) activity served as the cytoplasmic membrane marker, and the major outer membrane proteins (assessed by SDS PAGE) served as the outer membrane markers. Rhodanese activity was found in the inner membrane fractions obtained at the interface between 15% and 53% sucrose. Most of the lactate dehydrogenase activity was present in the same fractions (Fig. 2.3.3). Little or no YgaP, rhodanese or lactate dehydrogenase activity was found in the fractions containing the major outer membrane proteins. These results demonstrate YgaP is an integral membrane protein of the cytoplasmic membrane.

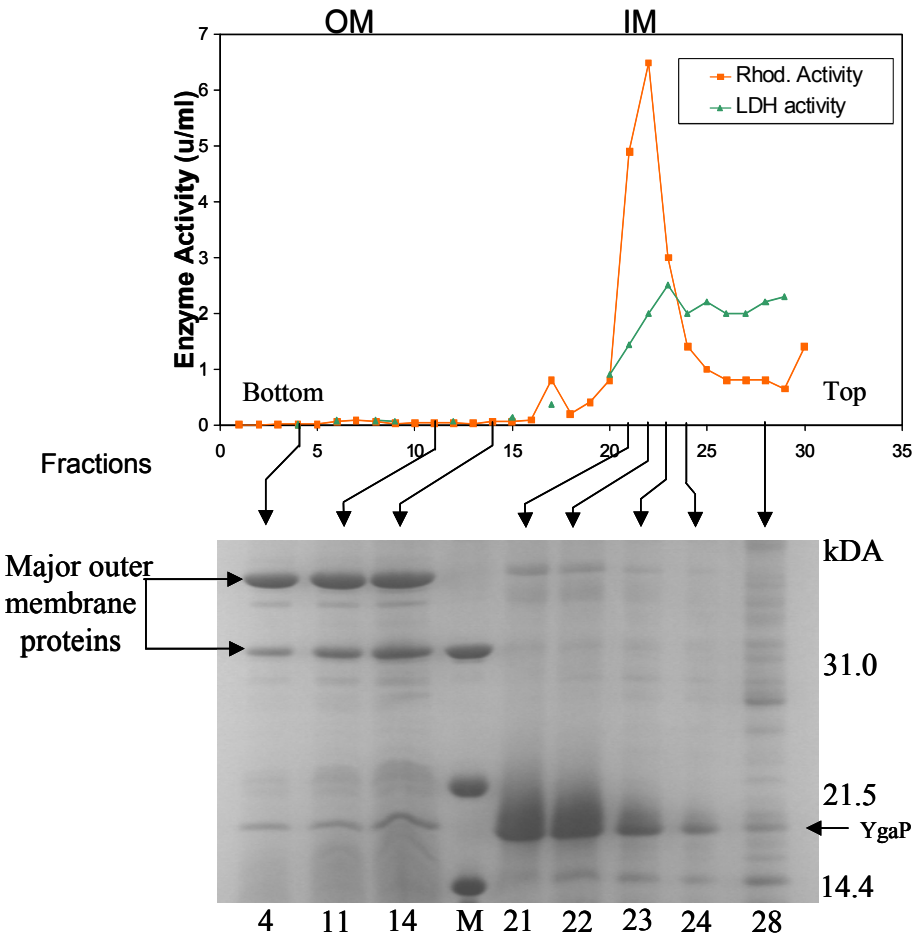


## FIG. 2.3.3. Co-sedimentation of YgaP with the cytoplasmic membrane

Sucrose density layer ultracentrifugation was used to determine the cellular location of YgaP. Upper Panel; Plot of rhodanese activity and lactate dehydrogenase activity of fractions collected after sucrose density layer ultracentrifugation of the crude extract of YgaP-expressing cells. Lower panel; SDS PAGE of indicated fractions. Fractions 4, 11 and 14 correspond to outer membrane (OM) proteins and fractions 21, 23, 24 correspond to inner membrane (IM) proteins. Fraction 28 represents cytoplasmic proteins. M is molecular mass marker.

### 2.3.3. Purification of YgaP-$His_6$.

Expression of YgaP with a C-terminal polyhistidine tag facilitated the purification of the enzyme by immobilized metal affinity chromatography. After solubilization of the protein from the membrane by detergent treatment, the detergent extract was subjected to a Talon $Co^{2+}$ resin and purified in batches by centrifugation as described in the manufacturer's protocol (BD Bioscience). The majority of the nonspecifically bound proteins were washed from the resin with buffer containing 50 mM sodium phosphate and 300 mM NaCl. Fractions containing rhodanese activity were eluted with a 150 mM imidazole buffer. The major protein found in the pooled fractions was approximately 20 kDa as visualized by SDS PAGE (Fig. 2.3.4), which corresponds to the calculated size of YgaP-$His_6$. The resulting protein was 90% homogenous (SDS PAGE). However a second protein of a lower intensity and approximately twice the size of YgaP-$His_6$ was seen in the purified fractions. Mass spectroscopy was performed to identify the second polypeptide.

From a 500 ml culture, 7 mg of YgaP-$His_6$ was purified to a specific activity of 2.4 U/mg (Table 2.3.2). The purified enzyme stored at –20$^{o}$C retained activity for 2-3 months (in the presence or absence of 15 % glycerol) after which the activity was lost gradually due to oxidation as described for other rhodaneses (6). The enzyme could be reactivated to some degree by addition of micromolar concentrations of cysteine. The purified rhodanese could not be stored at 4$^{o}$C due to rapid loss of activity within a few days.

Table 2.3.2. Purification of YgaP-$His_6$ from *E. coli*

| Fractions/purification steps | Volume (ml) | Amt. of Protein (mg) | Activity (U) | Sp. Activity (U/mg) | Yield (%) |
|---|---|---|---|---|---|
| Crude Extract | 20 | 120 | 112 | 0.9 | 100 |
| Membrane Fraction | 1.8 | 27 | 49 | 1.8 | 44 |
| Detergent Extract | 1.2 | 21 | 78 | 3.6 | 70 |
| Purified protein | 14 | 7 | 17 | 2.4 | 15 |

The values for purified protein were obtained by calculation. Fifty microliters of detergent extract was purified on Talon-$Co^{2+}$ resin to yield 0.3 mg of protein.

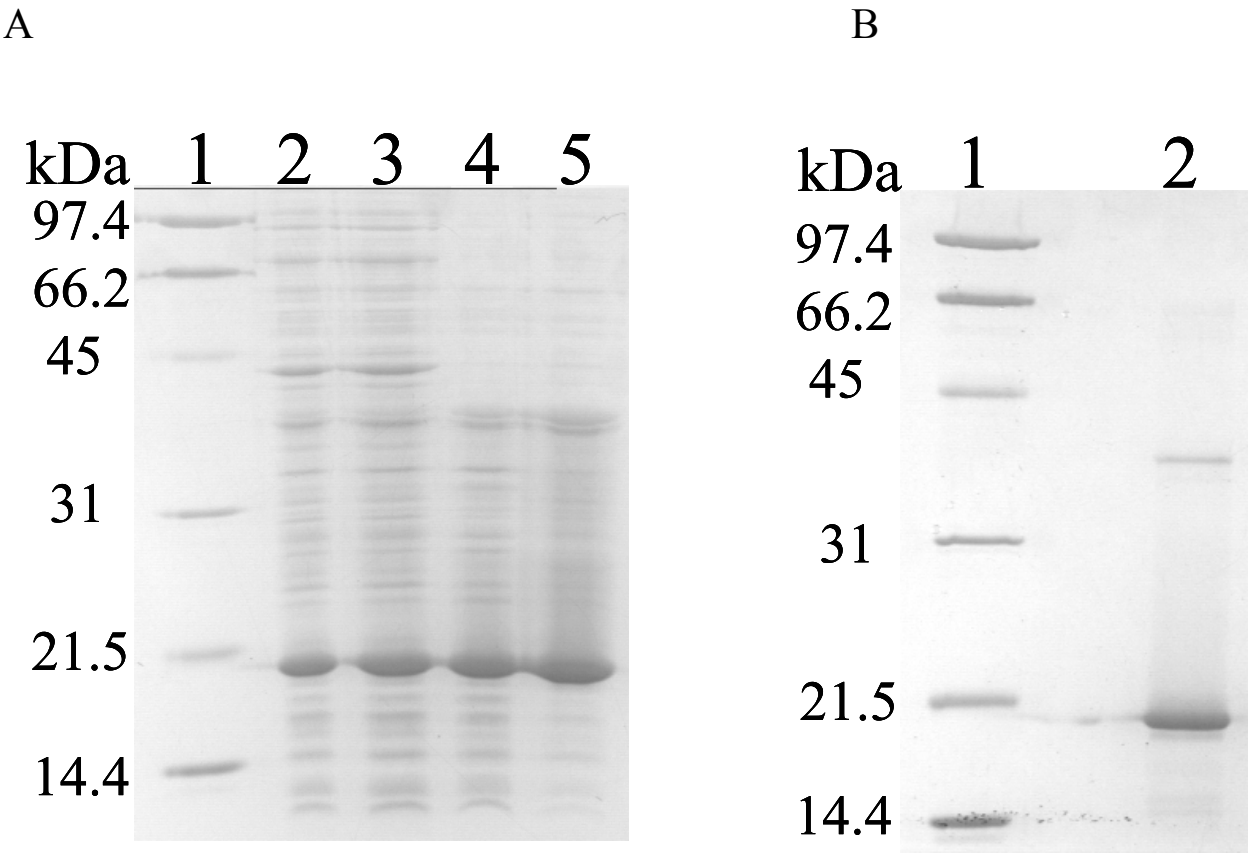


**FIG. 2.3.4. SDS PAGE illustrating the cellular fractionation and purification of YgaP-His$_6$.**
(A) Lane 1, Molecular mass markers; lanes 2 and 3, crude extract; lane 4, membrane fraction; lane 5, soluble fraction after detergent extraction. (B) Lane 1, molecular mass markers; lane 2, purified YgaP-His$_6$.

## 2.3.4. MALDI TOF Mass Spectrometry to identify the second polypeptide.

Upon purification of YgaP-$His_6$ a protein of approximately 40 kDa was constantly observed as a minor contaminant seen by SDS PAGE analysis. To find out whether this second polypeptide is a dimer of YgaP-$His_6$ or a protein that interacts with YgaP, MALDI-TOF mass spectrometry was performed. Protein band for the second polypeptide was excised from the gel, digested with trypsin and prepared for mass spectrometry as described in materials and methods. Four peptide peaks of mass/charge ratios of 629.51, 769.6, 881.61 and 985.5 were detected for the trypsin digest of the second polypeptide band that matched the theoretical peptide masses for digestion of YgaP-$His_6$ with trypsin (Table 2.3.3). Trypsin digestion of the YgaP-$His_6$ protein band also detected the same four peptide peaks. The peptide peak 629.51 of YgaP-$His_6$ was of the highest intensity and was therefore represented as 1. The intensities for all the other peaks are given relative to the intensity of this peak. Although some of the peaks were not strong, they were detected for both polypeptides in repeated experiments. A control experiment was run using a SDS polyacrylamide gel piece that did not contain any protein. Peptide peaks obtained for this gel piece did not match those obtained for purified YgaP-$His_6$, the second polypeptide or the theoretical peptide masses for a YgaP-$His_6$ trypsin digest. These data suggested that the second polypeptide on SDS polyacrylamide gel of purified YgaP-$His_6$ represents a dimer of YgaP-$His_6$.

Table 2.3.3. Peptide Masses Obtained from Mass Spectrometry of YgaP Monomer and Dimer

| Theoretical Peptide Mass | Position | YgaP Monomer | | YgaP Dimer | |
|---|---|---|---|---|---|
| | | Experimental Peptide Mass | Relative Intensity | Experimental Peptide Mass | Relative Intensity |
| 1866.97 | 1-17 | N/O | | N/O | |
| 629.39 | 21-25 | 629.51 | 1 | 629.62 | 0.15 |
| 881.4 | 26-32 | 881.61 | 0.45 | 881.5 | 0.7 |
| 2314.23 | 33-54 | N/O | | N/O | |
| 1410.70 | 57-68 | N/O | | N/O | |
| 749.34 | 70-76 | N/O | | N/O | |
| 2213.19 | 77-97 | N/O | | N/O | |
| 868.53 | 99-107 | N/O | | N/O | |
| 941.52 | 108-115 | N/O | | N/O | |
| 4761.57 | 116-163 | N/O | | N/O | |
| 831.40 | 168-173 | N/O | | N/O | |
| 769.46 | 174-180 | 769.6 | 0.31 | 769.7 | 0.38 |
| 985.46 | 181-188 | 985.5 | 0.05 | 985.47 | 0.27 |

N/O: A peak representing this peptide mass was not obtained.

Peptide masses greater than 500 daltons are shown.

## 2.3.5. Catalytic properties of YgaP

The well-characterized rhodaneses from different organisms including the bovine liver rhodanese as well as GlpE from *E. coli* carry out catalysis by a double displacement (ping-pong) mechanism (6;27;164). Kinetic data from activity measurements of purified YgaP-$His_6$ with various concentrations of cyanide at fixed concentrations of thiosulfate were fit to the Lineweaver Burk equation. Kinetic data from activity measurements of membrane bound YgaP were also generated under similar conditions and fit to the same equation. Both YgaP-$His_6$ and the membrane bound YgaP displayed the same kinetic pattern. The double reciprocal plots for both YgaP-$His_6$ and membrane bound YgaP form parallel lines (FIG. 2.3.5A and 2.3.6A), indicating a double displacement (ping-pong) mechanism. The secondary plots of apparent maximum velocities versus thiosulfate concentrations (FIG. 2.3.5B and 2.3.6B) were used to determine the $K_m$ for thiosulfate and cyanide. The $K_m$ values for purified YgaP-$His_6$ were 55 mM and 1.5 mM, respectively and those for the membrane bound YgaP were 69 mM and 0.7 mM respectively. The $k_{cat}$ based on YgaP-$His_6$ functioning as a monomer was 1 $s^{-1}$.

Despite the similarity between rhodaneses and mercaptopyruvate sulfurtransferases, substitution of 3-mercaptopyruvate for thiosulfate in the standard rhodanese assay with YgaP resulted in less than 1% of the activity for thiocyanate formation (data not shown). These results were identical to those obtained with GlpE, which also did not use 3-mercaptopyruvate as a sulfur donor at an appreciable rate.

Previous studies with the bovine rhodanese as well as the *E. coli* accessible rhodanese indicate that they are inhibited by certain anions (35;165). GlpE from *E. coli* however showed little or no inhibition by anions (6). Results of anion inhibition studies of YgaP were similar to GlpE for sulfate, chloride and acetate. Addition of sodium sulfate and sodium chloride at a

concentration of 0.3 M and sodium sulfite at a concentration of 50 mM resulted in 20 –30 % loss of rhodanese activity. Addition of sodium acetate at similar concentrations did not cause any loss of activity. However, sodium phosphate at a concentration of 0.25 mM resulted in 50% loss of enzyme activity. For GlpE rhodanese, sodium phosphate did not cause a significant loss in activity.

(A)

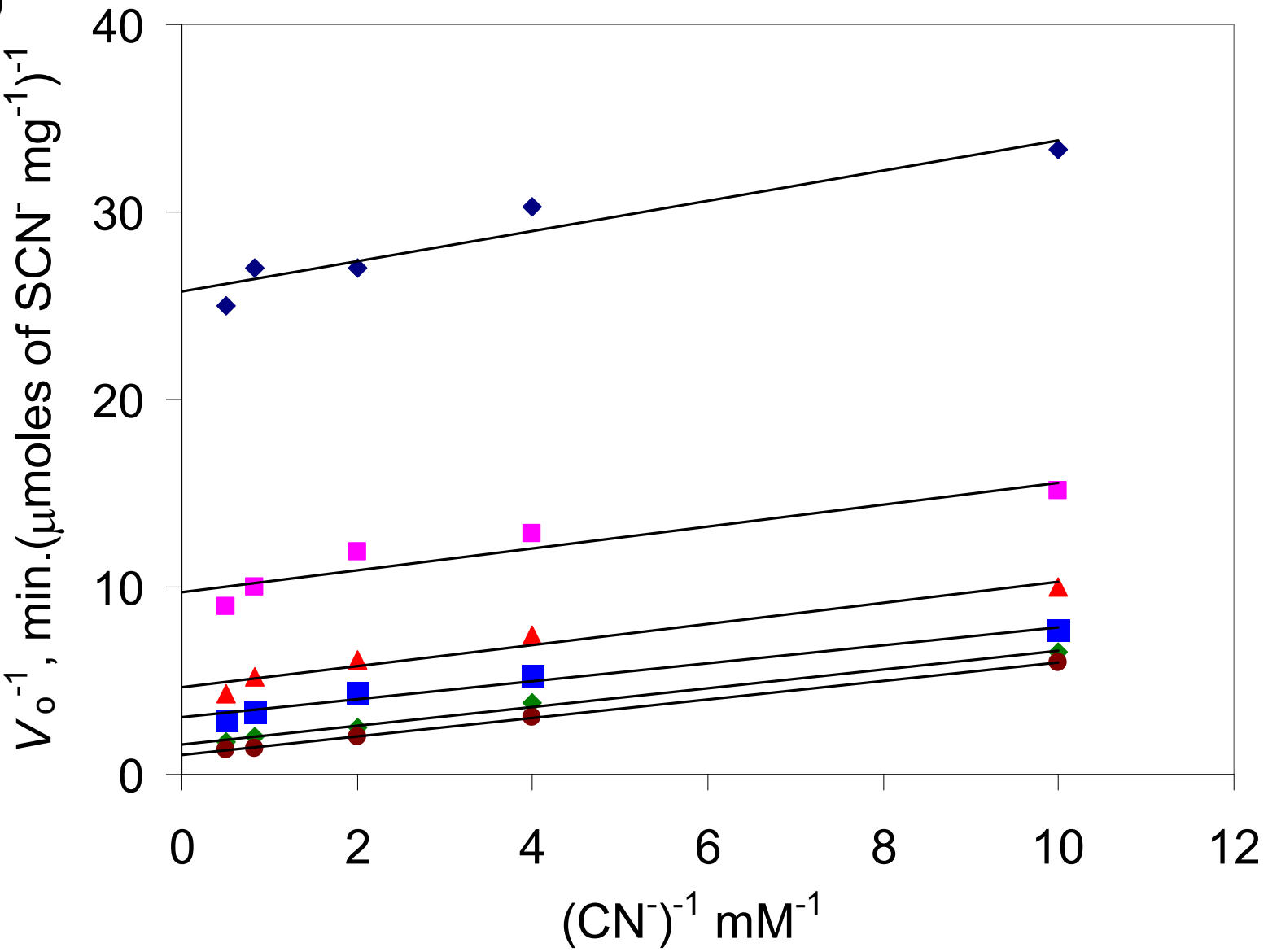

(B)

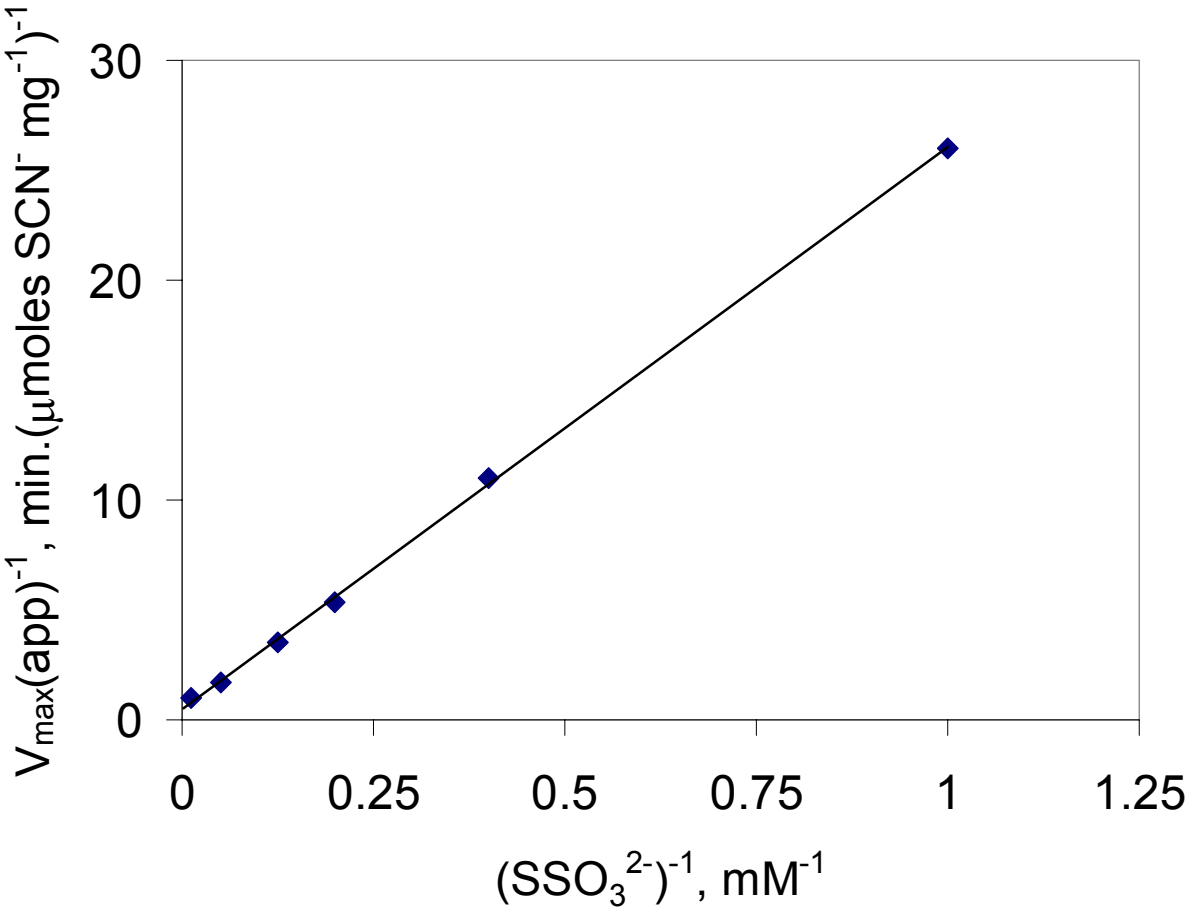


**FIG. 2.3.5. Kinetic measurements of purified YgaP-His$_6$ catalyzed thiosulfate:cyanide sulfurtransferase reaction.**

A. Double reciprocal plot of the rate of thiocyanate formation versus cyanide concentration at various fixed concentrations of thiosulfate: 1 mM (◆), 2.5 mM (■), 5 mM (▲), 8 mM (■), 20 mM (◆) and 80 mM (●). B. Secondary double reciprocal plot of apparent Vmax from the data in A versus thiosulfate concentration.

(A).

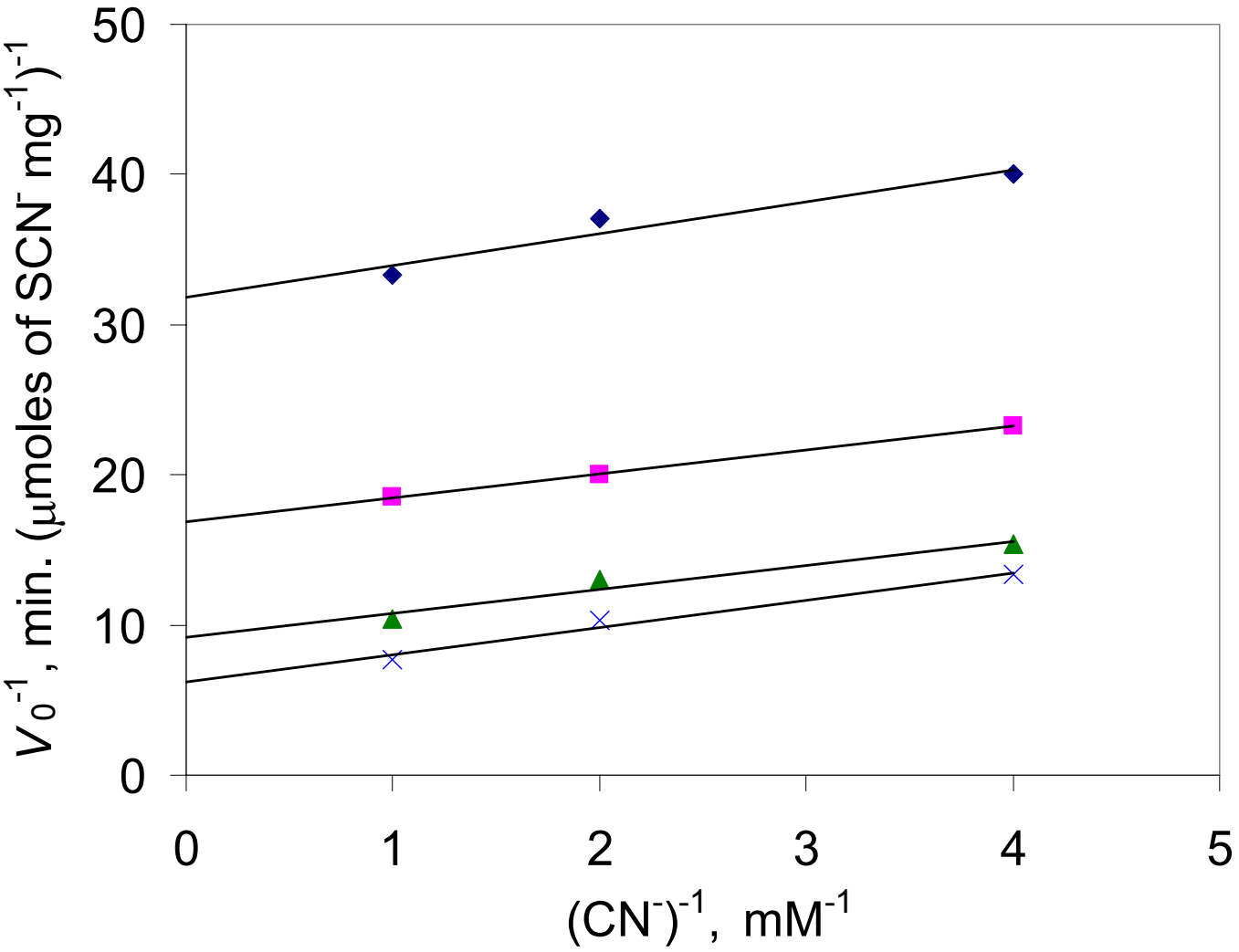

(B)

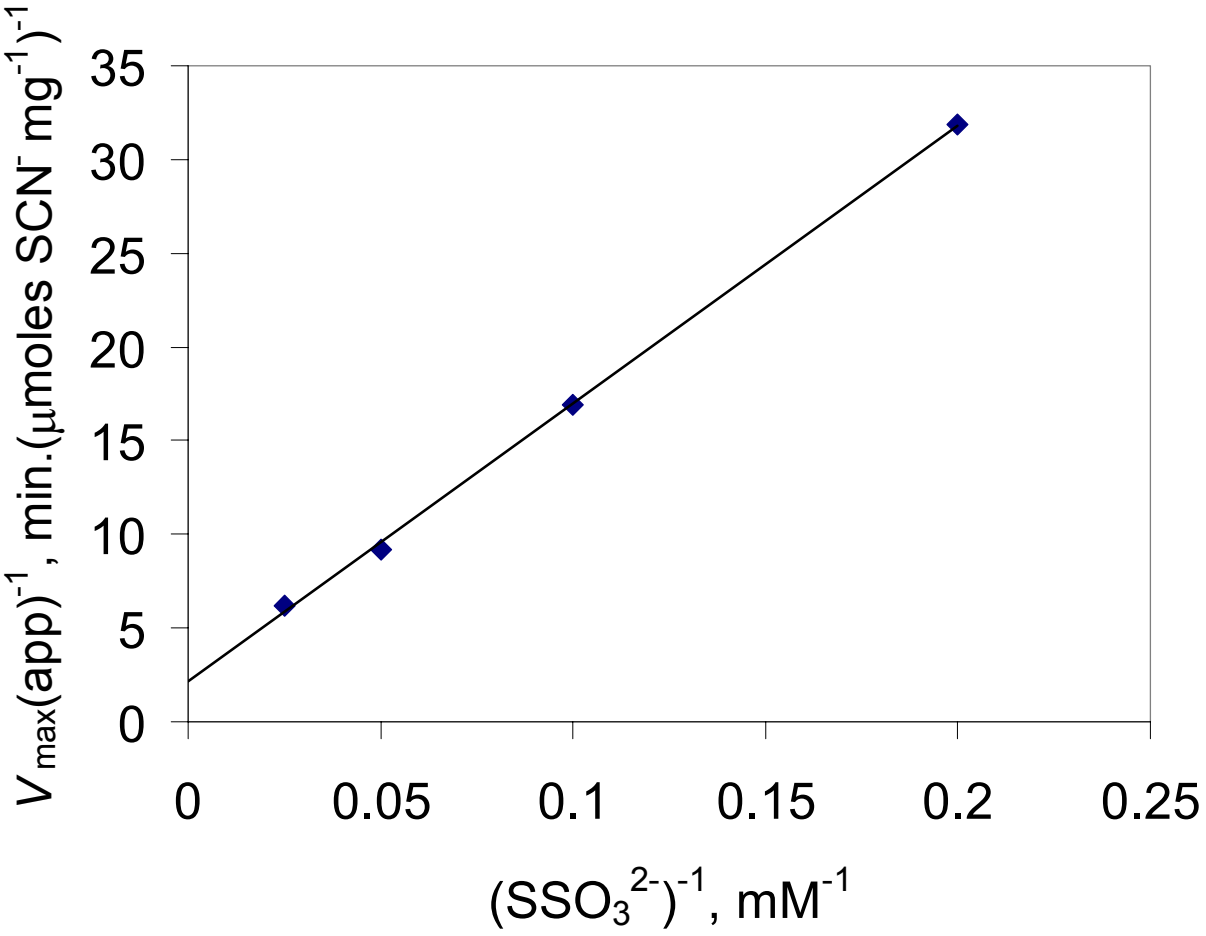


**FIG. 2.3.6. Kinetic measurements of the thiosulfate:cyanide sulfurtransferase reaction catalyzed by membrane fraction of YgaP.**

A. Double reciprocal plot of the rate of thiocyanate formation versus cyanide concentration at various fixed concentrations of thiosulfate: 5 mM (♦), 10 mM (■), 20 mM (▲) and 40 mM (×). B. Secondary plot of apparent Vmax from data in A versus thiosulfate concentration.

## 2.3.6. Disruption of chromosomal *ygaP*

As an approach to investigate the role of YgaP in *E. coli*, a gene disruption was created by replacing 418 base pairs of the coding sequence of *ygaP* with a $Km^r$ cassette flanked by FRT sites (145;146). The genotype of the resulting *ygaP*::$Km^r$ strain was verified by PCR after excision of the $Km^r$ cassette by FLP recombinase. The observed sizes of the PCR products were close to the expected values of 1121 bp and 828 bp for the wild-type and the *ygaP* deletion strain, respectively (Fig. 2.3.7).

The location of $Km^r$ cassette in the *E. coli* chromosome was further verified by P1 transduction using a donor strain with a *Tn*10 (*srlD3131*::*Tn*10) near *ygaP*. After transduction of strain FA001 with a P1 lysate of CAG18642, $Tc^r$ colonies were selected and then scored for $Km^r$. Of the 426 colonies scored, 85 were $Km^s$ (20%). The results are consistent with the $Km^r$ cassette being present at its expected location, because the anticipated cotransduction frequency of *slrD3131*::*Tn*10 and *ygaP* is 30%.

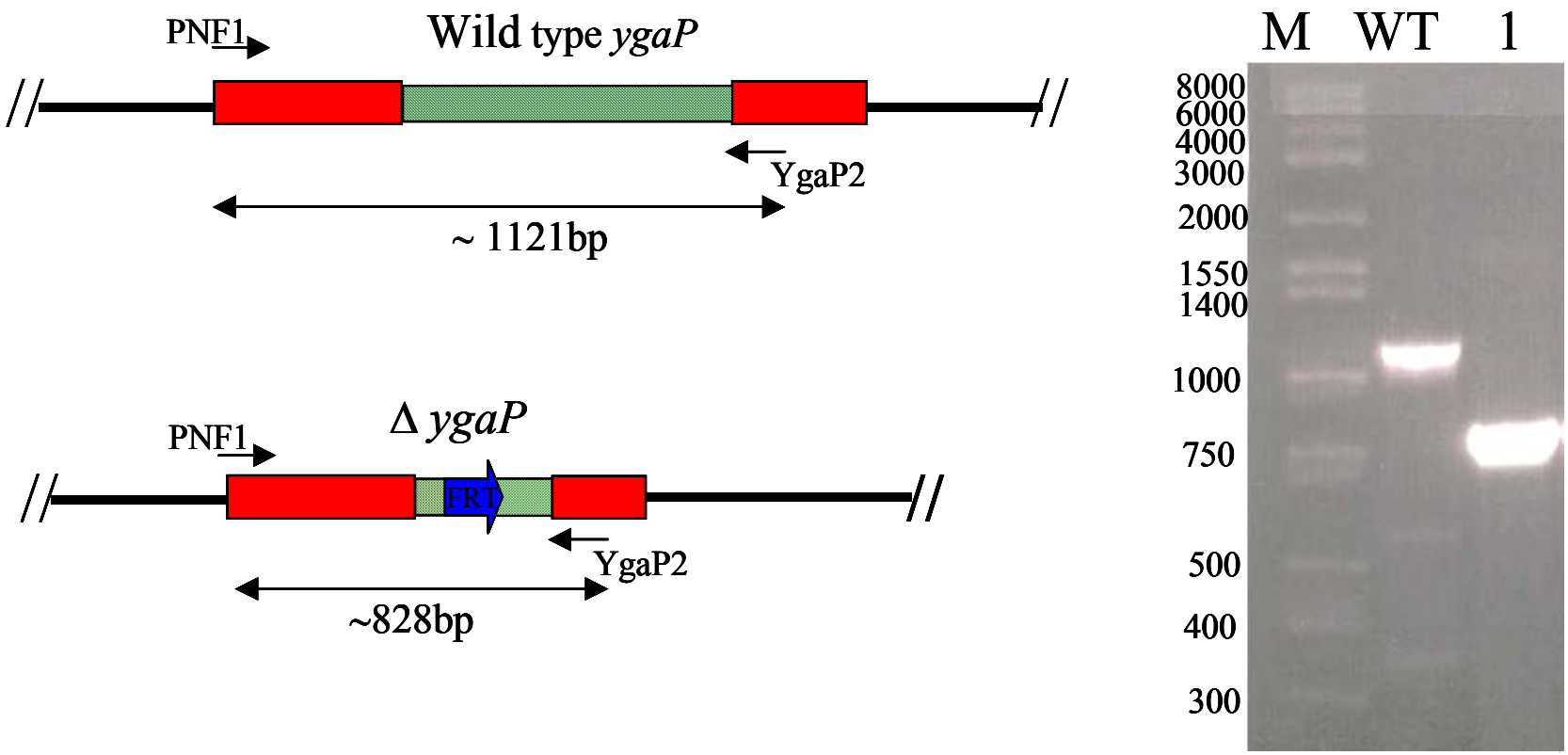


**FIG. 2.3.7. PCR for verification of Δ*ygaP* in the genome.**

The expected sizes of PCR products obtained using chromosomal DNA templates from the wild type and the Δ*ygaP* strain are shown on the left. Analysis of the PCR reactions by agarose gel electrophoresis is shown on the right. Lane M, molecular weight markers; lane WT, wild type; lane 1, DNA from Δ*ygaP* strain

.

### 2.3.7. Phenotypic characterization of the Δ*ygaP* mutant and multiple sulfurtransferase mutants

To obtain information regarding the physiological function of YgaP in *E. coli*, the Δ*ygaP* mutant was studied under various growth conditions. The Δ*ygaP* mutant grew at a rate similar to that of the wild type (TL524) in LB as well as in minimal media (AB glucose or glycerol) without any supplements at 37 °C.

It is hypothesized that rhodaneses may be involved in the biosynthesis of essential sulfur-containing compounds in the cell. To test the ability of the Δ*ygaP* mutant to synthesize sulfur-containing cofactors like thiamin, biotin or lipoic acid, the mutant was grown in glucose minimal medium (M9 or AB noble agar) with or without the essential cofactors. The Δ*ygaP* mutant did not show any growth auxotrophy compared to the wild type (TL524). The *thiI* (strain JLD26501) and *thiC* mutants (strain FA037), the *bioB* mutant (strain R875) and the *lipA* mutant (strain JRG33) served as controls for thiamin, biotin and lipoic acid biosynthesis, respectively, to ensure that the medium was free of any trace amounts of the cofactors. The *thiI* and the *thiC* mutant, the *bioB* mutant and the *lipA* mutant were unable to grow in the defined medium unless supplemented with the required cofactors.

Molybdopterin is an essential cofactor for many molybdenum-containing enzymes including nitrate reductase of *E. coli*. The immediate source of sulfur for molybdopterin biosynthesis is not known (57). In some organisms the MoeB protein, an MPT synthase sulfurase, contains a rhodanese domain fused to its C-terminus. The *E. coli* MoeB does not contain a C-terminal rhodanese domain. Therefore the possibility that rhodaneses have a role in molybdopterin synthesis was investigated. The Δ*ygaP* mutant was tested for chlorate sensitivity

under anaerobic conditions. The molybdopterin-containing enzyme nitrate reductase that reduces $NO_3^-$ to $NO_2^-$ can also convert chlorate to the more toxic chlorite anion. Mutants defective in nitrate reductase, including those unable to produce molybdopterin, are chlorate resistant under anaerobic conditions. The Δ*ygaP* mutant and the wildype (TL524) were chlorate sensitive but the *moaA* mutant (S1247) serving as a control was chlorate resistant. The result indicated that YgaP was not essential for molybdopterin biosynthesis.

The Δ*ygaP* mutant was also tested for its ability to synthesize $s^2U$ and $s^4U$ in tRNA (C. Lauhon, Univ. of Wisconsin). It was found that strains deficient in YgaP were still capable of $s^2U$ and $s^4U$ synthesis.

Since there is redundancy in proteins containing the rhodanese homology domain in *E. coli*, disruption of a single rhodanese gene may not confer a discernible phenotype. Strains having multiple sulfurtransferase gene disruptions were therefore constructed and tested for their ability to synthesize the various sulfur-containing cofactors (thiamin, biotin, lipoic acid, molybdopterin) and thionucleosides in tRNAs. Strains with single, triple (FA024, *sseA*::$Sp^r$ Δ*ygaP* Δ*glpE*), quadruple (FA025, *sseA*::$Sp^r$ Δ*ygaP* Δ *ynjE* Δ*glpE*), pentuple (JLD17302, *sseA*::$Sp^r$ Δ*ygaP* Δ*ynjE* Δ*glpE* Δ*pspE*), sextuple (JLD20502, *sseA*::$Sp^r$ Δ*ygaP* Δ *ynjE* Δ*glpE* Δ*pspE* Δ*yceA*) and heptuple (FA036, *sseA*::$Sp^r$ Δ*ygaP* Δ *ynjE* Δ*glpE* Δ*pspE* Δ*yceA* Δ*ybbB*::$Km^r$ and JLD26503, *sseA*::$Sp^r$ Δ*ygaP* Δ *ynjE* Δ*glpE* Δ*pspE* Δ*yceA* Δ*thiI* ) sulfurtransferase gene mutations were analyzed for their thiamin requirement for growth compared to the wild type (Janet Donahue). All of the mutants except for the single *thiI* mutant and the heptuple mutant (JLD26503) that has a *thiI* disruption grew as well as the wild type (TL524) on minimal plates without thiamin, biotin or lipoic acid (M9 glucose noble agar). The single *thiI* mutant and the heptuple mutant required thiamin for their growth. ThiI has a rhodanese domain fused to the C-

terminus of the protein and it has been shown to be involved in thiamin biosynthesis (17;50). These results demonstrate that none of the sulfurtransferases in *E. coli* are essential for thiamin, biotin or lipoic acid biosynthesis.

The mutant strains deficient in multiple sulfurtransferase genes were also analyzed for their ability to synthesize molybdopterin. These strains included a double mutant FA013 (*sseA*::Sp$^r$ Δ*ygaP*::Km$^r$), two triple mutants FA014 (*sseA*::Sp$^r$ Δ*ygaP*::Km$^r$ Δ*ynjE*) and FA024 (*sseA*::Sp$^r$ Δ*ygaP* Δ*glpE*) , a quadruple mutant FA025 (*sseA*::Sp$^r$ Δ*ygaP* Δ *ynjE* Δ*glpE*), a pentuple mutant JLD17302 (*sseA*::Sp$^r$ Δ*ygaP* Δ*ynjE* Δ*glpE* Δ*pspE*), a sextuple mutant JLd20502 (*sseA*::Sp$^r$ Δ*ygaP* Δ *ynjE* Δ*glpE* Δ*pspE* Δ*yceA*) and two heptuple mutants JLD27003 (*sseA*::Sp$^r$ Δ*ygaP* Δ *ynjE* Δ*glpE* Δ*pspE* Δ*yceA* Δ*thiI*) and FA036 (*sseA*::Sp$^r$ Δ*ygaP* Δ *ynjE* Δ*glpE* Δ*pspE* Δ*yceA* Δ*ybbB*::Km$^r$). All of the strains with multiple sulfurtransferase gene disruptions including the heptuple mutants were chlorate sensitive, similar to the wild-type. The *moaA* mutant (S1247, *moaA29*) served as the chlorate-resistant control. These results indicate that none of the sulfurtransferases are essential for biosynthesis of molydopterin.

The multiple sulfurtransferase mutants including the heptuple mutant FA036 were not deficient in $s^2U$, $s^4U$ (C. Lauhon, Univ. of Wisconsin) or $mS^2i6A$ (Pierrel and Fontecave, Grenoble, France) in tRNAs.

It has been proposed that rhodaneses may be involved in the mobilization of sulfur for biosynthesis or repair of iron sulfur clusters (137;166). As a tool to investigate the role of rhodaneses in repair of iron sulfur clusters, the mutants were exposed to oxidative stress by treatment with 2% $H_2O_2$ or 0.1 M methyl viologen (Janet Donahue). The mutants were grown in M9 glucose, and spread on M9 glucose plates with M9 top agar. Sterile filter disks soaked in 2% $H_2O_2$ or 0.1 M methyl viologen were placed on M9 plates and incubated overnight at 37$^o$C. Clear

zones were seen around the filter disks indicating growth inhibition due to $H_2O_2$ or methyl viologen exposure while the rest of the plate had lawns of bacterial growth. However, there was no difference in the size of the zones of inhibition between the wild type and the mutants. These results suggested that the susceptibility of the mutants to oxidative stress was similar to that of the wild type and therefore the rhodaneses may not be involved in repairing damage to iron sulfur clusters caused by oxidative stress.

Cyanide detoxification has also been proposed as a possible role for rhodaneses (167). The heptuple mutant FA036 was grown to log phase in LB medium (liquid) and then exposed to 0.3 mM potassium cyanide (Hui Cheng). The mutant grew as well as the wild-type, suggesting that the rhodaneses in *E. coli* are not involved in cyanide detoxification.

The sulfurtransferase mutants were grown on different sulfur sources to investigate whether any of the mutants are defective in utilizing the sulfur compounds (Janet Donahue). The single mutants FA012 (Δ *ygaP*), PJ1 (Δ *sseA*::$Sp^r$) and JLD17204 (Δ*glpE*) were grown overnight in M9 glucose minimal medium with limiting sulfur source (65 μM $MgSO_4$). The cells were grown to log phase then washed and transferred into fresh medium of the same composition containing either 65 μM $MgSO_4$ or 65 μM cysteine as the sulfur source. There was no difference in growth for the single mutants compared to the wild-type when $MgSO_4$ was used as the sulfur source (FIG. 2.3.8A). However when cysteine (65 μM) was used the Δ*ygaP* mutant showed a longer lag phase compared to the wild-type (FIG. 2.3.8B).

A

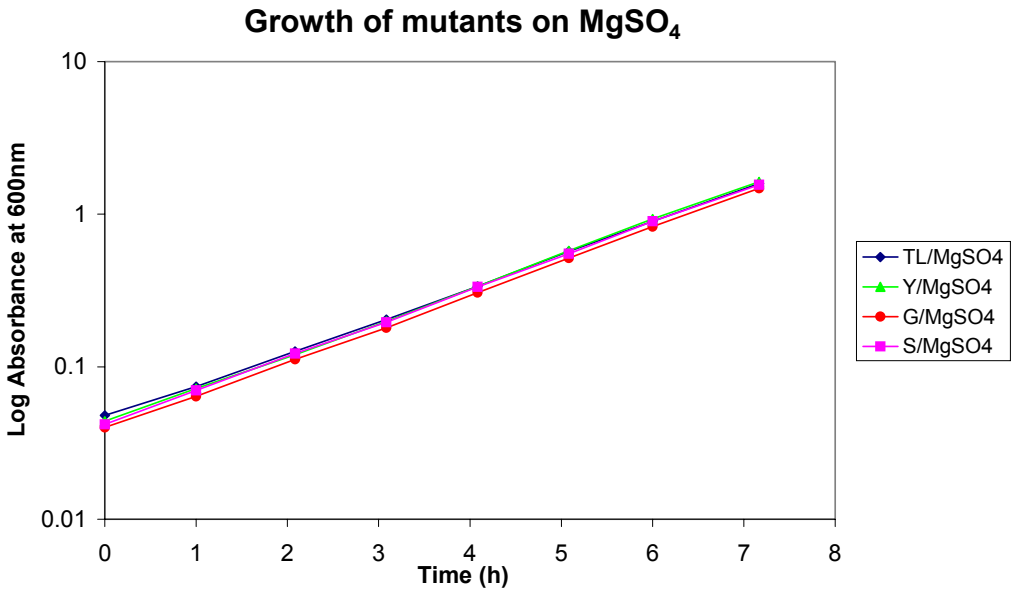


B

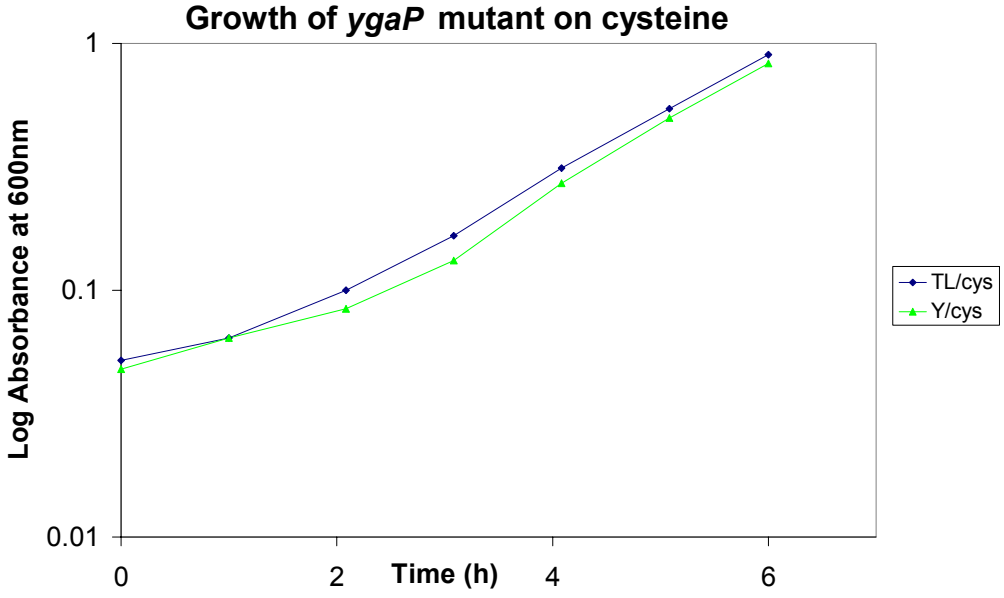


## FIG. 2.3.8. (A & B) Growth of mutants on various sulfur sources

A. The wild-type and the mutants grown with 65 µM MgSO4. TL, wild-type (TL524); Y, *ygaP* mutant (FA012); G, *glpE* mutant (JLD17204); S, *sseA* mutant (PJ1). B. The wild-type and the *ygaP* mutant (FA012) grown with 65 µM cysteine as the sulfur source.

C

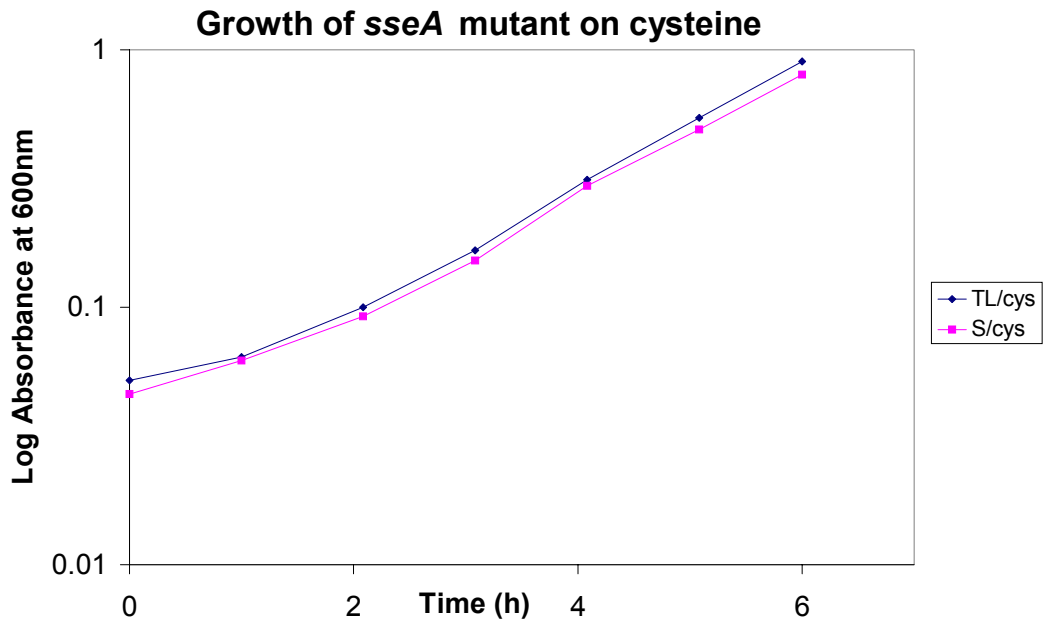


D

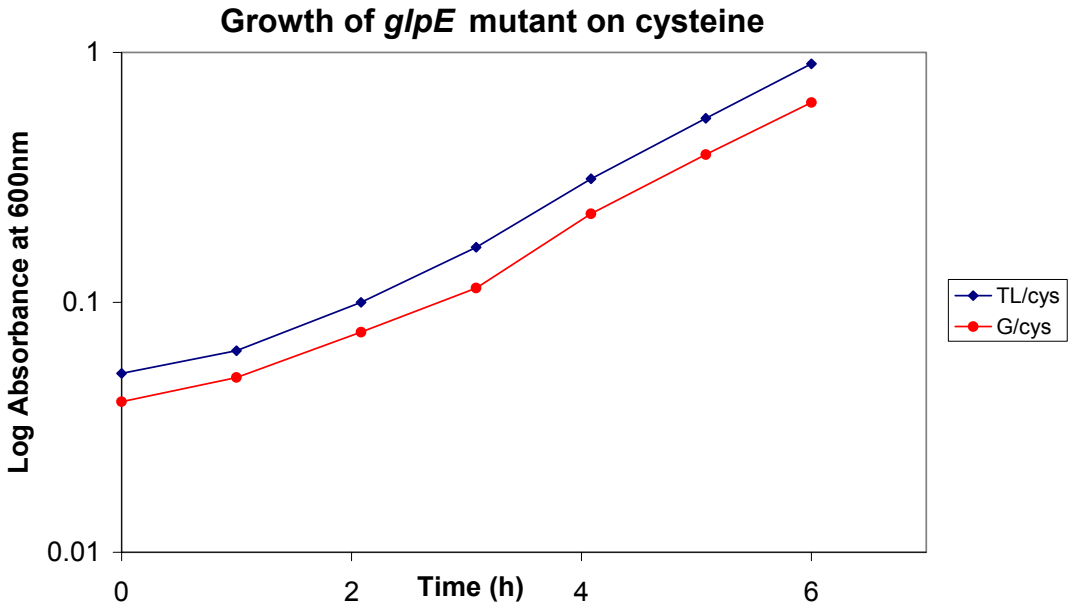


**FIG. 2.3.8.(C & D) Growth of mutants on various sulfur sources**

C. The wild-type (TL524) and the *sseA* mutant (PJ1) grown with 65 μM cysteine as the sulfur source.

D. The wild-type (TL524) and the *glpE* mutant (JLD17204) grown with 65 μM cysteine as the sulfur source.

## 2.4. Discussion.

### 2.4.1. Comparison of YgaP with other rhodaneses

*E. coli* is predicted to encode nine proteins containing one or more rhodanese homology domains. YgaP has a single rhodanese homology domain fused to a C-terminal membrane anchor. The other *E. coli* rhodaneses, GlpE and PspE, consist simply of a single rhodanese domain. The GlpE rhodanese of *E. coli* is the prototype of a single-domain rhodanese (7) composed of a 12-kDa rhodanese homology domain. GlpE displays sequence similarity to the C-terminal domain of the well-characterized bovine liver rhodanese (Rhobov) and to the *Azotobacter vinelandii* rhodanese (RhdA) (7). Rhobov and RhdA (3;4) are composed of two identically folded rhodanese domains with the active site cysteine located in the C-terminal domain of both enzymes. Despite the limited sequence similarity between the two domains, the very similar three-dimensional conformation suggests that the two domains in Rhobov and RhdA may have originated from ancestral gene duplication (3). SseA, a mercaptopyruvate sulfurtransferase of *E. coli*, also displays sequence similarity to Rhobov and RhdA with similarly arranged tandem domains (168). Another *E. coli* rhodanese, ThiI, involved in thiamin and 4-thiouridine biosynthesis, is a multidomain protein having an amino-terminal ThiI domain fused to a carboxy-terminal rhodanese domain (16;17).

The fact that YgaP has a hydrophobic extension at the carboxy terminus of the rhodanese domain and that it is solubilized from the membrane with detergents suggests that YgaP is an integral membrane protein. Sucrose density layer centrifugation further localized YgaP to the cytoplasmic membrane. The other *E. coli* rhodaneses GlpE and PspE are located in the cytoplasm and the periplasm, respectively (6;130). An important step in the characterization of

an integral membrane protein is to determine its membrane topology, that is, the number of transmembrane helices and the location of the N- and C-termini of the protein relative to the membrane (169). A number of topology prediction methods are available which are widely used as tools in understanding the topology of an integral membrane protein. The best current methods are known to predict the correct topology with a success rate of 65-70% (170). Topology prediction methods, TMHMM, HMMTOP and SOSUI were used to predict the membrane topology of YgaP. All of these methods suggested that the N-terminal rhodanese domain of YgaP is in the cytoplasm, with the protein anchored to the membrane by two transmembrane helices at the C-terminus that traverse the membrane (FIG. 2.4.1). TMHMM is one of the highly reliable and the best performing topology prediction methods currently used (170) suggesting that the topology predicted for YgaP is correct.

Catalytic properties of YgaP were determined using purified YgaP-$His_6$ and compared with those of the membrane-associated YgaP. The kinetic patterns as well as the $K_m$s for thiosulfate (55 and 69 mM) and cyanide (1.5 and 0.7 mM) for purified YgaP-$His_6$ and membrane-associated YgaP, respectively, were similar, indicating that the detergent solubilized, purified YgaP-$His_6$ behaved in a manner similar to that of the native enzyme anchored to the membrane. Like bovine rhodanese and the *E.coli* rhodaneses (GlpE and PspE), YgaP utilized a double displacement reaction mechanism. The low affinity of YgaP for thiosulfate is similar to that of GlpE ($K_m$ for thiosulfate 78 mM) suggesting that neither of these enzymes uses thiosulfate as the physiological substrate. Compared to GlpE and PspE, YgaP has a high affinity for cyanide ($K_m$ of about 1 mM compared to 17 and 43 mM for GlpE and PspE, respectively), which suggests that the enzyme may have a role in cyanide detoxification. However, the possibility of cyanide serving as a physiological substrate is unlikely, since 1 mM cyanide is known to

severely inhibit growth of the wild type as well as rhodanese mutants (130). The cyanide sensitivity of the wild type was comparable to rhodanese mutants indicating that the *E. coli* rhodaneses are not involved in cyanide detoxification (130). The physiological relevance of the high apparent affinity of YgaP for cyanide therefore remains unclear. The turnover number ($k_{cat}$) for YgaP (1 $s^{-1}$) is much lower than that of GlpE or PspE (115 $s^{-1}$ and 72 $s^{-1}$ per GlpE or PspE monomer, respectively). The low catalytic efficiency of YgaP could be due to the tight binding of cyanide to the enzyme-persulfide intermediate that allows the release of the product, thiocyanate at a very slow rate. Results of anion inhibition studies show that YgaP exhibits a similar pattern of inhibition to most anions as GlpE, except for phosphate, which inhibits YgaP activity more strongly than GlpE. Anion inhibition was observed for bovine rhodanese which was linked to the presence of certain basic residues near the active site (R186, R248 and K249) (171). These positively charged residues have also been implicated in substrate recognition. Although these residues are not conserved in YgaP, two positively charged residues, lysine and arginine are present in the active site loop of the enzyme that may contribute to the binding of the enzyme to the substrate.

Bovine rhodanese and the two soluble *E. coli* rhodaneses undergo autoxidation and lose activity (6;35;130). The inactive enzymes could be reactivated by micromolar concentration of cysteine. YgaP is also activated by addition of cysteine to the assay mixture. YgaP has two cysteine residues, one in its active site loop and the other near the C-terminus that may undergo autoxidation through intra/intermolecular interactions. The data from MALDI mass analysis and SDS PAGE of purified YgaP-$His_6$ suggest that YgaP forms a very stable dimer. Dimerization of YgaP might occur due to hydrophobic interaction between the transmembrane helices that may be closely packed in the membrane. Detergent and reduction resistant dimers were also observed

for PspC, a protein of the phage shock operon of *E. coli*. PspC has an N-terminal cytoplasmic domain, a single transmembrane domain and a periplasmic C-terminal domain containing a leucine zipper motif, which is suggested to participate in dimerization of the protein (172).

### 2.4.2. Physiological role of YgaP and other *E. coli* rhodaneses

Rhodaneses have been proposed to be involved in the biosynthesis of sulfur- containing cofactors like thiamin, biotin, molybdopterin and lipoic acid, biosynthesis of thiolated nucleosides of tRNAs, synthesis and repair of Fe-S clusters and selenium metabolism. In fact, the rhodanese domain of ThiI in *E. coli* has been shown to transfer sulfur for thiamin and 4-thiouridine biosynthesis (16;16;18;173). However, our work showed that besides ThiI, none of the proteins containing the rhodanese homology domain in *E. coli* are essential for the biosynthesis of the sulfur containing cofactors or thionucleosides in tRNAs.

Bovine rhodanese is able to reconstitute the Fe-S clusters of ferredoxin (138;166), succinate dehydrogenase (137) and mitochondrial NADH dehydrogenase (139) *in vitro* when incubated with thiosulfate, iron ions and reducing agents. Comparison of the sensitivity to oxidative stress of the wild type and the rhodanese mutants show that the rhodaneses are probably not involved in Fe-S cluster repair or biosynthesis. Since IscS and its homologs play a major role in Fe-S cluster biosynthesis in different organisms (80),(174) the participation of rhodaneses in Fe-S cluster biosynthesis could be insignificant (175).

It is hypothesized that rhodaneses may be involved in various aspects of sulfur metabolism (8;176). However, the *ygaP* mutant and the different rhodanese mutants did not require sulfur-containing cofactors or amino acids for growth on minimal medium and were not deficient in thionucleosides. The growth rates of rhodanese mutants were also similar to the wild

type on various sulfur sources. An exception may be the Δ*ygaP* mutant, which had a longer lag phase in cysteine-containing medium compared to the wild type. The implication of this result is not clear.

The presence of multiple rhodaneses predicted from genome sequence could be indicative of functional redundancy. However, the distinct cellular locations and domain architectures of the *E. coli* rhodaneses indicate diverse biological roles for these proteins. Among the nine proteins containing the rhodanese homology domain, YgaP is the only cytoplasmic membrane-associated rhodanese in *E. coli*. The unique cellular location of the protein along with the genome context of *ygaP* indicates an important and unique role for this rhodanese. The genomic context of *ygaP* in *E. coli* as well as in a wide variety of eubacteria (*P. aeruginosa*, *C. crecentus*, *Synechocystis*, *S. coelicolor*) suggest that it is the second gene in an operon with *ygaV*, which is predicted to encode a protein homologous to the ArsR-SmtB family of transcriptional regulators. A number of these bacterial metalloregulatory proteins have been described recently, including ArsRs which are repressors of arsenic resistance operons (177), SmtB of *Synechococcus* which is a $Zn^{+2}$- and $Cd^{+2}$- responsive repressor (177), NmtR of *Mycobacterium*, a cobalt and nickel sensing repressor (178) and NolR of rhizobium, which controls rhizobial nodulation genes and also functions as a global regulator (179). These regulators have helix-turn-helix DNA binding motifs that bind to operator sites, which facilitates regulation of transcription of downstream genes. Upon binding specific metal ions, these transcription factors dissociate from DNA and allow expression of genes that are involved in detoxification or homeostatis of metals in the cell. Sequence alignment of YgaV to the SmtB family of transcriptional regulators showed that YgaV has a conserved helix-turn-helix motif (FIG. 2.4.2). Furthermore the conserved Gly-X-X sequence (X represents hydrophobic residues)

at the end of the second helix found in all except SmtB and NolR is also present in YgaV. Finally, there is a cluster of hydrophilic residues following the Gly-X-X region in SmtB and other regulators that is also found in YgaV. The metal-binding ligands in SmtB include Cys61, Asp64, His97, Asp104, His106, His117 and Glu120. Although some of these residues are conserved in other metalloregulators, most are not. For ArsR the arsenic ligands are Cys32, Cy34 and Cys37. The difference in the metal binding residues indicates that the binding sites are unique for each metal-specific member of the family. The fact that *ygaP* is in the same operon with *ygaV* suggest that YgaV is an autoregulatory repressor or activator that regulates the expression of both *ygaV* and *ygaP* in response to some effector molecule. The effector could be a metal sulfide that interacts with YgaP to efflux or sequester the metal in the cell. It will be interesting to find out whether the expression of *ygaP* is under the control of YgaV and if the two genes are cotranscribed. Results of these studies could provide greater insights into the function of YgaP.

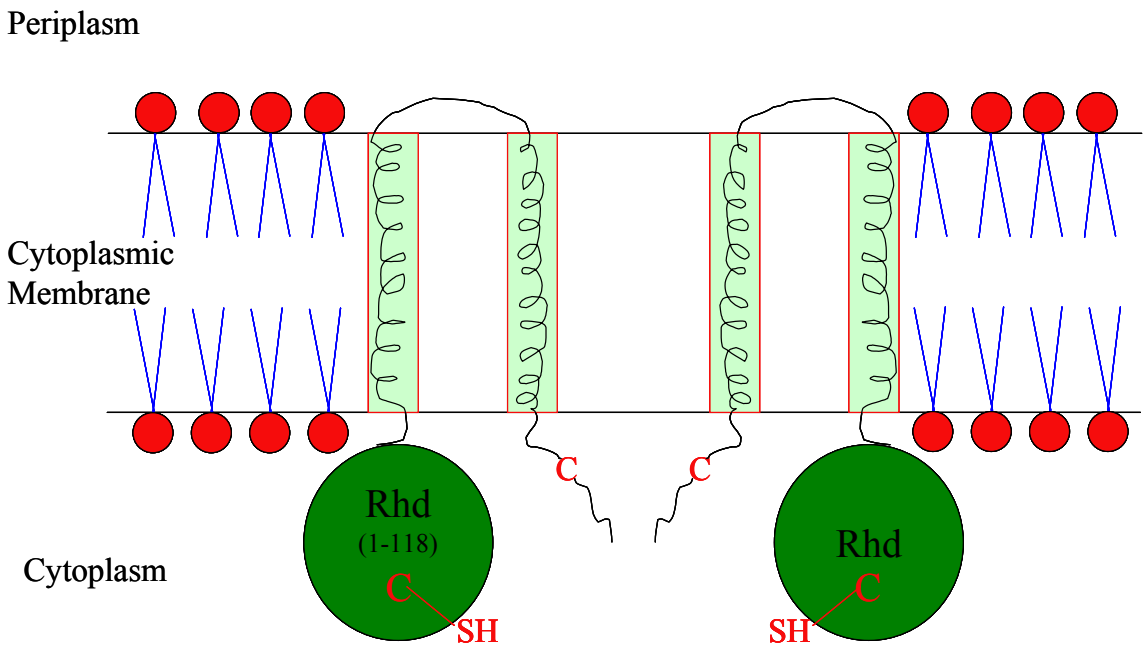


**FIG. 2.4.1. Membrane Topology of YgaP.**
Topology prediction methods predict this orientation of the protein. The rhodanese domain represented as a green circle is predicted to contain 118 amino acid residues. Residues 119-142 and residues 146-166 represent the two membrane spanning domains. The two conserved cysteine residues in the protein are shown in red.

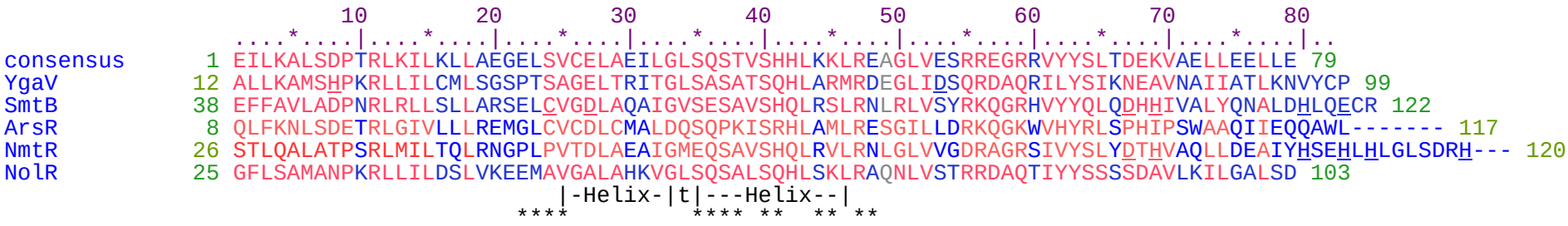


**FIG. 2.4.2. Comparison of YgaV to ArsR homologs.**

Residues shown in red are identical or similar to the consensus sequence. YgaV is a ArsR type transcriptional regulator from *E. coli*. SmtB is a Zinc-responsive dimeric repressor of *Synechococcus*. The underlined residues in SmtB are possible Zinc-binding residues. ArsR is the repressor protein for arsenic resistance operons of bacteria. NmtR is a nickel and cobalt-binding protein from *Mycobacterium tuberculosis*. Substitutions at the underlined residues affect nickel and cobalt binding. NolR is a global regulator that controls many proteins along with the rhizobial nodulation proteins.

# Chapter Three

# YbbB, a rhodanese paralog of *E. coli*, is a selenouridine synthase

## 3.1. Introduction.

Selenium is an essential component of various enzymes and macromolecules. It is present as a selenocysteine residue in many selenoproteins from prokaryotic and eukaryotic sources (97). Selenium is also found in the wobble position of several bacterial tRNAs as the modified base 5-methyl-amino-methyl-2-selenouridine and in tRNAs from plants, animals and archaea (93;95;119;125) . Isoaccepting species of lysine, glutamate and glutamine tRNA are the most abundant seleno-tRNAs found in bacteria (118;180) . Specific incorporation of selenium into tRNA and protein requires monoselenophosphate, since *selD* mutants of *Escherichia coli* or *Salmonella typhimurium* deficient in selenophosphate synthetase are unable to incorporate selenium into proteins or tRNAs (125;126) . While the pathway of selenium incorporation into protein is known (97;104) the steps or enzymes involved in the incorporation of selenium into tRNA are not completely defined. It is known that seleno-tRNA is derived from 2-thiouridine tRNA by replacement of the sulfur with selenium (119). A partially purified enzyme from *S. typhimurium*, termed tRNA 2-selenouridine synthase, was shown to catalyze the conversion of 2-thiouridine in tRNA to 2-selenouridine when supplemented with selenophosphate (127). However, the gene encoding tRNA 2-selenouridine synthase has not been defined.

Sulfurtransferases containing a rhodanese homology domain are ubiquitous proteins that catalyze the transfer of a sulfane sulfur atom from thiosulfate (rhodanese) or from 3-mercaptopyruvate (mercaptopyruvate sulfurtransferase) to thiophillic sulfur acceptors such as cyanide *in vitro* (1). These enzymes have a conserved cysteine residue at their active site that is known to participate in catalysis (7;15;162) . Proteins containing a single rhodanese homology domain of approximately 110 amino acids have been characterized (6;129;181) . In addition, rhodanese domains are found fused to a variety of protein domains of known or unknown function (1). The diversity in structure and fusion partners for the rhodanese homology domain suggests that this family of proteins functions in a variety of metabolic pathways.

The genome of *E. coli* is predicted to encode nine proteins containing a rhodanese homology domain. GlpE, PspE, YgaP and ThiI have rhodanese activity (6;17;129;130) , and SseA has mercaptopyruvate sulfurtransferase activity (11). ThiI, containing a carboxy-terminal rhodanese homology domain, is required for biosynthesis of 4-thiouridine in tRNA (16;18) and for the biosynthesis of the thiazole ring of thiamin (182). The physiological functions of the other eight *E. coli* rhodanese paralogs remain undefined.

Recent investigations aimed at defining the physiological functions of sulfurtransferases suggested involvement of these enzymes in selenium metabolism. First, it was found that a cysteine perselenide was generated on bovine rhodanese, presumably at the active site cysteine, by incubation of the enzyme with selenite in the presence of glutathione. The selenium-loaded rhodanese was capable of serving as a selenium donor for selenophosphate synthetase (91). Second, we observed that the *selD*

operon of several Gram-negative bacteria contained a second gene (*E. coli ybbB* orthologs) predicted to encode a protein with an amino-terminal rhodanese domain and a carboxy-terminal ATP-binding domain (FIG. 1.5.2). These observations suggested that YbbB might participate in selenium metabolism. The rhodanese homology domain of YbbB has two adjacent cysteine residues at its putative active site. In this work, an *E. coli* mutant deficient in *ybbB* was constructed and was found to be deficient in incorporation of selenium into tRNA. Purified YbbB protein was shown to possess tRNA 2-selenouridine synthase activity. The cysteine residue (Cys97) of YbbB that aligns most closely with the active site cysteine of the rhodanese domain was essential for activity. Thus, the physiological role of YbbB has been discovered, and the results indicate that the rhodanese homology domain functions as a selenium transfer protein for synthesis of 2-selenouridine in tRNA.

## 3.2. Materials and Methods.

### 3.2.1. Bacterial strains and plasmids

The bacterial strains and plasmids used in this study are described in Table 3.2.1 and 3.2.2, respectively. All strains are *E. coli* K-12 derivatives except for BL21*(DE3) which is derived from *E. coli* B. DH5αZ1 (141) was used as a host during plasmid construction.

### 3.2.2. Growth media and conditions

In general, cultures were grown in Luria-Bertani (LB) broth (144) supplemented with the appropriate antibiotic (200 μg/ml ampicillin, 25 μg/ml kanamycin or 10 μg/ml tetracycline). All cultures were grown at 37$^{o}$C unless indicated otherwise.

For overexpression of YbbB-His$_6$, cultures were grown anaerobically as described in later part of this section (see 3.2.4). Deletion of *ybbB* was carried out by the method of Datsenko and Wanner (145). The Km$^r$ cassette was excised from the Δ*ybbB*::Km$^r$-disrupted strain by transforming the cells with plasmid pCP20. pCP20 is an Ap$^r$ and Cm$^r$ plasmid that has a temperature sensitive origin of replication and thermal induction of yeast FLP recombinase synthesis (146). The ampicillin resistant transformants were selected at 30$^{o}$C and then colonies were purified on nonselective medium at 43°C. Loss of the Km$^r$ cassette and pCP20 was verified by plating the cells on medium supplemented with kanamycin and ampicillin or chloramphenicol.

Minimal media containing M9 salts and the following supplements: 0.2% glucose, 2 μg/ml thiamin and 0.01mM $MgSO_4$, was used for testing growth impairment of *ybbB* deletion strain.

P1 transduction was done according to the methods described by Silhavy et.al. (148)

Table 3.2.1. Bacterial Strains

| Strains | Genotype/Property | Derivation or Reference |
|---|---|---|
| MG1655 | $F^-$ *rph-1 ilvG rfb-50* $\lambda^-$ | (149) |
| TL524 | MG1655 *Δ(lacZYA-argF) U169* | (150) |
| BL21(DE3) | $F^-$ *ompT hsdS*$_B$ ($r_B^- m_B^-$) *gal dcm* (*λcIts857 ind1 Sam7 nin5 lacUV5-T7 gene1* | |
| BL21*(DE3) | BL21(DE3) *rne131* | (152) |
| BW25113 | *lacI*$^q$ *rrnB*$_{T14}$ *ΔlacZ*$_{WJ16}$ *hsdR514 ΔaraBAD*$_{AH33}$ *ΔrhaBAD*$_{LD78}$ | (145) |
| CAG12171 | MG1655 *purK79*::Tn*10* $\lambda^-$ *rph-1* | (153) |
| FA026 | BW25113 (Δ*ybbB*::$Km^r$) | This work |
| FA027 | BW25113 Δ*ybbB*::*FRT*[a] | FLP mediated removal of $Km^r$ of FA026 |
| FA029 | BW25113 (Δ*ybbB*::$Km^r$ *purK79*::Tn*10*) | P1 (CAG12171) → FA026 |
| FA031 | TL524 (Δ*ybbB*::$Km^r$ *purK79*::Tn*10*) | P1 (FA029) →TL524 |
| FA034 | TL524 (Δ*ybbB*::*FRT*[a] *purK79*::Tn*10*) | FLP mediated removal of $Km^r$ of FA031 |
| FA036 | TL524 Δ *sseA*::$Sp^r$ Δ*ynjE*[a] Δ*ygaP*[a] Δ*glpE*[a] Δ*pspE*[a] Δ*yceA*[a] Δ*ybbB*::$Km^r$ | P1 (FA029) → JLD20502 |
| JLD20502 | TL524 Δ *sseA*::$Sp^r$ Δ*ynjE*[a] Δ*ygaP*[a] Δ*glpE*[a] Δ*pspE*[a] Δ*yceA*[a] | FLP-mediated removal of $Km^r$ of JLD19902 |

[a] FLP-mediated excision of $Km^r$ cassette leaves and 88 bp FRT "scar"

Table 3.2.2. Plasmids used or constructed in the study of YbbB

| Plasmids | Genotype/Property | Derivation or Reference |
|---|---|---|
| pCP20 | $FLP^+$ $Ap^r$ $Cm^r$ $rep^{ts}$ | (146) |
| pT7-7 | ColEI origin, $Ap^r$, T7 promoter | (142) |
| pGZ117 | $(His)_6$ linker between *Sal*I and *Hin*dIII of pT7-7 | (143) |
| pFRT-K | Gene disruption plasmid, FRT-flanked $Km^r$ cassette in *Eco*RI/*Hin*dIII of pBS $KS^+$ | This work |
| pKD46 | OriR101 $Ap^r$ *repA*$^{ts}$ *araC*-$P_{araB}$ λRed (γ β *exo*) | (145) |
| pFA202 | *ybbB* cloned into *Nde*I and *Sal*I of pLK100 | This work |
| pFA204 | Derivative of pFA202, *Nde*I/ *Hin*dIII cloned into pT7-7 | This work |
| pFA150 | 5' flanking region of *ybbB* cloned into *Sal*I/*Hin*dIII of pFRTK | This work |
| pFA151 | 3' flanking region of *ybbB* cloned into *Bam*HI/*Eco*RI of pFA150 | This work |
| pFA218 | Derivative of pFA204 | This work |
| pFA210 | Derivative of pFA204 | This work |

Table 3.2.3. Oligonucleotides

| Name | Oligonucleotide sequence 5'-3'[a] | Restriction site |
|---|---|---|
| ybbBF | CTTTTAcaTATGCAAGAGAGACAC | *Nde*I |
| YbbB-His R | TCCCgtcgacCCGCGCCTTAACCCATTC | *Sal*I |
| BNRI | CAAGGAAgCTTGATTTTTAACTGC | *Hin*d*III* |
| BNFI | ACTGGTCgaCCGGGTAATCCCAAC | *Sal*I |
| BCRI | ATAAGGATcCGACACTCATATC | *Bam*HI |
| BCFI | GGCGGAATtcGTTAAGGCGCGG | *Eco*R*I* |
| YBBB2[a] | AAGGCCATGTGTCAGATCtAGTCG | *Bgl*II |
| BBCS-1[b] | AATTGCCACGGGCGCA***GCt***GAGAATACC | *Btg*I |
| BBCS-2[b] | AATTGCCACGGGC***GCt***GCAGAGAATACC | *Btg*I |

a. Lower case letters indicate base substitutions to create restriction sites or mutations. Restriction sites are underlined.

b. YBBB2 is approximately 50 bp downstream of the stop codon of *ybbB*

c. Letters in bold and italicized indicate Cys-Ser mutation

### 3.2.3. Construction of YbbB-$His_6$ expression plasmid.

The gene for *ybbB* was amplified by PCR using forward and reverse primers ybbBF and ybbBHisR, respectively (Table 3.2.3). After PCR, the *Nde*I and *Sal*I fragment was cloned into pGZ117 between the $T_7$ promoter and the region encoding a $(His)_6$ affinity tag and thrombin cleavage site (FIG. 3.2.1) (143). Replacement of the stop codon of *ybbB* with a *Sal*I siteand subsequent cloning resulted in expression of YbbB-$His_6$ with the C-terminal amino acid sequence AR|VDLVPR*$GSH_6$ where the residues to the right of the vertical line are the additional residues at the C-terminal end of YbbB; the asterisk indicates the thrombin cleavage site. Sequencing of the insert in the resulting plasmid pFA202, revealed a 6 bp duplication (ATACAT) between the ribosome binding site and the start codon of the gene ($^{rbs}$AAGGAGATATACAT*ATACAT* $^{startcodon}$ATG). However, the sequence of YbbB was correct. pFA202 was digested with *Nde*I and *Hin*dIII and the resulting fragment consisting of *ybbB* with the additional residues at the C-terminus encoding the his-tail was cloned into pT7-7 (FIG. 3.2.1). The resulting clone (pFA204) was sequenced from the ribosome binding site to the end of *ybbB*. The sequence of YbbB and the ribosome binding site was correct.

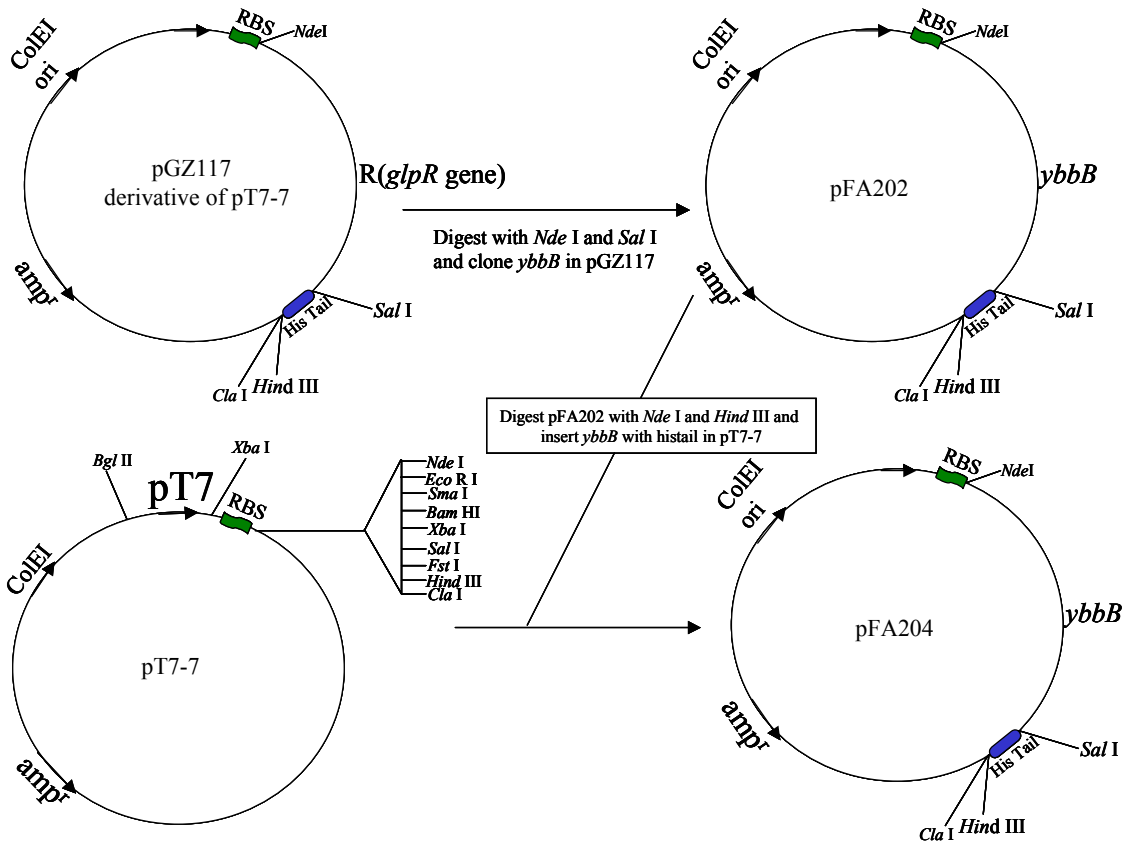


**SalI to HindIII Sequence in pGZ117**

SalI HindIII

GTC GAC CTG GTT CCG CGT GGA TCC $(CAC)_5$ CAT TAA GCT T

CAG CTG GAC CAA GGC GCA CCT AGG $(GTG)_5$ GTA ATT CGA A

V D L V P R G S $H_5$ H

**Sequence of *ybbB* near C-terminus after cloning(pFA202)**

SalI HindIII

*ybbB*...GCG CGG GTC GAC CTG GTT CCG CGT GGA TCC $(CAC)_5$ CAT TAA GCT T

*ybbB* CGC GCC CAG CTG GAC CAA GGC GCA CCT AGG $(GTG)_5$ GTA ATT CGA A

A R V D L V P R G S $H_5$ H

14 Additional amino acid residues

**FIG. 3.2.1. Construction of YbbB expression plasmid**

### 3.2.4. Overexpression and purification of YbbB.

It was observed that expression of YbbB under anaerobic conditions was approximately 2 times higher than under aerobic conditions. A 100 ml overnight culture of BL21*(DE3) (pFA204) was grown aerobically for 8-9 hours to an $OD_{600}$ of ~ 1.0-1.5. Cells were collected by centrifugation, resuspended in 2 ml of LB and injected into 1 L of anaerobic LB media supplemented with formate (2 mM), selenite (0.1 μM) and ampicillin. The culture was grown anaerobically at 37°C to an $OD_{600}$ of 0.3 and induced with 0.5 mM IPTG for 2.5-3 hours.

For comparison of YbbB expression under aerobic conditions, cells were grown overnight, harvested by centrifugation and resuspended in same volume of LB. Following fifty fold dilution into LB supplemented with ampicillin, the culture was grown to an $OD_{600}$ of 0.4-0.6 and overexpression of YbbB was achieved by induction with 0.5 mM IPTG for 2.5-3 hours.

YbbB-$His_6$ was purified from a 1 liter culture grown anaerobically. After induction the cells were harvested by centrifugation and resuspended in 10 ml of 20 mM sodium phosphate buffer, 0.5 M NaCl, 10 mM imidazole (pH 7.5). The cells were lysed by two passages through a French pressure cell at 12,000-16,000 psi. The cell lysate was centrifuged at 3000 × g for 6 min at 4°C to remove cell debris and unbroken cells. The clarified supernatant was brought to 1% streptomycin sulfate, kept on ice for 30 min and then centrifuged at 30,000 × g for 30 min to remove nucleic acids. The resulting supernatant was brought to 40% saturation with $(NH_4)_2SO_4$. The $(NH_4)_2SO_4$ suspension was kept on ice for 30 min and centrifuged at 30,000 × g for 30 min at 4°C . The $(NH_4)_2SO_4$ pellet (containing YbbB) was dissolved in 1 ml of 20 mM sodium phosphate

buffer, 0.5 M NaCl, 10 mM imidazole (pH 7.5) and loaded on a Talon cobalt resin column (BD Bioscience, Clonetech) equilibrated with the same buffer containing 10 mM 2-mercaptoethanol. After washing with 10 column volumes of the same buffer, YbbB was eluted with 5 bed volumes of a gradient of 50-500 mM imidazole. YbbB eluted from the column at 150 mM imidazole.

### 3.2.5. Construction of a chromosomal *ybbB* gene disruption.

Construction of strains having a *ybbB* gene disruption was carried out using a modification of the method of Datsenko and Wanner (145) where λ Red recombinase facilitated replacement of the *ybbB* gene with a kanamycin resistance cassette flanked by FRT sites. For our experiments pFRT-K (Table 3.2.2) was constructed by introducing a 1.5 kb kanamycin-resistance cassette ($Km^r$) flanked by *FRT* sites (FLP recombinase site) from pCP15 (146) into the *Eco*RI-*Hin*dIII sites of pBluescript-$KS^+$ (Stratagene). Thus, pFRT-K contains multiple cloning sites on each side of the $Km^r$ cassette for cloning chromosomal DNA sequences that target the gene disruption.

For construction of the *ybbB* knockout strain, a 182 bp fragment, ending 52 bp upstream of the ATG codon of *ybbB* was amplified by PCR using the primers BNFI and BNRI (Table 3.2.3). A 119 bp fragment consisting of the 3' flanking region of YbbB including 22 bp of the coding region at the C-terminal end of *ybbB* was amplified using primers BCFI and BCRI (Table 3.2.3). The C-terminal PCR product was digested with *Bam*HI and *Eco*RI and ligated into the same site of pFRT-K creating pFA150. Subsequently the N-terminal PCR product was digested with *Hin*dIII and *Sal*I and cloned

into the same site of pFA150, creating plasmid pFA151 (FIG.3.2.2). pFA151 was linearized with *Sal*I and *Bam*HI and the resulting 1.8 kb DNA fragment harboring the $Km^r$-FRT cassette flanked by N-terminal and C-terminal flanking regions of *ybbB* was introduced by transformation into BW25113 (pKD46) by selecting for kanamycin resistance (Strain FA026). The $Km^r$ cassette of FA026 was excised by yeast FLP recombinase of pCP20 that allows homologous recombinations between the FRT sites flanking the $Km^r$ cassette (146). pCP20 is an $Ap^r$ and $Cm^r$ plasmid that has a temperature sensitive origin of replication and thermal induction of yeast FLP recombinase synthesis (146). After transformation of FA026 with pCP20, the ampicillin resistant transformants were selected at 30°C and then colonies were purified on nonselective medium at 43°C. Loss of the $Km^r$ cassette and pCP20 was verified by plating the cells on medium supplemented with kanamycin and ampicillin. The resulting strain FA027 was $Km^s$ and $Am^s$.

The deletion removes most of the gene leaving only 22 bp from the C-terminal coding region of *ybbB*. Colonies with the *ybbB* gene deletion were verified by PCR using primers YBBB2 and BNFI (Table 3.2.3). Further evidence for the chromosomal location of *ybbB*::$Km^r$ was obtained by showing cotransduction of *ybbB*::$Km^r$ with a nearby Tn*10* insertion (*purK79::*Tn*10*). The *purK79*::Tn*10* marker was introduced into strain FA026 by P1 transduction, with selection for $Tc^r$, creating strain FA029. A P1 lysate of strain FA029 was made and *ybbB*::$Km^r$ was subsequently moved to strain TL524 by P1 transduction, with selection for $Tc^r$ generating FA031. The $Km^r$ cassette was excised from strain FA031 by FLP recombinase creating strain FA034.

### 3.2.6. Construction of Cys-Ser variants of YbbB.

Expression vectors for production of Cys96Ser and Cys97Ser variants of YbbB were constructed by performing PCR amplification of the region containing the two cysteines using plasmid vector pFA204 as the template and ybbBF and BBCS-1 or ybbBF and BBCS-2 as primers (Table 3.2.3). After amplification the PCR products were digested with *Nde*I and *Btg*I and cloned into the same sites of pFA204 replacing the wild type sequence with the PCR products. The 300 bp *Nde*I – *Btg*I regions of the resulting plasmids (pFA218 and pFA210) were subsequently sequenced and found to be correct.

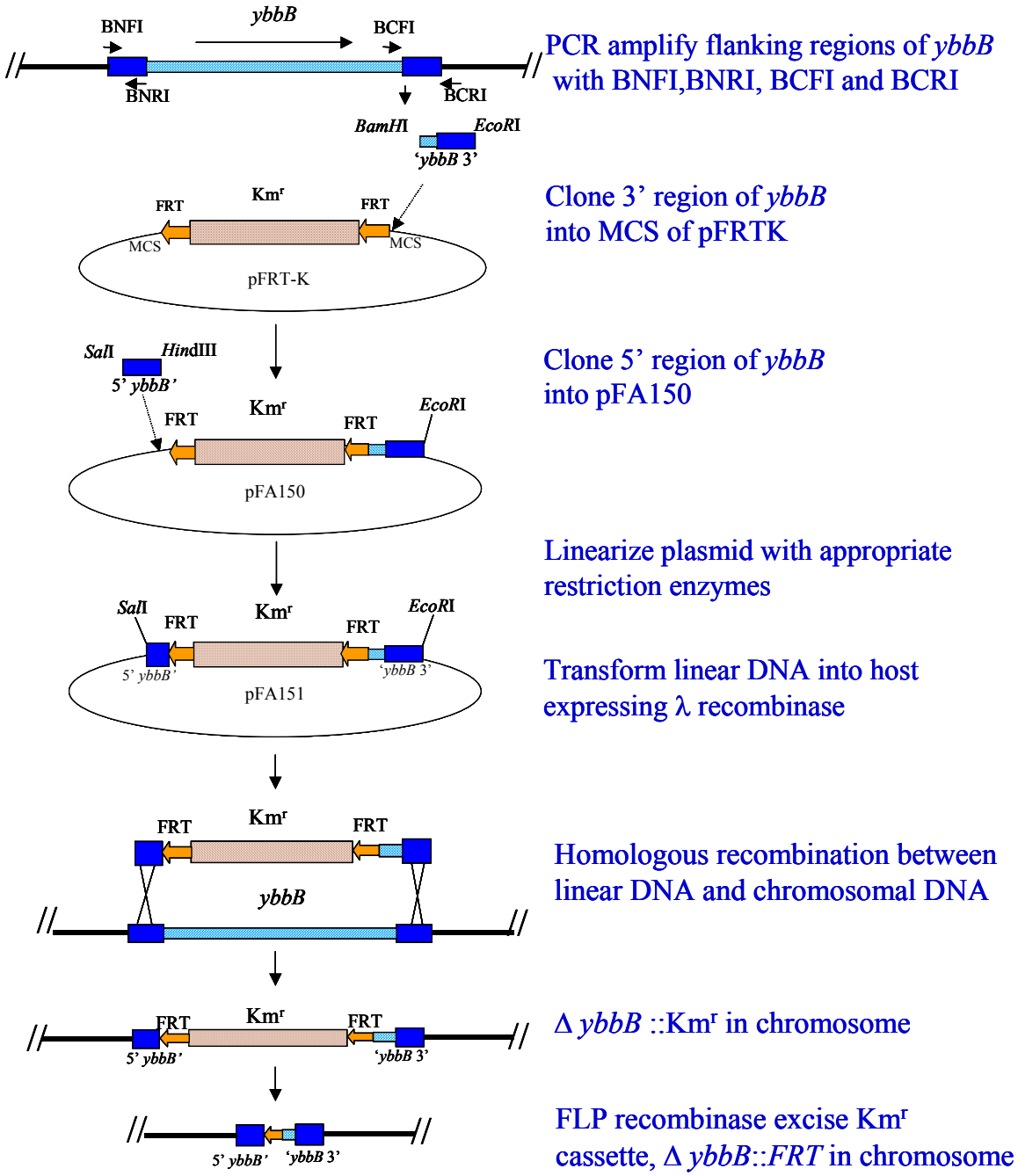


**FIG. 3.2.2. Construction of chromosomal *ybbB* gene disruption**

N- and C-terminal flanking regions of *ybbB* are represented in dark blue. *ybbB* is represented by blue dots. FRT is FLP recombinase target site.

## 3.3. Results.

### 3.3.1. Disruption of chromosomal *ybbB*.

To address the function of YbbB in *E. coli*, 1070 bp of the coding sequence of *ybbB* was replaced with a 1.5 kb $Km^r$ cassette flanked by FRT sites (145;146). After removal of the $Km^r$ cassette by FLP recombinase, *ybbB* deletion was verified by PCR analysis of genomic DNA with primers BNFI and YBBB2 flanking *ybbB*. FIG. 3.3.1 shows the PCR products for the wild-type and the *ybbB* deletion strain. The observed PCR products were close to the expected sizes of 1372 and 328 bp for the wild-type *ybbB* gene and the *ybbB* deletion strain, respectively.

P1 transduction was used for mapping Δ*ybbB*::$Km^r$ in the *E. coli* genome. A donor strain with a *Tn*10 marker (*purK79*::*Tn*10) near *ybbB* was used for this purpose. After P1 transduction into the recipient (FA026, Δ*ybbB*::$Km^r$), colonies were selected for $Tc^r$ and then scored for $Km^r$. Of the 100 $Tc^r$ transductants, 57 were $Km^s$. The distance between *ybbB* and (*purK79*::*Tn*10) is 0.45 min (20,829 bp) on the *E. coli* chromosome having a calculated cotransduction frequency of 49%. The observed cotransduction frequency of *ybbB* and (*purK79*::*Tn*10) was close to the expected value suggesting that the *ybbB* deletion is present in its target location.

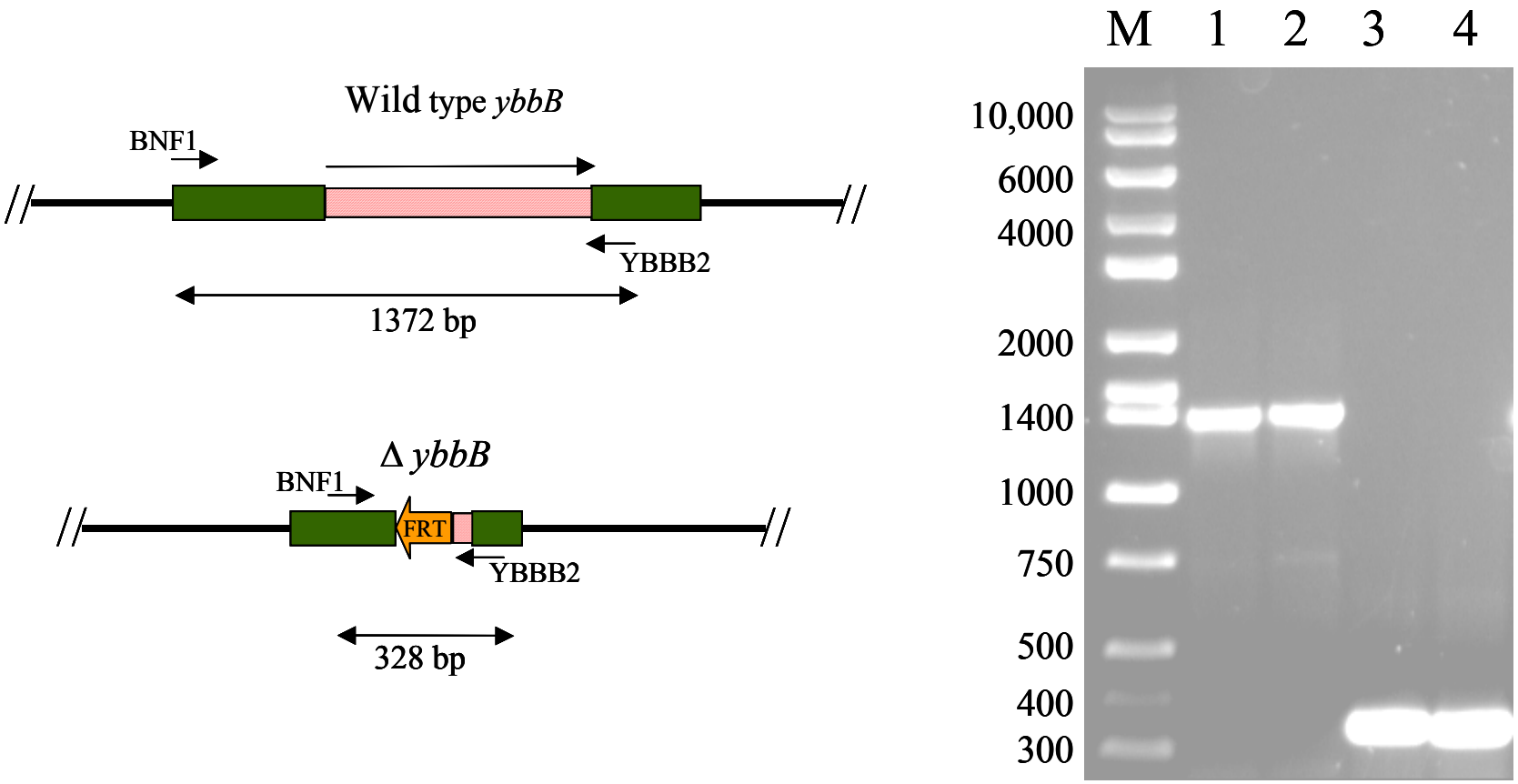


**FIG. 3.3.1. Verification of *ybbB* deletion**

The expected sizes of PCR products obtained using chromosomal DNA templates from the wild-type and the Δ*ybbB* strain (after excision of the Km$^r$ cassette) are shown on the left. Analysis of the PCR reactions by agarose gel electrophoresis is shown on the right. Lane M, DNA size markers (bp); lane 1 and 2, wild type; lane 3 and 4, DNA from two isolates from Δ*ybbB* strain.

### 3.3.2. Characterization of Δ*ybbB* strain

To find out whether *ybbB* deletion causes growth impairment, the mutant strain (FA034) was grown on M9 glucose minimal media without any supplements. However there was no difference in growth between the wild-type and the mutant suggesting that the deletion of *ybbB* does not cause an apparent growth defect. The genome context of *ybbB* in *P. aeruginosa* suggests a possible role for YbbB in selenium metabolism. To investigate whether the Δ*ybbB* strain is capable of incorporating selenium into tRNAs or proteins, the Δ*ybbB* strain and the wild-type were grown overnight anaerobically in LB supplemented with 0.1μM $SeO_3^{2-}$ and 20 μCi$^{75}$ $SeO_3^{2-}$. Extracts of these cells were analyzed for $^{75}$Se labeling by 12% SDS-PAGE gel and PhosphoImager analysis. FIG. 3.3.2A shows the SDS-PAGE of $^{75}$Se-labeled proteins and tRNAs in the wild-type and Δ*ybbB* strain. The top bands (FIG. 3.3.2) correspond to $^{75}$Se-labeled formate dehydrogenase present in both the wild type and the Δ*ybbB* strain. The $^{75}$Se-labeled tRNA band, observed at the lower end of the image for the wild type was absent from the Δ*ybbB* strain. The tRNA band was also missing from the heptuple rhodanese mutant (FA036) that contains deletion of seven rhodanase like genes including *ybbB* (FIG. 3.3.2B). However, the sextuple rhodanese mutant (JLD20502), precursor of the heptuple mutant, without the *ybbB* deletion, displayed the labeled tRNA band. These results show that the *ybbB* mutant is unable to incorporate $^{75}$Se into tRNAs. However, *ybbB* deletion does not affect specific incorporation of $^{75}$Se into proteins. The presence of active selenium-containing formate dehydrogenase ($FDH_H$) in the Δ*ybbB* strain was also verified by benzyl viologen overlay assay (G. Lacourciere, NIH). For the assay, the cells

from the Δ*ybbB* strain and the wild-type were grown overnight anaerobically at 37ºC on LB agar plates. To identify potential formate dehydrogenase mutants, a dye overlay solution, containing agar (0.75%), benzyl viologen (1 mg/ml) and sodium formate (0.25 mM) was poured over the growth plates and placed under anaerobic conditions. After a few minutes purple colored colonies appeared on both plates as a result of the reduction of benzyl viologen, which is consistent with the presence of active selenium-containing formate dehydrogenase ($FDH_H$) in the *ybbB* disrupted strain as well as the wild-type (FIG. 3.3.3).

The absence of seleno-tRNAs in the *ybbB* mutant (FA034) was further investigated by HPLC analysis (G. Lacourciere, NIH) of nucleosides derived from the tRNAs of both the wild-type and *ybbB* deletion strain. The wild-type and the Δ*ybbB* strain were grown in the presence of [$^{75}$Se]selenite and bulk tRNA was isolated and digested with P1 nuclease and alkaline phosphatase. The resulting nucleosides were separated by HPLC on a C-18 column and $^{75}$Se labeling was detected with a scintillation counter. The HPLC data shows that in the wild type [$^{75}$Se]mnm$^5$se$^2$U eluted at the retention time expected for the elution of this nucleoside. No peak for [$^{75}$Se]mnm$^5$se$^2$U was detected in the *ybbB* deletion strain (FIG. 3.3.4). These results suggest that YbbB is involved in the biosynthesis of seleno tRNAs in *E. coli*.

Since 2-selenouridine tRNAs are made from 2-thiouridine tRNAs (119;121;183), it is conceivable that the *ybbB* deletion could affect either the conversion of 2-thiouridine to 2-selenouridine or the biosynthesis of the precursor 2-thiouridine tRNAs itself. HPLC analysis of nucleosides from tRNAs of wild-type and the *ybbB* mutant showed that both

strains possess 2-thiouridine in their tRNAs(C. Lauhon, Univ. of Wisconsin), indicating that YbbB is specifically involved in the incorporation of selenium into tRNAs.

To find out if the *ybbB* deletion could be complemented by the cloned wild-type *ybbB* gene, the mutant strain was transformed with a plasmid containing cloned *ybbB*. The reapperance of the $^{75}$Se-labeled tRNA band in the mutant strain seen in FIG. 3.3.2A (lane 3) suggests that the phenotype of the mutant strain is in fact due solely to the *ybbB* deletion in the genome.

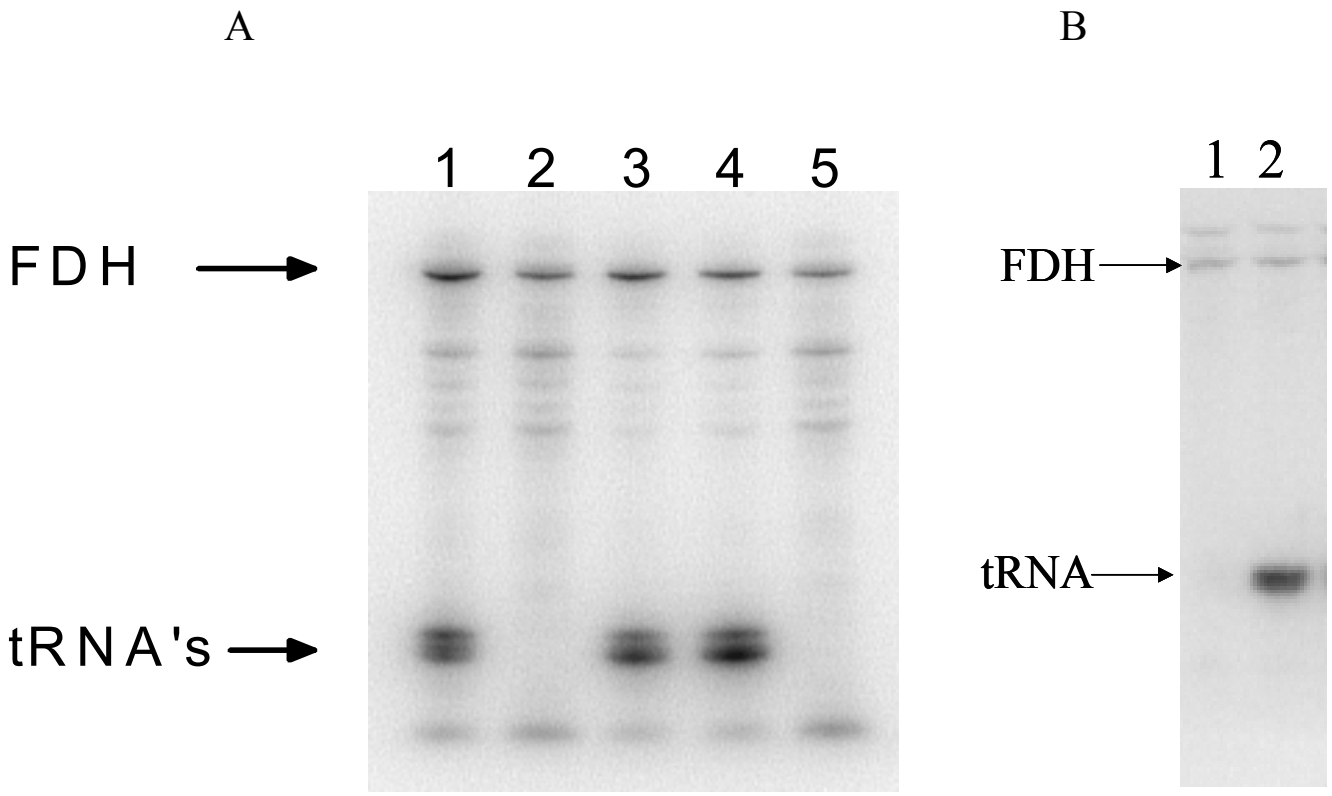


**FIG. 3.3.2. SDS-PAGE of wild-type and mutant strains**
Image of SDS PAGE showing $^{75}$Se labeled tRNA and protein. A .Lane 1, wild-type (TL524); lane 2, Δ*ybbB* strain (FA034); lane 3, Δ*ybbB* strain with cloned *ybbB* (FA034, pFA204); lane 4, Δ*ybbB* strain transformed with *ybbB*$^{C96S}$ clone (FA034, pFA218) and lane 5, Δ*ybbB* strain transformed with *ybbB*$^{C97S}$ clone (FA034, pFA210). B. Lane 1, heptuple mutant (FA036); lane 2, sextuple mutant (JLD20502).

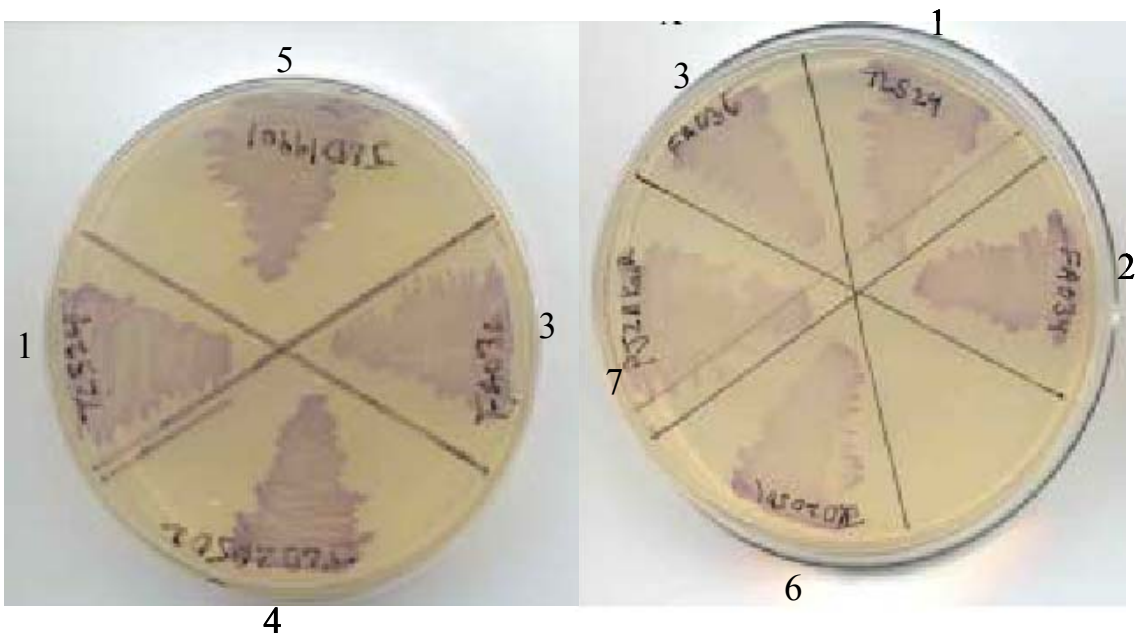


**FIG. 3.3.3. Benzyl viologen overlay assay for wild-type and mutant strains**

Purple colored colonies observed for the wild-type and mutant strains. 1, wild-type (TL524); 2, Δ*ybbB* strain (FA034); 3, heptuple mutant (FA036); 4, sextuple mutant (JLD20502) and 5, pentuple mutant (JLD19901). The assay was also done for 6, Δ*yceA* strain (JLD20501) and 7, Δ*ynjE* strain (PJ2).

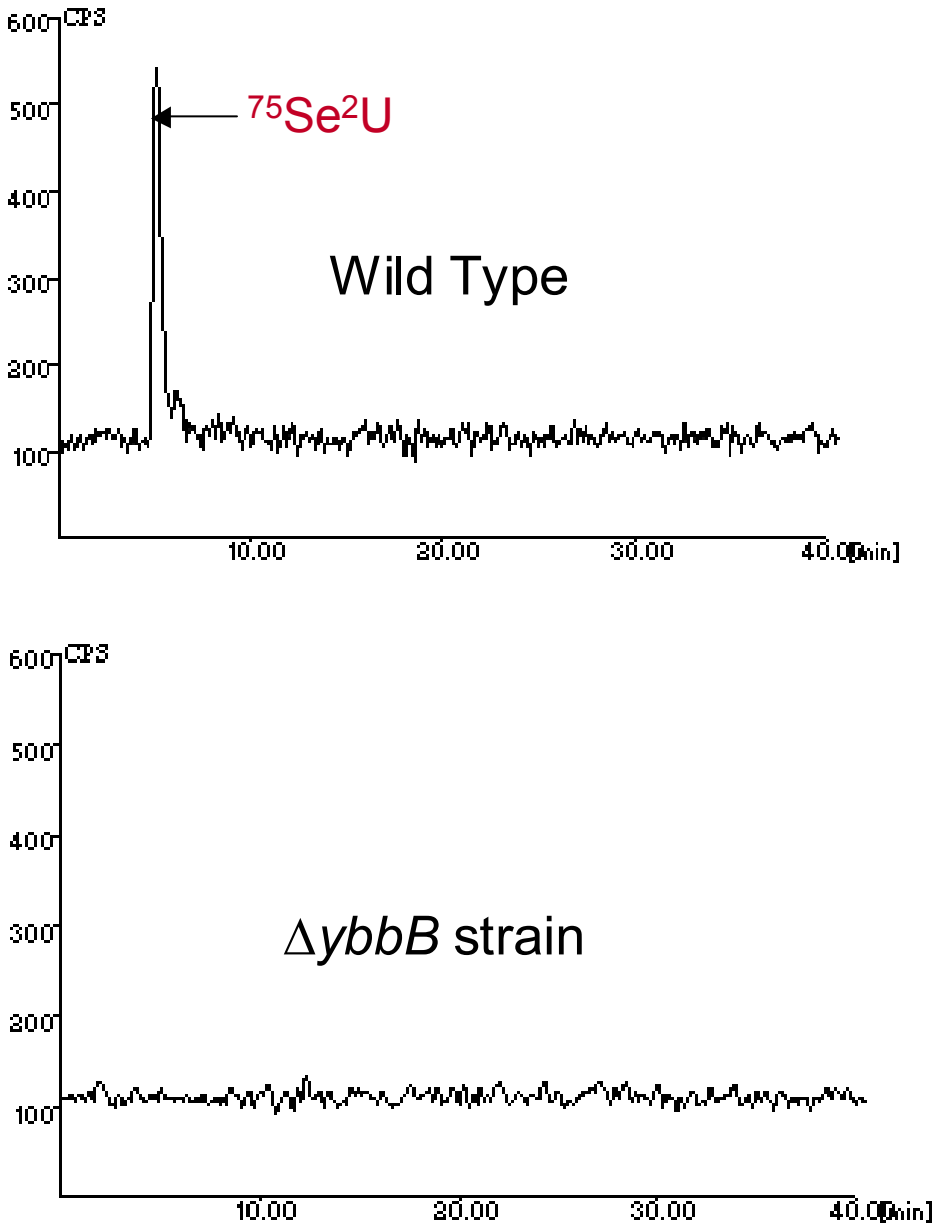


**FIG. 3.3.4. HPLC analysis of nucleosides from $^{75}$Se labeled tRNA from wild-type and Δ*ybbB* strain**

The $^{75}$Se labeled peak for mnm$^5$Se$^2$U is present in the wild type but not in Δ*ybbB* strain.

Proteins containing the rhodanese homology domain have a conserved cysteine residue in their active site that is known to participate in catalysis. YbbB has two adjacent cysteine residues Cys96 and Cys97. Cys97 aligns with the active site cysteine of the rhodaneses. To investigate whether either of these cysteines participates in YbbB activity, the two cysteines were individually mutated to serine. *ybbB* clones carrying the Cys to Ser mutations were used for complementation of the *ybbB* deletion. The $ybbB^{C96S}$ clone complemented the *ybbB* deletion but the y$bbB^{C97S}$ clone did not. These results show that Cys97 is required for the synthesis of $mnm^5se^2U$ *in vivo*, and Cys96 is not required (FIG. 3.3.2A, lanes 4 and 5).

### 3.3.3. Purification of YbbB-$His_6$.

YbbB was expressed with a C-terminal hexahistidine tag from the T7 promoter in pFA204. After disruption of the cells, a cell free extract was recovered and subjected to streptomycin sulfate treatment followed by $NH_4SO_4$ precipitation to remove impurities from the soluble fraction containing YbbB. Immobilized metal affinity chromatography using Talon $Co^{2+}$resin was used for purification of YbbB-$His_6$. A 1 liter culture yielded 1.2 mg of purified YbbB-$His_6$. An apparent molecular weight of about 43 kDa was observed on SDS-PAGE (FIG. 3.3.5), which is close to the expected value of 42,754. Spectral analysis of purified YbbB-$His_6$ showed a strong peak with maximum absorbance at 260 nm, suggesting that YbbB might be bound to nucleic acids. Assay of rhodanese activity of purified YbbB-$His_6$, using 20 μg of purified protein and a reaction time of 40 min showed that the enzyme had low activity (0.017-0.03 μmoles/min/mg) compared to

other known rhodaneses (270 and 150 μmoles/min/mg for purified GlpE and PspE, respectively) suggesting that the enzyme does not function as a rhodanese.

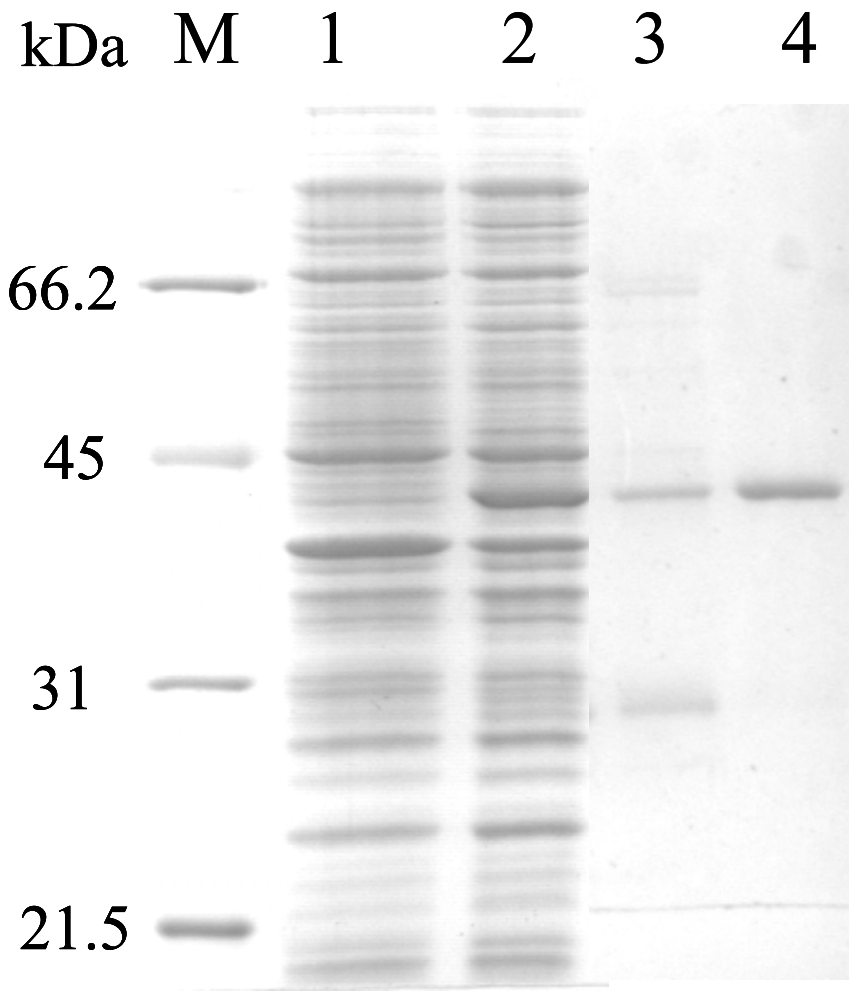


**FIG. 3.3.5. SDS PAGE of overexpressed and purified YbbB-His$_6$**
Lane M, Molecular weight markers; lane 1, crude extract from vector control BL21*(DE3)(pT7-7); lane 2, crude extract from strain BL21*(DE3)(pFA204) overexpressing YbbB; lane 3 and 4, purified fractions.

## 3.4. Discussion.

YbbB is one of the nine proteins in *E. coli* that contains a rhodanese homology domain. It is a multidomain protein that has an amino-terminal rhodanese domain consisting of ~ 110 amino acid residues and a carboxy-terminal domain containing a "P-loop" motif. The multi-domain nature of YbbB is comparable to ThiI, another multidomain protein in *E. coli* involved in the synthesis of thionuclosides in tRNAs and the thiazole ring of thiamin (17). ThiI has an amino-terminal THUMP domain, a central P-loop ATPase domain and a carboxy-terminal rhodanese domain (133). The THUMP domain (named after thiouridine synthases, methylases and pseudouridine synthases) is predicted to be involved in RNA binding and is shared by enzymes that carry out RNA modification, namely, methylation, pseudouridinylation and thiouridinylation. The central P-loop ATPase domain together with the carboxy terminal rhodanese domain catalyzes the formation of 4-thiouridine. A search for the THUMP domain in YbbB did not detect this region. The THUMP domain was also not detectable in other thionucleoside synthases like MnmA or MiaB which are involved in the synthesis of thiolated uridine and adenine derivatives respectively, indicating that this domain is not present in all RNA modifying enzymes. The P-loop motif is a conserved glycine rich region that typically forms a flexible loop between a hydrophobic beta-strand and an alpha helix and is found in proteins that bind ATP or GTP (184). In YbbB, the P-loop is present in the central region of the protein adjacent to the amino-terminal rhodanese domain. Its sequence is similar to the consensus pattern: [GA]$X_2$GXGK[ST] (FIG. 3.4.1).

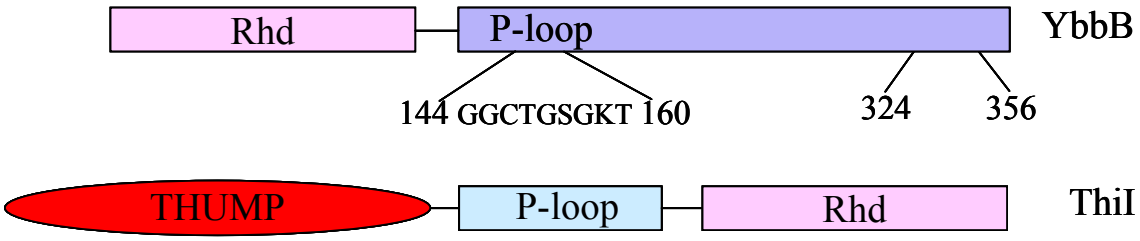


**FIG. 3.4.1. Domain architecture of YbbB and ThiI**
Residues 324-356 represent putative tRNA synthetase-like domain

1– MQERHTEQDYRALLIADTPIIDVRAPIEFEHGAMPAAINLPLMNNDERAAVGTCYKQQGSDAALALGHKLVAGEIRQQRM

DAWRAACLQNPQGILCCARGGQRSHIVQSWLHAAGIDYPLVEGGYKALRQTAIQATIELAQKPIVLIGGCTGSGKTLLVQ

QQPNGVDLEGLARHRGSAFGRTLQPQLSQASFENLLAAEMLKTDARQNLRLWVLEDESRMIGSNHLPECLRERMTQAAIA

VVEDPFEIRLERLNEEYFLRMHHDFTHAYGDEQGWQEYCEYLHHGLSAIKRRLGLQRYNELAARLDAALTTQLTTGSTDG

HLAWLVPLLEEYYDPMYRYQLEKKAEKVVFRGEWAEVAEWVKAR – 364

**FIG. 3.4.2. Sequence of YbbB showing the rhodanese domain and P-loop motif**

The rhodanese domain is underlined in red and the P-loop is underlined in blue. Cys96 and Cys97 are highlighted.

YbbB has a small region at its extreme C-terminus (residues 324-356) that is similar in sequence to Isoleucyl tRNA synthetase (IleS residues 762-793). The crystal structure of isoleucyl tRNA synthetase from *Staphylococcus. aureus* has been determined (185) which shows that this region of IleS is in the so-called helical domain of IleS, one of three domains that contributes to binding of the anticodon loop of the tRNA. However, the residues in this region of IleS are not in direct contact with the tRNA. It would be interesting to assess the effect of a 30 - 40 amino acid C-terminal truncation on YbbB activity.

Homologs of YbbB with an amino-terminal rhodanese domain and a carboxy-terminal P-loop motif are present in a wide variety of eubacteria (Table 3.4.1), which suggests an important role for this protein.

In an attempt to understand the function of YbbB, we created a Δ*ybbB* strain and showed that the mutant was deficient in 2-selenouridine containing tRNAs but was able to produce selenocysteine-containing proteins and 2-thiouridine in tRNAs normally. The pathway for the biosynthesis of 2-thiouridine in tRNA has been defined. MnmA together with IscS was shown to be involved for the *in vitro* synthesis of $s^2U$ in tRNAs (87). Since *ybbB* mutants produced normal levels of $s^2U$ in tRNAs, it is likely that YbbB is required for the replacement of sulfur with selenium for formation of seleno-tRNAs. A partially purified enzyme from *Salmonella typhimurium* was shown to catalyze the formation of 2-selenouridine tRNAs from 2-thiouridine tRNAs in the absence of ATP (127). The enzyme was termed 2-selenouridine synthase, which required selenophosphate, the product of *selD*. However, the gene encoding this protein was not identified. We propose that the YbbB homolog in *S. typhimurium* is one of the major

components in the partially purified enzyme preparation, necessary for the synthesis of 2-selenouridine tRNAs.

Our work also showed that Cys97, which aligns with the active site cysteine in rhodaneses, is required for YbbB activity *in vivo*, but Cys96 is not required. Cys97 of YbbB is conserved in all YbbB homologs. Cys96 is not conserved, but is usually a Tyr or Phe. Rhodaneses are known to catalyze the transfer of sulfur through the formation of a persulfide intermediate on the cysteine residue at its active site (27). The ThiI protein, involved in the synthesis of $s^4U$ and thiamin in *E. coli* also has a cysteine residue in its rhodanese domain that aligns with the active site cysteine of rhodaneses. Catalysis by ThiI was shown to proceed via a persulfide intermediate formed at Cys 456 and it is this form of the enzyme that transfers the sulfur to uridine to form $s^4U8$ tRNA (17;18;51). Like Cys 97 of YbbB, Cys 456 of ThiI is required for activity since a Cys456_Ala mutant does not form $s^4U$ in tRNA. It was shown that a perselenide could be formed on the active site cysteine of bovine rhodanese and this selenium-substituted rhodanese could function as a selenium donor to SelD for formation of selenophosphate (91). In light of all these findings we hypothesize that Cys97 in YbbB could function via the formation of a cysteine perselenide that serves as the immediate selenium donor for 2-selenouridine synthesis. However the exact mechanism for this reaction is not clear.

YbbB was expressed with a C-terminal histidine tag and the protein was purified by metal affinity chromatography. Initial characterization of YbbB was carried out by Matt Wolfe (Thressa Stadtman's lab) at NIH. Matt showed that purified YbbB had an absorbance maximum at 260 nm, which was diminished to one third of its original intensity upon treatment of YbbB with RNase. These results were similar to my

observation of a 260 nm peak for purified YbbB and suggested that YbbB is bound to RNA, most likely tRNA. The molecular mass of YbbB-$His_6$ monomer as calculated from its predicted amino acid sequence (42,754 Da) was confirmed by SDS PAGE. Gel filtration chromatography was used to determine the apparent molecular mass of native YbbB (M. Wolfe, NIH). The results showed that purified YbbB-$His_6$ eluted at an elution time corresponding to a molecular weight of ~129,000. However, when the purified protein was pretreated with RNase, the protein chromatographed with a molecular weight of about 40,000. Since the calculated molecular weight of tRNA is about 24,000, the observed molecular weight of purified YbbB-$His_6$ can be attributed to its dimerization, with each monomer bound to a tRNA molecule.

The reaction requirements for incorporation of selenium into tRNA were investigated *in vitro* using different combinations of reactants: YbbB, selenophosphate synthetase (SelD), ATP and tRNA (Matt Wolfe). Radiolabeled $^{75}Se^{2-}$ was used as the selenium substrate and the production of $^{75}Se^{2}U$ tRNA was measured. The results showed that YbbB and selenophosphate were essential for seleno-tRNA synthesis. To detect the specific tRNA species that interacts with YbbB, *in vitro* experiments are being carried out using purified 2-thiouridine tRNA and YbbB without bound tRNA.

Although the YbbB mutant was defective in the biosynthesis of $mnm^5se^2U$ in tRNAs, no observable growth phenotype was associated with this mutation. The selenium-containing base 5-methylaminomethyl-2-selenouridine ($mnm^5se^2U$) is present at position 1 (wobble position) of the anticodon of $tRNA^{Lys,\ Glu\ and\ Gln}$. Modifications at this position have been proposed to have roles in codon-anticodon interaction (74), aminoacylation of tRNA (73), reading frame maintainance (75) and binding of the tRNA

to the ribosome (76). Suppressor tRNAs derived from normal cellular tRNAs have been used as a tool to study the function of these modification in tRNA-codon interaction(125). Suppressor tRNAs also possess modified bases in the wobble position and the effect of these modifications on the function of suppressor tRNAs provide a tool to understand role of these modification on the codon specificity of tRNA.

In *E. coli* the *mnmA* mutant lacking the 2-thiouridine ($s^2U$) modification in the wobble position of the tRNA was shown to suppress nonsense mutations less efficiently than the wild-type suppressor strain suggesting that the $s^2U$ modification may be necessary for codon-anticodon interaction (123). However, 2-thiouridine ($s^2U$) is a precursor to 2-selenouridine ($se^2U$). Therefore, the decreased efficiency of suppression seen in *mnmA* mutant strains could be due to the deficiency of selenium modified-tRNAs and/ or the lack of thiolated tRNAs. To test this hypothesis, the Δ*ybbB* mutation was introduced into a SupF strain, which contains a UAA/UAG suppressor tRNA derived from $tRNA^{Lys}$. The resulting strain was tested for its efficiency to suppress an amber mutation in the *N* gene of phage lambda. Since N protein encodes an antiterminator needed for production of phage, the suppression of nonsense mutation in N would allow the phage to form plaques on host strains. Our initial experiments showed that the *supF* Δ*ybbB* strain produced similar number of plaques compared to *supF* only, indicating that YbbB, thus selenium modified tRNAs, may not affect the efficiency of nonsense suppression by SupF.

Table 3.4.1. Homologs of YbbB

| Organism | Taxonomical classification | % identities to *E. coli* YbbB | % positives *to E. coli* YbbB | Amino acids | Conservation of Cys96 of YbbB | Conservation of Cys97 of YbbB |
|---|---|---|---|---|---|---|
| *E. coli* | Proteobacteria, γ subdivision, enterobacteria | 100 | 100 | 364 | Cys | Cys |
| *Salmonella enterica* | Proteobacteria, γ subdivision, enterobacteria | 77 | 86 | 364 | Cys | Cys |
| *Shewanella oneidensis* MR-1 | Proteobacteria, γ subdivision, enterobacteria | 47 | 64 | 376 | Tyr | Cys |
| *Pseudomonas aeruginosa* | Proteobacteria, γ subdivision | 46 | 61 | 369 | Tyr | Cys |
| *Azotobacter vinelandii* | Proteobacteria, γ subdivision | 44 | 60 | 511 | Tyr | Cys |
| *Rhodobacter sphaeroids* | Proteobacteria, α subdivision | 38 | 52 | 350 | Tyr | Cys |
| *Magnetococcus* sp. MC-1 | Proteobacteria, unclassified | 37 | 50 | 343 | Tyr | Cys |
| *Burkholderia fungorum* | Proteobacteria β subdivision | 32 | 45 | 336 | Tyr | Cys |
| *Nitrosomonas europaea* | Proteobacteria β subdivision | 38 | 56 | 385 | Tyr | Cys |
| *Ralstonia mettalidurans* | Proteobacteria, β subdivision | 34 | 47 | 353 | Tyr | Cys |
| *Campylobacter jejuni* | Proteobacteria δ-ε subdivision | 31 | 47 | 332 | Tyr | Cys |
| *Clostridium perfringens* | Firmicutes (Gram +ve) | 30 | 47 | 356 | Phe | Cys |

| Organism | Taxonomical classification | % identities to *E. coli* YbbB | % positives to *E. coli* YbbB | Number of amino acids | Conservation of Cys96 of YbbB | Conservation of Cys97 of YbbB |
|---|---|---|---|---|---|---|
| *Synechococcus* | Cyanobacteria | 36 | 49 | 347 | Tyr | Cys |
| *Trichodesmium erythraeum* | Cyanobacteria | 35 | 49 | 339 | His | Cys |
| *Procholorococcus marinus* | Cyanobacteria | 32 | 46 | 366 | Tyr | Cys |
| *Methanococcus Jannaschii* MJ0052 [a] | Archaea | 31 | 53 | 222 | Phe | Cys |
| *M. Jannaschii* MJ0053 [a] | Archaea | 29 | 46 | 227 | Not conserved | Not conserved |

[a] MJ0052 an MJ0053 have a unique domain structure. Genome context suggests that MJ0052 and MJ0053 are present in a putative operon. MJ0052 is homologous to the rhodanese domain of YbbB whereas MJ0053 is homologus to the ATP domain of YbbB.

# Reference List


1 Bordo, D., Bork, P. (2002) The rhodanese/Cdc25 phosphatase superfamily: Sequence-structure-function relations. *EMBO Rep.* 3, 741-746

2 Fauman, E. B., Cogswell, J. P., Lovejoy, B., Rocque, W. J., Holmes, W., Montana, V. G., Piwnica-Worms, H., Rink, M. J., Saper, M. A. (1998) Crystal structure of the catalytic domain of the human cell cycle control phosphatase, Cdc25A. *Cell* 93, 617-625

3 Ploegman, J. H., Drent, G., Kalk, K. H., Hol, W. G., Heinrikson, R. L., Keim, P., Weng, L., Russell, J. (1978) The covalent and tertiary structure of bovine liver rhodanese. *Nature* 273, 124-129

4 Bordo, D., Deriu, D., Colnaghi, R., Carpen, A., Pagani, S., Bolognesi, M. (2000) The crystal structure of a sulfurtransferase from *Azotobacter vinelandii* highlights the evolutionary relationship between the rhodanese and phosphatase enzyme families. *J.Mol.Biol.* 298, 691-704

5 Reynolds, R. A., Yem, A. W., Wolfe, C. L., Deibel, M. R., Jr., Chidester, C. G., Watenpaugh, K. D. (1999) Crystal structure of the catalytic subunit of Cdc25B required for G2/M phase transition of the cell cycle. *J.Mol.Biol.* 293, 559-568

6 Ray, W. K., Potters, M. B., Mansuri, A. M., Larson, T. J. (2000) Characterization of a 12-kilodalton rhodanese encoded by *glpE* of *Escherichia coli* and its interaction with thioredoxin. *J.Bacteriol.* 181, 2277-2284

7 Spallarossa, A., Donahue, J. L., Larson, T. J., Bolognesi, M., Bordo, D. (2001) *Escherichia coli* GlpE is a prototype for single-domain sulfurtransferase (rhodanese) homology superfamily. *Structure* 9, 1117-1125

8 Klimmek, O., Kreis, V., Klein, C., Simon, J., Wittershagen, A., Kroger, A. (1998) The function of the periplasmic Sud protein in polysulfide respiration of *Wolinella succinogenes*. *Eur.J.Biochem* 253, 263-269

9 Mukhopadhyay, R., Zhou, Y., Rosen, B. P. (2003) Directed evolution of a yeast arsenate reductase into a protein-tyrosine phosphatase. *J.Biol.Chem.* 278, 24476-24480

10 Nagahara, N., Nishino, T. (1996) Role of amino acid residues in the active site of rat liver mercaptopyruvate sulfurtransferase. cDNA cloning, overexpression, and site-directed mutagenesis. *J.Biol.Chem.* 271, 27395-27401

11 Colnaghi, R., Cassinelli, G., Drummond, M., Forlani, F., Pagani, S. (2001) Properties of the *Escherichia coli* rhodanese-like protein SseA: contribution of the active-site residue Ser240 to sulfur donor recognition. *FEBS Lett.* 500, 153-156

12 Jutabha, P. Biochemical and genetic characterization of mercaptopyruvate sulfurtransferase and paralogous putative sulfurtransferases of *Escherichia coli*. 2001. Virginia Polytechnic Institute and State University

13 Keyse, S. M., Ginsburg, M. (1993) Amino acid sequence similarity between CL100, a dual-specificity MAP kinase phosphatase and cdc25. *Trends Biochem.Sci.* 18, 377-378

14 Hofmann, K., Bucher, P., Kajava, A. V. (1998) A model of Cdc25 phosphatase catalytic domain and CDK-interaction surface based on the presence of a rhodanese homology domain. *J.Mol.Biol.* 282, 195-208

15 Ploegman, J. H., Drent, G., Kalk, K. H., Hol, W. G. (1979) The structure of bovine liver rhodanese. II. The active site in the sulfur-substituted and the sulfur-free enzyme. *J.Mol.Biol.* 127, 149-162

16 Mueller, E. G., Buck, C. J., Palenchar, P. M., Barnhart, L. E., Paulson, J. L. (1998) Identification of a gene involved in the generation of 4-thiouridine in tRNA. *Nucleic.Acids.Res.* 26, 2606-2610

17 Palenchar, P. M., Buck, C. J., Cheng, H., Larson, T. J., Mueller, E. G. (2000) Evidence that ThiI, an enzyme shared between thiamin and 4-thiouridine biosynthesis, may be a sulfurtransferase that proceeds through a persulfide intermediate. *J.Biol.Chem.* 275, 8283-8286

18 Mueller, E. G., Palenchar, P. M., Buck, C. J. (2001) The role of the cysteine residues of ThiI in the generation of 4-thiouridine in tRNA. *J.Biol.Chem.* 276, 33588-33595

19 Appleyard, M. V., Sloan, J., Kana, Heck, I. S., Kinghorn, J. R., Unkles, S. E. (1998) The *Aspergillus nidulans cnxF* gene and its involvement in molybdopterin biosynthesis. Molecular characterization and analysis of *in vivo* generated mutants. *J.Biol.Chem.* 273, 14869-14876

20 Agar, J. N., Krebs, C., Frazzon, J., Huynh, B. H., Dean, D. R., Johnson, M. K. (2000) IscU as a scaffold for iron-sulfur cluster biosynthesis: sequential assembly of [2Fe-2S] and [4Fe-4S] clusters in IscU. *Biochemistry* 39, 7856-7862

21 Westley, J., Adler, H., Westley, L., Nishida, C. (1983) The sulfurtransferases. *Fundam.Appl.Toxicol.* 3, 377-382

22 Abdolrasulnia, R., Wood, J. L. (1979) Transfer of persulfide sulfur from thiocystine to rhodanese. *Biochim.Biophys.Acta* 567, 135-143

23 Westley, J. (1981) Thiosulfate: cyanide sulfurtransferase (rhodanese). *Methods Enzymol.* 77, 285-291

24 Ploegman, J. H., Drent, G., Kalk, K. H., Hol, W. G. (1978) Structure of bovine liver rhodanese. I. Structure determination at 2.5 Å resolution and a comparison of the conformation and sequence of its two domains. *J.Mol.Biol.* 123, 557-594

25 Westley, J., Schlesinger, P. (1974) An expanded mechanism of rhodanese catalysis. *J.Bacteriol.* 249, 780-788

26 Weng, L., Heinrikson, R. L., Westley, J. (1978) Active site cysteinyl and arginyl residues of rhodanese. A novel formation of disulfide bonds in the active site promoted by phenylglyoxal. *J.Biol.Chem.* 253, 8109-8119

27 Westley, J., Heyse, D. (1971) Mechanisms of sulfur transfer catalysis. Sulfhydryl-catalyzed transfer of thiosulfonate sulfur. *J.Biol.Chem.* 246, 1468-1474

28 Whitehouse, D. B., Pilz, A. J., Porta, G., Hopkinson, D. A. (1988) Rhodanese isozymes in human tissues. *Ann.Hum.Genet.* 52, 1-10

29 Weiland, K. L., Dooley, T. P. (1991) Molecular cloning, sequencing and characterization of cDNA to rat liver rhodanese, a thiosulphate sulphurtransferase. *Biochem J.* 275, 227-231

30 Hatzfeld, Y., Saito, K. (2000) Evidence for the existence of rhodanese (thiosulfate:cyanide sulfurtransferase) in plants: preliminary characterization of two rhodanese cDNAs from *Arabidopsis thaliana*. *FEBS Lett.* 470, 147-150

31 Bauer, M., Papenbrock, J. (2002) Identification and characterization of single-domain thiosulfate sulfurtransferases from *Arabidopsis thaliana*. *FEBS Lett.* 532, 427-431

32 Colnaghi, R., Pagani, S., Kennedy, C., Drummond, M. (1996) Cloning, sequence analysis and overexpression of the rhodanese gene of *Azotobacter vinelandii*. *Eur.J.Biochem* 236, 240-248

33 Aird, B. A., Heinrikson, R. L., Westley, J. (1987) Isolation and characterization of a prokaryotic sulfurtransferase. *J.Biol.Chem.* 262, 17327-17335

34 Villarejo, M., Westley, J. (1966) Sulfur metabolism of *Bacillus subtilis*. *Biochim.Biophys.Acta* 117, 209-216

35 Alexander, K., Volini, M. (1987) Properties of an *Escherichia coli* rhodanese. *J.Biol.Chem.* 262, 6595-6604

36 Bordo, D., Larson, T. J., Donahue, J. L., Spallarossa, A., Bolognesi, M. (2000) Crystals of GlpE, a 12 kDa sulfurtransferase from *Escherichia coli*, display 1.06 Å resolution diffraction: a preliminary report. *Acta Crystallogr.D.Biol.Crystallogr.* 56, 1691-1693

37 Roy, A. B., Trudinger, P. A. (1970) Rhodanese and 3-mercaptopyruvate sulfurtransferase. In *The Biochemistry of Inorganic Compounds of Sulfur* pp. 190-206, Cambridge University Press, Cambridge.

38 Jarabak, R. (1981) 3-Mercaptopyruvate sulfurtransferase. *Methods Enzymol.* 77, 291-297

39 Meister, A. (1953) Conversion of α -keto analog of cysteine to pyruvate and sulfur. *Fed.Proc.* 12, 245

40 Wood, J. L., Fiedler, H. (1953) β– mercaptopyruvate, a substrate for rhodanese. *J.Biol.Chem.* 205, 231-234

41 Jarabak, R., Westley, J. (1978) Steady-state kinetics of 3-mercaptopyruvate sulfurtransferase from bovine kidney. *Arch.Biochem Biophys.* 185, 458-465

42 Nagahara, N., Okazaki, T., Nishino, T. (1995) Cytosolic mercaptopyruvate sulfurtransferase is evolutionarily related to mitochondrial rhodanese. Striking similarity in active site amino acid sequence and the increase in the mercaptopyruvate sulfurtransferase activity of rhodanese by site-directed mutagenesis. *J.Biol.Chem.* 270, 16230-16235

43 Nakamura, T., Yamaguchi, Y., Sano, H. (2000) Plant mercaptopyruvate sulfurtransferases. Molecular cloning, subcellular localization and enzymatic activities. *Eur.J.Biochem* 267, 5621-5630

44 Papenbrock, J., Schmidt, A. (2000) Characterization of two sulfurtransferase isozymes from *Arabidopsis thaliana* . *Eur.J.Biochem* 267, 5571-5579

45 Vachek, H., Wood, J. L. (1972) Purification and properties of mercaptopyruvate sulfur transferase of *Escherichia coli*. *Biochim.Biophys.Acta* 258, 133-146

46 Begley, T. P., Downs, D. M., Ealick, S. E., McLafferty, F. W., Van, L. A., Taylor, S., Campobasso, N., Chiu, H. J., Kinsland, C., Reddick, J. J., Xi, J. (1999) Thiamin biosynthesis in prokaryotes. *Arch.Microbiol.* 171, 293-300

47 Xi, J., Ge, Y., Kinsland, C., McLafferty, F. W., Begley, T. P. (2001) Biosynthesis of the thiazole moiety of thiamin in *Escherichia coli*: Identification of an acyldisulfide-linked protein-protein conjugate that is functionally analogous to the ubiquitin/E1 complex. *Proc.Natl.Acad.Sci.U.S.A.* 98, 8513-8518

48 Taylor, S. V., Kelleher, N. L., Kinsland, C., Chiu, H. J., Costello, C. A., Backstrom, A. D., McLafferty, F. W., Begley, T. P. (1998) Thiamin biosynthesis in *Escherichia coli*. Identification of ThiS thiocarboxylate as the immediate sulfur donor in the thiazole formation. *J.Biol.Chem.* 273, 16555-16560

49 Begley, T. P., Xi, J., Kinsland, C., Taylor, S., McLafferty, F. (1999) The enzymology of sulfur activation during thiamin and biotin biosynthesis. *Curr.Opin.Chem.Biol.* 3, 623-629

50 Lauhon, C. T., Kambampati, R. (2000) The *iscS* gene in *Escherichia coli* is required for the biosynthesis of 4-thiouridine, thiamin, and NAD. *J.Biol.Chem.* 275, 20096-20103

51 Wright, C. M., Palenchar, P. M., Mueller, E. G. (2002) A paradigm for biological sulfur transfers via persulfide groups: a persulfide-disulfide-thiol cycle in 4-thiouridine biosynthesis. *Chem.Comm.* 2002, 2708-2709

52 Tatusov, R. L., Galperin, M. Y., Natale, D. A., Koonin, E. V. (2000) The COG database: a tool for genome-scale analysis of protein functions and evolution. *Nucleic Acids Res.* 28, 33-36

53 Gutzke, G., Fischer, B., Mendel, R. R., Schwarz, G. (2001) Thiocarboxylation of molybdopterin synthase provides evidence for the mechanism of dithiolene formation in metal-binding pterins. *J.Biol.Chem.* 276, 36268-36274

54 Rubio, L. M., Flores, E., Herrero, A. (1999) Molybdopterin guanine dinucleotide cofactor in *Synechococcus* sp. nitrate reductase: identification of *mobA* and isolation of a putative *moeB* gene. *FEBS Lett.* 462, 358-362

55 Leimkuhler, S., Rajagopalan, K. V. (2001) A sulfurtransferase Is required in the transfer of cysteine sulfur in the *in vitro* synthesis of molybdopterin from precursor Z in *Escherichia coli*. *J.Biol.Chem.* 276, 22024-22031

56 Rudolph, M. J., Wuebbens, M. M., Rajagopalan, K. V., Schindelin, H. (2001) Crystal structure of molybdopterin synthase and its evolutionary relationship to ubiquitin activation. *Nat.Struct.Biol.* 8, 42-46

57 Leimkuhler, S., Wuebbens, M. M., Rajagopalan, K. V. (2001) Characterization of *Escherichia col*i MoeB and its involvement in the activation of molybdopterin synthase for the biosynthesis of the molybdenum cofactor. *J.Biol.Chem.* 276, 34695-34701

58 Leimkuhler, S., Freuer, A., Araujo, J. A. S., Rajagopalan, K. V., Mendel, R. R. (2003) Mechanistic studies of human molybdopterin synthase reaction and characterization of mutants identified in group B patients of Molybdenum cofactor deficiency. *J.Biol.Chem.* 278, 26127-26134

59 Marquet, A., Bui, B. T., Florentin, D. (2001) Biosynthesis of biotin and lipoic acid. *Vitam.Horm.* 61, 51-101

60 Duin, E. C., Lafferty, M. E., Crouse, B. R., Allen, R. M., Sanyal, I., Flint, D. H., Johnson, M. K. (1997) [2Fe-2S] to [4Fe-4S] cluster conversion in *Escherichia coli* biotin synthase. *Biochemistry* 36, 11811-11820

61 Tse Sum Bui, B., Florentin, D., Fournier, F., Ploux, O., Mejean, A., Marquet, A. (1998) Biotin synthase mechanism: on the origin of sulphur. *FEBS Lett.* 440, 226-230

62 Gibson, K. J., Pelletier, D. A., Turner, I. M. (1999) Transfer of Sulfur to Biotin from Biotin Synthase (BioB protein). *Biochem Biophys.Res.Commun.* 254, 632-635

63 McIver, L., Baxter, R. L., Campopiano, D. J. (2000) Identification of the [Fe-S] cluster-binding residues of *Escherichia coli* biotin synthase. *J.Biol.Chem.* 275, 13888-13894

64 Ugulava, N. B., Gibney, B. R., Jarrett, J. T. (2000) Iron-sulfur cluster interconversions in biotin synthase: dissociation and reassociation of iron during conversion of [2Fe-2S] to [4Fe-4S] clusters. *Biochemistry* 39, 5206-5214

65 Tse Sum Bui, B., Escalettes, F., Chottard, G., Florentin, D., Marquet, A. (2000) Enzyme-mediated sulfide production for the reconstitution of [2Fe-2S] clusters into apo-biotin synthase of *Escherichia coli*. Sulfide transfer from cysteine to biotin. *Eur.J.Biochem.* 267, 2688-2694

66 Ollagnier-de-Choudens, S., Mulliez, E., Hewitson, K. S., Fontecave, M. (2002) Biotin synthase is a pyridoxal phosphate-dependent cysteine desulfurase. *Biochemistry* 41, 9145-9152

67 Miller, J. R., Busby, R. W., Jordan, S. W., Cheek, J., Henshaw, T. F., Ashley, G. W., Broderick, J. B., Cronan, J. E., Jr., Marletta, M. A. (2000) *Escherichia coli* LipA is a lipoyl synthase: *in vitro* biosynthesis of lipoylated pyruvate dehydrogenase complex from octanoyl-acyl carrier protein. *Biochemistry* 39, 15166-15178

68 Reed, K. E., Cronan, J. E. J. (1993) Lipoic acid metabolism in *Escherichia coli*: sequencing and functional characterization of the *lipA* and *lipB* genes. *J.Bacteriol.* 175, 1325-1336

69 Ollagnier-de, C. S., Fontecave, M. (1999) The lipoate synthase from *Escherichia coli* is an iron-sulfur protein. *FEBS Lett.* 453, 25-28

70 Rozenski, J., Crain, P. F., McCloskey, J. A. (1999) The RNA Modification Database: 1999 update. *Nucleic Acids Res.* 27, 196-197

71 Lauhon, C. T. (2002) Requirement for IscS in biosynthesis of all thionucleosides in *Escherichia coli*. *J.Bacteriol.* 184, 6820-6829

72 Lisowsky, T., Lee, J. E., Polimeno, L., Francavilla, A., Hofhaus, G. (2001) Mammalian augmenter of liver regeneration protein is a sulfhydryl oxidase. *Dig.Liver Dis.* 33, 173-180

73 Sylvers, L. A., Rogers, K. C., Shimizu, M., Ohtsuka, E., Soll, D. (1993) A 2-thiouridine derivative in $tRNA^{Glu}$ is a positive determinant for aminoacylation by *Escherichia coli* glutamyl-tRNA synthetase. *Biochemistry* 32, 3836-3841

74 Yokoyama, S., Watanabe, T., Murao, K., Ishikura, H., Yamaizumi, Z., Nishimura, S., Miyazawa, T. (1985) Molecular mechanism of codon recognition by tRNA species with modified uridine in the first position of the anticodon. *Proc.Natl.Acad.Sci.U.S.A.* 82(15), 4905-4909

75 Urbonavicius, J., Qian, Q., Durand, J. M. B., Hagervall, T. G., Bjork, G. R. (2001) Improvement of reading frame maintenance is a common function for several tRNA modifications. *EMBO J.* 20, 4863-4873

76 Ashraf, S. S., Sochacka, E., Cain, R., Guenther, R., Malkiewicz, A., Agris, P. F. (1999) Single atom modification (O-->S) of tRNA confers ribosome binding. *RNA.* 5, 188-194

77 Yasukawa, T., Suzuki, T., Ishii, N., Ohta, S., Watanabe, K. (2001) Wobble modification defect in tRNA disturbs codon-anticodon interaction in a mitochondrial disease. *EMBO J.* 20, 4794-4802

78 Beinert, H., Holm, R. H., Münck, E. (1997) Iron-Sulfur Clusters: Nature's Modular, Multipurpose Structures. *Science* 277, 653-659

79 Jacobson, M. R., Cash, V. L., Weiss, M. C., Laird, N. F., Newton, W. E., Dean, D. R. (1989) Biochemical and genetic analysis of the *nifUSVWZM* cluster from *Azotobacter vinelandii.* *Mol.Gen.Genet.* 219, 49-57

80 Zheng, L., White, R. H., Cash, V. L., Jack, R. F., Dean, D. R. (1993) Cysteine desulfurase activity indicates a role for NIFS in metallocluster biosynthesis. *Proc.Natl.Acad.Sci.U.S.A.* 90, 2754-2758

81 Zheng, L., Dean, D. R. (1994) Catalytic formation of a nitrogenase iron-sulfur cluster. *J.Biol.Chem.* 269, 18723-18726

82 Zheng, L., White, R. H., Cash, V. L., Dean, D. R. (1994) Mechanism for the desulfurization of L-cysteine catalyzed by the *nifS* gene product. *Biochemistry* 33, 4714-4720

83 Yuvaniyama, P., Agar, J. N., Cash, V. L., Johnson, M. K., Dean, D. R. (2000) NifS-directed assembly of a transient [2Fe-2S] cluster within the NifU protein. *Proc.Natl.Acad.Sci.U.S.A* 97, 599-604

84 Nakamura, M., Saeki, K., Takahashi, Y. (1999) Hyperproduction of recombinant ferredoxins in *Escherichia coli* by coexpression of the ORF1-ORF2-*iscS*-*iscU*-*iscA*-*hscB*-*hscA*-*fdx*-ORF3 gene cluster. *J.Biochem (Tokyo.)* 126, 10-18

85 Zheng, L., Cash, V. L., Flint, D. H., Dean, D. R. (1998) Assembly of iron-sulfur clusters. Identification of an *iscSUA-hscBA-fdx* gene cluster from *Azotobacter vinelandii*. *J.Biol.Chem.* 273, 13264-13272

86 Krebs, C., Agar, J. N., Smith, A. D., Frazzon, J., Dean, D. R., Huynh, B. H., Johnson, M. K. (2001) IscA, an alternate scaffold for Fe-S cluster biosynthesis. *Biochemistry* 40, 14069-14080

87 Kambampati, R., Lauhon, C. T. (2003) MnmA and IscS are required for *in vitro* 2-thiouridine biosynthesis in *Escherichia coli*. *Biochemistry* 42, 1109-1117

88 Mihara, H., Esaki, N. (2002) Bacterial cysteine desulfurases: their function and mechanisms. *Appl.Microbiol.Biotechnol.* 60, 12-23

89 Mihara, H., Maeda, M., Fujii, T., Kurihara, T., Hata, Y., Esaki, N. (1999) A *nifS*-like gene, *csdB*, encodes an *Escherichia coli* counterpart of mammalian selenocysteine lyase. Gene cloning, purification, characterization and preliminary x-ray crystallographic studies. *J.Biol.Chem.* 274, 14768-14772

90 Takahashi, Y., Tokumoto, U. (2002) A third bacterial system for the assembly of iron-sulfur clusters with homologs in archaea and plastids. *J.Biol.Chem.* 277, 28380-28383

91 Ogasawara, Y., Lacourciere, G., Stadtman, T. C. (2001) Formation of a selenium-substituted rhodanese by reaction with selenite and glutathione: Possible role of a protein perselenide in a selenium delivery system. *Proc.Natl.Acad.Sci.U.S.A.* 98, 171320998

92 Stadtman, T. C. (1991) Biosynthesis and function of selenocysteine-containing enzymes. *J.Biol.Chem.* 266, 16257-16260

93 Wittwer, A. J., Tsai, L., Ching, W. M., Stadtman, T. C. (1984) Identification and synthesis of a naturally occurring selenonucleoside in bacterial tRNAs: 5-[(methylamino)methyl]-2-selenouridine. *Biochemistry* 23, 4650-4655

94 Stadtman, T. C. (2002) Discoveries of vitamin B12 and selenium enzymes. *Annu.Rev.Biochem.* 71, 1-16

95 Politino, M., Tsai, L., Veres, Z., Stadtman, T. C. (1990) Biosynthesis of selenium-modified tRNAs in *Methanococcus vannielii*. *Proc.Natl.Acad.Sci.U.S.A.* 87, 6345-6348

96 Huang, KX., An, YX., Chen, ZX., Xu, HB. (2001) Isolation and partial characterization of selenium-containing tRNA from germinating barley. *Biol Trace Elem Res* 82 (1-3), 247-257

97 Stadtman, T. C. (1996) Selenocysteine. *Annu.Rev.Biochem.* 65, 83-100

98 Mizutani, T., Watanabe, T., Kanaya, K., Nakagawa, Y., Fujiwara, T. (1999) Trace 5-methylaminomethyl-2-selenouridine in bovine tRNA and the selenouridine synthase activity in bovine liver. *Mol Biol Rep* 26, 162-172

99 Stadtman, T. C. (1990) Selenium biochemistry. *Annu.Rev.Biochem.* 59, 111-127

100 Allan, C. B., Lacourciere, G. M., Stadtman, T. C. (1999) Responsiveness of selenoproteins to dietary selenium. *Annu.Rev.Nutr.* 19, 1-16

101 Rayman Margaret P. (2000) The importance of selenium to human health. *Lancet* 356, 231-241

102 Zinoni, F., Birkmann, A., Stadtman, T. C., Bock, A. (1986) Nucleotide sequence and expression of the selenocysteine-containing polypeptide of formate dehydrogenase (formate-hydrogen-lyase-linked) from *Escherichia coli*. *Proc.Natl.Acad.Sci.U.S.A.* 83, 4650-4654

103 Chambers, I., Frampton, J., Goldfarb, P., Affara, N., McBain, W., Harrison, P. R. (1986) The structure of the mouse glutathione peroxidase gene: the selenocysteine in the active site is encoded by the 'termination' codon, TGA. *EMBO J.* 5, 1221-1227

104 Bock, A., Forchhammer, K., Heider, J., Leinfelder, W., Sawers, G., Veprek, B., Zinoni, F. (1991) Selenocysteine: the 21st amino acid. *Mol.Microbiol.* 5, 515-520

105 Leinfelder, W., Forchhammer, K., Zinoni, F., Sawers, G., Berthelot-Mandrand, M. A., Bock, A. (1988) *Escherichia coli* genes whose products are involved in selenium metabolism. *J.Bacteriol.* 170, 540-546

106 Berg, B. L., Heider, J., Stewart, V. (1991) Nitrate-inducible formate dehydrogenase in *Escherichia coli* K-12. I. Nucleotide sequence of he fdnGHI operon and evidence that opal (UGA) encodes selenocysteine. *J.Biol.Chem.* 266(33), 22380-22385

107 Sawers, G., Heider, J., Zehelein, E., Bock, A. (1991) Expression and operon structure of the *sel* genes of *Escherichia coli* and identification of a third selenium-containing formate dehydrogenase isoenzyme. *J.Bacteriol.* 173, 4983-4993

108 Gladyshev, V. N., Khangulov, S. V., Stadtman, T. C. (1994) Nicotinic acid hydroxylase from *Clostridium barkeri* : Electron paramagnetic resonance studies show that selenium is coordinated with molybdenum in the catalytically active selenium-dependent enzyme. *Proc.Natl.Acad.Sci.U.S.A.* 91, 232-236

109 Self, W. T., Stadtman, T. C. (2000) Selenium-dependent metabolism of purines: A selenium-dependent purine hydroxylase and xanthine dehydrogenase were purified from Clostridium purinolyticum and characterized. *Proc.Natl.Acad.Sci.U.SA.* 97, 7208-7213

110 Sliwkowski, M. X., Stadtman, T. C. (1985) Incorporation and distribution of selenium into thiolase from *Clostridium kluyveri*. *J.Biol.Chem.* 260, 3140-3144

111 Leinfelder, W., Forchhammer, K., Veprek, B., Zehelein, E., Bock, A. (1990) *In vitro* Synthesis of Selenocysteinyl-tRNA$_{UCA}$ from Seryl-tRNA$_{UCA}$: Involvement and characterization of the *selD* Gene product. *Proc.Natl.Acad.Sci.U.S.A.* 87, 543-547

112 Veres, Z., Kim, I. Y., Scholz, T. D., Stadtman, T. C. (1994) Selenophosphate synthetase. Enzyme properties and catalytic reaction. *J.Biol.Chem.* 269, 10597-10603

113 Lacourciere, G. M., Stadtman, T. C. (1999) Catalytic properties of selenophosphate synthetases: Comparison of the selenocysteine-containing enzyme from *Haemophilus influenzae* with the corresponding cysteine-containing enzyme from *Escherichia coli*. *Proc.Natl.Acad.Sci.U.S.A.* 96, 44-48

114 Lacourciere, G. M., Stadtman, T. C. (1998) The NIFS protein can function as a selenide delivery protein in the biosynthesis of selenophosphate. *J.Biol.Chem.* 273, 30921-30926

115 Lacourciere, G. M., Mihara, H., Kurihara, T., Esaki, N., Stadtman, T. C. (2000) *Escherichia coli* NifS-like proteins provide selenium in the pathway for the biosynthesis of selenophosphate. *J.Biol.Chem.* 275, 23769-23773

116 Ching, W. M. (1984) Occurance of selenium-containing tRNAs in mouse leukemia cells. *Proc.Natl.Acad.Sci.U.S.A.* 81(10), 3010-3013

117 Ching, W. M., Stadtman, T. C. (1982) Selenium-containing tRNA$^{Glu}$ from *Clostridium sticklandii*: correlation of aminoacylation with selenium content. *Proc.Natl.Acad.Sci.U.S.A.* 79, 374-377

118 Wittwer, A. J. (1983) Specific incorporation of selenium into lysine- and glutamate-accepting tRNAs from *Escherichia coli*. *J.Biol.Chem.* 258, 8637-8641

119 Wittwer, A. J., Stadtman, T. C. (1986) Biosynthesis of 5-methylaminomethyl-2-selenouridine, a naturally occurring nucleoside in *Escherichia coli* tRNA. *Arch.Biochem.Biophys.* 248, 540-550

120 Ching, W. M., Alzner-DeWeerd, B., Stadtman, T. C. (1985) A selenium-containing nucleoside at the first position of the anticodon in seleno-tRNA$^{Glu}$ from *Clostridium sticklandii*. *Proc.Natl.Acad.Sci.U.S.A.* 82, 347-350

121 Veres, Z., Tsai, L., Politino, M., Stadtman, T. C. (1990) *In vitro* incorporation of selenium into tRNAs of *Salmonella typhimurium*. *Proc.Natl.Acad.Sci.U.S.A.* 87, 6341-6344

122 Ikemura, T. (1981) Correlation between the abundance of *Escherichia coli* transfer RNAs and the occurrence of the respective codons in its protein genes. *J.Mol.Biol.* 146, 1-21

123 Sullivan, M. A., Cannon, J. F., Webb, F. H., Bock, R. M. (1985) Antisuppressor mutation in *Escherichia coli* defective in biosynthesis of 5-methylaminomethyl-2-thiouridine. *J.Bacteriol.* 161, 368-376

124 Elseviers, D., Petrullo, LA., Gallagher, PJ. (1984) Novel *E. coli* mutants deficient in biosynthesis of 5-methylaminomethyl-2-thiouridine. *Nucl.Acids.Res.* 12 (8), 3521-3534

125 Kramer, G. F., Ames, B. N. (1988) Isolation and characterization of a selenium metabolism mutant of *Salmonella typhimurium*. *J.Bacteriol.* 170, 736-743

126 Stadtman, T. C., Davis, J. N., Zehelein, E., Bock, A. (1989) Biochemical and genetic analysis of *Salmonella typhimurium* and *Escherichia coli* mutants defective in specific incorporation of selenium into formate dehydrogenase and tRNAs. *BioFactors* 2, 35-44

127 Veres, Z., Stadtman, T. C. (1994) A purified selenophosphate-dependent enzyme from *Salmonella typhimurium* catalyzes the replacement of sulfur in 2-thiouridine residues in tRNAs with selenium. *Proc.Natl.Acad.Sci.U.S.A.* 91, 8092-8096

128 Allan, C. B. (2000) Evidence that multiple proteins from *Salmonella typhimurium* are required for the biosynthesis of 5-methylaminomethyl-2-selenouridine in tRNAs. *BioFactors* 11, 87-89

129 Adams, H., Teertstra, W., Koster, M., Tommassen, J. (2002) PspE (phage-shock protein E) of *Escherichia coli* is a rhodanese. *FEBS Lett.* 518, 173-176

130 Cheng, H. Characterization of PspE, a secreted sulfurtransferase of *Escherichia coli*. 1-74. 2003. Virginia Polytechnic Institute and State University.

131 Brissette, J. L., Weiner, L., Ripmaster, T. L., Model, P. (1991) Characterization and sequence of the *Escherichia coli* stress-induced *psp* operon. *J.Mol.Biol.* 220, 35-48

132 Model, P., Jovanovic, G., Dworkin, J. (1997) The *Escherichia coli* phage-shock-protein (*psp*) operon. *Mol.Microbiol.* 24, 255-261

133 Aravind, L., Koonin, E. V. (2001) THUMP - a predicted RNA-binding domain shared by 4-thiouridine, pseudouridine synthetases and RNA methylases. *Trends Biochem.Sci.* 26, 215-217

134 Volini, M., Ogata, K., Alexander, K. (1983) Molecular forms of the rhodaneses. In *Frontiers in Biochemical and Biophysical Studies of Proteins and Membranes* (Liu, T.Y., Sakakibara, S., Schechter, A. N., Yagi, K., Yajima, H., and Yasunobu, K. T., eds) pp. 183-192, Elsevier Science Publishing, Inc., New York.

135 Altschul, S. F., Madden, T. L., Schaffer, A. A., Zhang, J., Zhang, Z., Miller, W., Lipman, D. J. (1997) Gapped BLAST and PSI-BLAST: a new generation of protein database search programs. *Nucleic Acids Res.* 25, 3389-3402

136 Nagahara, N., Ito, T., Minami, M. (1999) Mercaptopyruvate sulfurtransferase as a defense against cyanide toxication: molecular properties and mode of detoxification. *Histol.Histopathol.* 14, 1277-1286

137 Bonomi, F., Pagani, S., Cerletti, P., Cannella, C. (1977) Rhodanese-mediated sulfur transfer to succinate dehydrogenase. *Eur.J.Biochem* 72, 17-24

138 Pagani, S., Bonomi, F., Cerletti, P. (1984) Enzymic synthesis of the iron-sulfur cluster of spinach ferredoxin. *Eur.J.Biochem* 142, 361-366

139 Pagani, S., Galante, Y. M. (1983) Interaction of rhodanese with mitochondrial NADH dehydrogenase. *Biochim.Biophys.Acta* 742, 278-284

140 Kambampati, R., Lauhon, C. T. (2000) Evidence for the transfer of sulfane sulfur from IscS to ThiI during the *in vitro* biosynthesis of 4-thiouridine in *Escherichia coli* tRNA. *J.Biol.Chem.* 275, 10727-10730

141 Lutz, R., Bujard, H. (1997) Independent and tight regulation of transcriptional units in *Escherichia coli* via the LacR/O, the TetR/O and AraC/$I_1$-$I_2$ regulatory elements. *Nucleic Acids Res.* 25, 1203-1210

142 Tabor, S., Richardson, C. C. (1985) A bacteriophage T7 RNA polymerase/promoter system for controlled exclusive expression of specific genes. *Proc.Natl.Acad.Sci.U.S.A.* 82, 1074-1078

143 Zeng, G., Larson, T. J. (1996) Use of engineered thrombin cleavage site for determination of translational reading frames. *BioTechniques* 21, 822-824

144 Miller, J. H. (1972) *Experiments in Molecular Genetics*.Cold Spring Harbor Laboratory, Cold Spring Harbor, N.Y.

145 Datsenko, K. A., Wanner, B. L. (2000) One-step inactivation of chromosomal genes in *Escherichia coli* K-12 using PCR products. *Proc.Natl.Acad.Sci.U.S.A* 97, 6640-6645

146 Cherepanov, P. P., Wackernagel, W. (1995) Gene disruption in *Escherichia coli*: $Tc^R$ and $Km^R$ cassettes with the option of Flp-catalyzed excision of the antibiotic-resistance determinant. *Gene* 158, 9-14

147 Johnson, M. E., Rajagopalan, K. V. (1987) Involvement of *chlA, E, M*, and *N* loci in *Escherichia coli* molybdopterin biosynthesis. *J.Bacteriol.* 169, 117-125

148 Silhavy, T. J., Berman, M. L., Enquist, L. W. (1984) *Experiments with Gene Fusions*.Cold Spring Harbor Laboratory, Cold Spring Harbor, NY.

149 Blattner, F. R., Plunkett, G., Bloch, C. A., Perna, N. T., Burland, V., Riley, M., Collado-Vides, J., Glasner, J. D., Rode, C. K., Mayhew, G. F., Gregor, J., Davis, N. W., Kirkpatrick, H. A., Goeden, M. A., Rose, D. J., Mau, B., Shao, Y. (1997) The complete genome sequence of *Escherichia coli* K-12. *Science* 277, 1453-1462

150 Donahue, J. L., Bownas, J. L., Niehaus, W. G., Jr., Larson, T. J. (2000) Purification and characterization of *glpX*-encoded fructose 1,6-bisphosphatase, a new enzyme of the glycerol 3-phosphate regulon of *Escherichia coli*. *J.Bacteriol.* 182, 5624-5627

151 Studier, F. W., Moffatt, B. A. (1986) Use of bacteriophage T7 RNA polymerase to direct selective high-level expression of cloned genes. *J.Mol.Biol.* 189, 113-130

152 Lopez, P. J., Marchand, I., Joyce, S. A., Dreyfus, M. (1999) The C-terminal half of RNase E, which organizes the *Escherichia coli* degradosome, participates in mRNA degradation but not rRNA processing *in vivo*. *Mol.Microbiol.* 33, 188-199

153 Nichols, B. P., Shafiq, O., Meiners, V. (1998) Sequence analysis of Tn*10* insertion sites in a collection of *Escherichia coli* strains used for genetic mapping and strain construction. *J.Bacteriol.* 180, 6408-6411

154 Herbert, A., Guest, J. R. (1968) Biochemical and genetic studies with lysine + methionine mutants of *Escherichia coli*: Lipoic acid and α-ketoglutarate dehydrogenase-less mutants. *J.Gen.Microbiol.* 53, 363-381

155 Cleary, P., Campbell, A. (1972) Deletion and complementation analysis of biotin gene cluster of *Escherichia coli*. *J.Bacteriol.* 112, 830-839

156 Campillo-Campbell, A., Campbell, A. (1982) Molybdenum cofactor requirement for biotin sulfoxide reduction in *Escherichia coli*. *J.Bacteriol.* 149, 469-478

157 Tabor, S., Richardson, C. C. (1995) A single residue in DNA polymerases of the *Escherichia coli* DNA polymerase I family is critical for distinguishing between deoxy- and dideoxyribonucleotides. *Proc.Natl.Acad.Sci.U.S.A.* 92, 6339-6343

158 Ito, K., Sato, T., Yura, T. (1977) Synthesis and assembly of the membrane proteins in *E. coli*. *Cell* 11, 551-559

159 Laemmli, U. (1970) Cleavage of structural proteins during the assembly of the head of bacteriophage T4. *Nature* 227, 680-685

160 Bradford, M. M. (1976) A rapid and sensitive method for the quantitation of microgram quantities of protein utilizing the principle of protein-dye binding. *Anal.Biochem.* 72, 248-254

161 Pratt, E. A., Fung, L. W., Flowers, J. A., Ho, C. (1979) Membrane-bound D-lactate dehydrogenase from *Escherichia coli*: purification and properties. *Biochemistry* 18, 312-316

162 Bordo, D., Forlani, F., Spallarossa, A., Colnaghi, R., Carpen, A., Bolognesi, M., Pagani, S. (2001) A persulfurated cysteine promotes active site reactivity in *Azotobacter vinelandii* rhodanese. *Biol.Chem.* 382, 1245-1252

163 Schnaitman, C. A. (1971) Solubilization of the cytoplasmic membrane of *Escherichia coli* by Triton X-100. *J.Bacteriol.* 108, 545-552

164 Volini, M., Westley, J. (1966) The mechanism of the rhodanese-catalyzed thiosulfate-lipoate reaction. Kinetic analysis. *J.Biol.Chem.* 241, 5168-5176

165 Wang, S. F., Volini, M. (1973) The interdependence of substrate and protein transformations in rhodanese catalysis. I. Enzyme interactions with substrate, product, and inhibitor anions. *J.Biol.Chem.* 248, 7376-7385

166 Cerletti, P. (1986) Seeking a better job for an under-employed enzyme: rhodanese. Trends Biochem.Sci. 11, 369-372.

167 Vennesland, B., Castric, P. A., Conn, E. E., Solomonson, L. P., Volini, M., Westley, J. (1982) Cyanide metabolism. *Fed.Proc.* 41, 2639-2648

168 Spallarossa, A., Carpen, A., Forlani, F., Pagani, S., Bolognesi, M., Bordo, D. (2003) SseA, a 3-mercaptopyruvate sulfurtransferase from *Escherichia coli*: crystallization and preliminary crystallographic data. *Acta Crystallogr.D.Biol.Crystallogr.* 59, 168-170

169 Drew, D., Sjostrand, D., Nilsson, J., Urbig, T., Chin, C., de Gier, J. W., Von Heijne, G. (2002) Rapid topology mapping of *Escherichia coli* inner-membrane proteins by prediction and PhoA/GFP fusion analysis. *Proc.Natl.Acad.Sci.U.S.A.* 99, 2690-2695

170 Melén, K., Krogh, A., Von Heijne, G. (2003) Reliability measures for membrane protein topology prediction algorithms. *J.Mol Biol.* 327, 735-744

171 Lijk, L. J., Torfs, C. A., Kalk, K. H., De Maeyer M.C., Hol, W. G. (1984) Differences in the binding of sulfate, selenate and thiosulfate ions to bovine liver rhodanese, and a description of a binding site for ammonium and sodium ions. An X-ray diffraction study. *Eur.J.Biochem* 142, 399-408

172 Adams, H., Teertstra, W., Demmers, J., Boesten, R., Tommassen, J. (2003) Interactions between phage-shock proteins in *Escherichia coli*. *J.Bacteriol.* 185, 1174-1180

173 Mueller, E. G., Palenchar, P. M. (1999) Using genomic information to investigate the function of ThiI, an enzyme shared between thiamin and 4-thiouridine biosynthesis. *Protein Sci.* 8, 2424-2427

174 Frazzon, J., Fick, J. R., Dean, D. R. (2002) Biosynthesis of iron-sulphur clusters is a complex and highly conserved process. *Biochem.Soc.Trans.* 30, 680-685

175 Frazzon, J., Dean, D. R. (2003) Formation of iron-sulfur clusters in bacteria: an emerging field in bioinorganic chemistry. *Curr.Opin.Chem.Biol.* 7, 166-173

176 Donadio, S., Shafiee, A., Hutchinson, C. R. (1990) Disruption of a rhodanese-like gene results in cysteine auxotrophy in *Saccharopolyspora erythraea*. *J.Bacteriol.* 172, 350-360

177 Cook, W. J., Kar, S. R., Taylor, K. B., Hall, L. M. (1998) Crystal structure of the cyanobacterial metallothionein repressor SmtB: a model for metalloregulatory proteins. *J.Mol.Biol.* 275, 337-346

178 Cavet, J. S., Meng, W., Pennella, M. A., Appelhoff, R. J., Giedroc, D. P., Robinson, N. (2002) A nickel-cobalt-sensing ArsR-SmtB family repressor. Contributions of cytosol and effector binding sites to metal selectivity. *J.Biol.Chem.* 277, 38441-38448

179 Chen, H., Higgins, J., Kondorosi, E., Kondorosi, A., Djordjevic, M. A., Weinman, J. J., Rolfe, B. G. (2000) Identification of *nolR*-regulated proteins in *Sinorhizobium meliloti* using proteome analysis. *Electrophoresis* 21, 3823-3832

180 Wittwer, A. J., Ching, W. M. (1989) Selenium-containing tRNA(Glu) and tRNA(Lys) from *Escherichia coli*: purification, codon specificity and translational activity. *BioFactors* 2, 27-34

181 Klimmek, O., Stein, T., Pisa, R., Simon, J., Kroger, A. (1999) The single cysteine residue of the Sud protein is required for its function as a polysulfide-sulfur transferase in *Wolinella succinogenes*. *Eur.J.Biochem* 263, 79-84

182 Webb, E., Claas, K., Downs, D. M. (1997) Characterization of *thiI*, a new gene involved in thiazole biosynthesis in *Salmonella typhimurium*. *J.Bacteriol.* 179, 4399-4402

183 Veres, Z., Tsai, L., Scholz, T. D., Politino, M., Balaban, R. S., Stadtman, T. C. (1992) Synthesis of 5-methylaminomethyl-2-selenouridine in tRNAs: $^{31}$P NMR studies show the labile selenium donor synthesized by the *selD* gene product contains selenium bonded to phosphorus. *Proc.Natl.Acad.Sci.U.S.A.* 89, 2975-2979

184 Koonin, E. V. (1993) A superfamily of ATPases with diverse functions containing either classical or deviant ATP-binding motif. *J.Mol Biol.* 229, 1165-1174

185 Silvian, L. F., Wang, J., Steitz, T. A. (1999) Insights into editing from an ile-tRNA synthetase structure with $tRNA^{Ile}$ and mupirocin. *Science* 285, 1074-1077

# Vitae

Farzana Ahmed
Engel Hall, Virginia Tech
Blacksburg 24061
(540)-231-7861
fahmed@vt.edu

**EDUCATION**

*Ph.D*., *Biochemistry*
Virginia Polytechnic Institute and State University, expected summer 2003
*M. S., Biochemistry*, 1994
Dhaka University, Bangladesh,
*B.S., Biochemistry,* (Honours), 1992
Dhaka University, Bangladesh.

**PUBLICATIONS**

Ahmed F, Rahim, K. A., Fattah, S. A., Islam, A. and Ahmed A. (1996). "Comparative study of changes of liver function tests of patients with viral hepatitis and liver cirrhosis," The Dhaka University Journal of Biological Science. 5(1).

Ahmed F. and Larson, T.J. "YgaP, a novel cytoplasmic membrane associated sulfurtransferase of *Escherichia coli*", manuscript under preparation.

Ahmed F., Wolfe M. D., Lacourciere G., Stadtman T. C. and Larson T. J. " The YbbB rhodanese paralog of *Escherichia coli* is a selenouridine synthase", manuscript under preparation

**HONORS AND AWARDS**

James H. Eheart Scholarship (2002), Department of Biochemistry, Virginia Tech.

**ACTIVITIES**

Student Member, American Society of Microbiology (2002-present)
President, Association of Bangladeshi Students, Virginia Tech (8/98-8/99)

**PRESENTATIONS**

American Society for Microbiology 102$^{nd}$ general meeting, Salt Lake City, Utah, May 19-23, 2002. Topic: "YgaP, a novel cytoplasmic membrane associated sulfurtransferase of *Escherichia coli*."

American Society for Microbiology 103$^{rd}$ general meeting, Washington D.C., May 18-22, 2003. Topic: " The YbbB rhodanese paralog of *Escherichia coli* is a selenouridine synthase*"*